ผลของบรรยากาศการแคลไซน์ของไทเทเนียโซล-เจลต่อสมบัติในการเร่งปฏิกิริยาของตัวเร่งปฏิกิริยาแพลทินัมบนไทเทเนียในปฏิกิริยาไฮโดรจิเนชันแบบเลือกเกิดของ3-ไนโตรสไตรีน

นางสาวศศิธร คูหาอุดมลาภ

วิทยานิพนธ์นี้เป็นส่วนหนึ่งของการศึกษาตามหลักสูตรปริญญาวิศวกรรมศาสตรมหาบัณฑิต
สาขาวิชาวิศวกรรมเคมี ภาควิชาวิศวกรรมเคมี
คณะวิศวกรรมศาสตร์ จุฬาลงกรณ์มหาวิทยาลัย
ปีการศึกษา 2558

The effect of calcination atmospheres of sol-gel TiO_2 on the catalytic properties of Pt/TiO_2 catalysts in selective hydrogenation of 3-nitrostyrene

Miss Sasithorn Kuhaudomlap

A Thesis Submitted in Partial Fulfillment of the Requirements
for the Degree of Master of Engineering Program in Chemical Engineering
Department of Chemical Engineering
Faculty of Engineering
Chulalongkorn University
Academic Year 2015

Thesis Title	The effect of calcination atmospheres of sol-gel TiO_2 on the catalytic properties of Pt/TiO_2 catalysts in selective hydrogenation of 3-nitrostyrene
By	Miss Sasithorn Kuhaudomlap
Field of Study	Chemical Engineering
Thesis Advisor	Associate Professor Joongjai Panpranot, Ph.D.

Accepted by the Faculty of Engineering, Chulalongkorn University in Partial Fulfillment of the Requirements for the Master's Degree

.....Dean of the Faculty of Engineering

(Associate Professor Supot Teachavorasinskun, D.Eng.)

THESIS COMMITTEE

.....Chairman

(Associate Professor Anongnat Somwangthanaroj, Ph.D.)

.....Thesis Advisor

(Associate Professor Joongjai Panpranot, Ph.D.)

.....Examiner

(Assistant ProfessorSuphot Phatanasri, Ph.D.)

.....External Examiner

(Assistant Professor Okorn Mekasuwandumrong, D.Eng.)

ศศิธร คูหาอุดมลาภ : ผลของบรรยากาศการแคลไซน์ของไทเทเนียโซล-เจลต่อสมบัติในการเร่งปฏิกิริยาของตัวเร่งปฏิกิริยาแพลทินัมบนไทเทเนียในปฏิกิริยาไฮโดรจิเนชันแบบเลือกเกิดของ3-ไนโตรสไตรีน (The effect of calcination atmospheres of sol-gel TiO_2 on the catalytic properties of Pt/TiO_2 catalysts in selective hydrogenation of 3-nitrostyrene) อ.ที่ปรึกษาวิทยานิพนธ์หลัก: รศ. ดร. จูงใจ ปั้นประณต, 113 หน้า.

ไทเทเนียมไดออกไซด์เฟสอนาเทสขนาดนาโนถูกเตรียมด้วยวิธีโซลเจลและแคลไซน์ภายใต้บรรยากาศไฮโดรเจน อากาศ ไนโตรเจน ออกซิเจน และอาร์กอนที่อุณหภูมิ ๓๕๐ องศาเซลเซียส เป็นเวลา ๒ ชั่วโมง และใช้เป็นตัวรองรับสำหรับการเตรียมตัวเร่งปฏิกิริยา ๐.๕ เปอร์เซนต์โดยน้ำหนักของแพลทินัมบนไทเทเนียด้วยวิธีการเตรียมแบบคลือบฝัง วิเคราะห์คุณลักษณะของตัวเร่งปฏิกิริยาด้วยเทคนิคการเลี้ยวเบนของรังสีเอ็กซ์ การดูดซับทางกายภาพด้วยแก๊สไนโตรเจน เอ็กซเรย์โฟโตอิเล็กตรอนสเปกโตรสโกปี การรีดักชันของไฮโดรเจนด้วยการโปรแกรมอุณหภูมิ อินฟราเรดสเปกโตรสโกปีของการดูดซับด้วยคาร์บอนมอนอกไซด์ การดูดซับทางเคมีด้วยแก๊สคาร์บอนมอนอกไซด์ อิเล็กตรอนสปินเรโซแนนซ์ และ กล้องจุลทรรศน์อิเล็กตรอนแบบส่องผ่าน ตัวเร่งปฏิกิริยาแพลทินัมบนไทเทเนียที่แคลไซน์ภายใต้บรรยากาศไฮโดรเจนและไนโตรเจนแสดงประสิทธิภาพของตัวเร่งปฏิกิริยาสูงสุดได้ค่าการเปลี่ยนของสามไนโตรสไตรีน (ประมาณ ๗๐ เปอร์เซนต์) โดยที่ค่าการเลือกเกิดของสามไวนิลอนิลิน มากกว่า ๙๐ เปอร์เซนต์ ภายในเวลาการทำปฏิกิยา ๒๐ นาที เมื่อทำการรีดิวซ์ที่อุณหภูมิ ๒๐๐ องศาเซลเซียส ความว่องไวในปฏิกิริยาไฮโดรจิเนชันแบบเลือกเกิดของสามไนโตรสไตรีนของตัวเร่งปฏิกิริยาแพลทินัมบนไทเทเนีย สอดคล้องกับการกระจายตัวของแพลทินัมที่สูงบนตัวรองรับไทเทเนีย และค่าการเลือกเกิดของผลิตภัณฑ์ที่ต้องการคือ สามไวนิลอนิลินสัมพันธ์กับการมีอยู่ของพื้นผิวแพลทินัมแบบโลว์โคออดิเนต และอันตรกิริยาระหว่างโลหะกับตัวรองรับที่แข็งแรง ซึ่งได้รับอิทธิพลมาจากความบกพร่องบนตัวรองรับไทเทเนีย การเตรียมตัวเร่งปฏิกิริยาด้วยวิธีการดูดซับทางไฟฟ้าสถิตที่แข็งแรงช่วยปรับปรุงความสามารถในการเปลี่ยนไปเป็นผลิตภัณฑ์ของสามไนโตรสไตรีนจาก ๒๙ เปอร์เซนต์ไปเป็น ๖๔ เปอร์เซนต์ของตัวเร่งปฏิกิริยาแพลทินัมบนไทเทเนียที่ถูกแคลไซน์ภายใต้อากาศ เมื่อเปรียบเทียบกับตัวเร่งปฏิกิริยาที่เตรียมด้วยวิธีการเคลือบฝัง แต่ไม่ส่งผลต่อประสิทธภาพของตัวเร่งปฏิกิริยาแพลทินัมบนไทเทเนียที่แคลไซน์ภายใต้ไฮโดรเจน ทั้งนี้อาจเนื่องมาจากตัวเร่งปฏิกิริยามีการกระจายตัวที่ดีอยู่แล้ว

ภาควิชา วิศวกรรมเคมี ลายมือชื่อนิสิต .....

สาขาวิชา วิศวกรรมเคมี ลายมือชื่อ อ.ที่ปรึกษาหลัก .....

ปีการศึกษา 2558

5770306621 : MAJOR CHEMICAL ENGINEERING

KEYWORDS: SELECTIVE HYDROGENATION / CALCINATION ATMOSPHERE / SOL-GEL / PT/TIO2

SASITHORN KUHAUDOMLAP: The effect of calcination atmospheres of sol-gel TiO_2 on the catalytic properties of Pt/TiO_2 catalysts in selective hydrogenation of 3-nitrostyrene. ADVISOR: ASSOC. PROF. JOONGJAI PANPRANOT, Ph.D., 113 pp.

Nanocrystalline anatase TiO_2 were synthesized by a sol-gel method and calcined under H_2, air, N_2, O_2 and Ar atmosphere at 350 °C for 2 h and used as the supports for preparation of 0.5%Pt/TiO_2 catalysts by incipient wetness impregnation (IW) method. The characteristics and catalytic properties of Pt (0.5wt% Pt) were analyzed by X-ray diffraction (XRD), N_2-physisorption, X-ray photoelectron spectroscopy (XPS), H_2-temperature programmed reduction (H_2-TPR), infrared spectroscopy of adsorbed CO (CO-IR), CO-pulses chemisorption, electron spin resonance (ESR) and transmission electron microscopy (TEM). The 0.5%Pt supported on the TiO_2 calcined under H_2 and N_2 atmosphere exhibited the best catalytic performances. High conversion of 3-NS (~70%) with high selectivity to 3-VA (>90%) could be obtained after 20 min reaction time upon reduction at 200 °C. The catalytic activities of Pt/TiO_2 were correlated with Pt dispersion and the selectivity of 3-VA desired product was related to the presence of low coordinated Pt sites and the metal-support interaction, which were influenced by defects on the TiO_2 support. Preparation by the strong electrostatic adsorption (SEA) method improved the conversion of 3-NS from 29% to 64% of the Pt/TiO_2-air catalysts but for the Pt/TiO_2-H_2, preparation by SEA method did not improve both conversion of 3-NS and 3-VA selectivity, due probably to that the catalyst already had high Pt dispersion, comparing to the one prepared by the incipient wetness impregnation method.

Department: Chemical Engineering Student's Signature .....

Field of Study: Chemical Engineering Advisor's Signature .....

Academic Year: 2015

ACKNOWLEDGEMENTS

I am deeply grateful to my thesis advisor, Assoc. Prof. Dr. Joongjai Panpranot for her invaluable help and constant encouragement throughout the course of this research. I am most grateful for teaching and advice. I would not have achieved this far and this thesis would not have been completed without all the support that I have always received from her.

In additional, the author would also be grateful to Assoc. Prof. Dr. Anongnat Somwangthanaroj, as the chairman, Asst. Prof. Dr. Suphot Phatanasri, and Asst. Prof. Dr. Okorn Mekasuwandumrong as a member of the thesis committee and for your brilliant comments and suggestions.

I most gratefully acknowledge my parent and my friends for all their support throughout the period of this research.

Finally, I would like to thank the financial support to this work under The Institutional Research Grant (The Thailand Research Fund), IRG 5780014, and Chulalongkorn University, Contract No. RES_57_411_21_076.

Sasithorn Kuhaudomlap

CONTENTS

Page

Page

Page

Page

Page

LIST OF TABLES

Page

LIST OF FIGURES

Page

Page

CHARPTER I

INTRODUCTION

1.1 Introduction

The selective hydrogenation of nitrostyrene (NS) to vinylaniline (VA) is an important reaction because functionalized anilines such as VA are high value chemicals that are industrially important intermediates for pharmaceuticals, polymers, herbicides, and other fine chemicals. They are conventionally produced by selective hydrogenation of nitroaromatics (e.g. NS). The compound consists of two functional group a c=c double bond and a nitro group [1, 2]. Nitrostyrene hydrogenation is quite a complex reaction, which involves a nitro group reduction towards 3-vinylaniline, which can be further transformed to the undesired 3-ethylaniline and 3-ethylnitrobenzene which can be further converted to 3-ethylaniline. Highly selective catalysts including Au, Ag, and Mo were developed for NS hydrogenation, but they showed low activity [3-6]. Pt-based catalysts are used in the hydrogenation of NS because of their high catalytic activity but the catalysts simultaneously hydrogenate both functional groups, leading to undesired products [3, 7]. It is difficult to obtain high selectivity of product at high conversion. Thus, many attempts have been made to improve catalytic performances such as the addition of modifiers, changing pretreatment conditions and catalyst support [3].

Titanium dioxide is one of the most frequently used supports that promotes active metal dispersion for hydrogenation reaction. As a catalyst support, TiO_2 exhibits attractive characteristics such as chemical stability, non-toxicity, environmental and low cost. Reduction with H_2 at high temperature results in the SMSI effect for the TiO_2 supported Pt nanocatalysts. The SMSI effect appears to be necessary for high catalytic performance of the Pt/TiO_2 catalysts. The properties of TiO_2 such as crystallite size, crystalline phase composition, surface area, and morphology of particles depended on the synthesis method and conditions, post-synthesis treatment conditions [8], and the addition of a second metal. TiO_2 nanocatalysts have been prepared by several methods such as solvothermal [9], sol-gel [10], deposition-precipitation method [11], metal–organic chemical vapor deposition method (MOCVD) [12], one-step flame spray

pyrolysis (FSP) [13], and thermal decomposition [14]. Thus, Pt is an expensive noble metal widely used in NS hydrogenation and TiO_2 support is an important factor for controlling and improving the catalytic performances of dispersed Pt particles and it exhibited the strong metal-support interaction (SMSI) effect under high temperature reduction [15]. In the present work, TiO_2 was selected as the support for preparation of Pt/TiO_2 catalysts in the selective hydrogenation of 3-NS.

Sol-gel method is an easy route and widely employed to the preparation of high purity titanium dioxide nanopowders at low temperature. Their advantages are good homogeneity, highly crystalline, and the efficient controlling of the crystal phases and the particle sizes of titania, but the powder obtained is amorphous in nature and further heat treatment is required for crystallization [16, 17]. The properties of sol-gel derived TiO_2 were found to be influenced by calcination atmospheres. The metallic vacancy and oxygen are the common point defects and affected by the preparation process. The use of H_2-treated sol–gel derived TiO_2 resulted in higher Pd dispersion and improved catalytic performance of Pd/TiO_2 catalysts in the selective hydrogenation of acetylene, compared to the TiO_2 calcined in air [18]. Rutile TiO_2 prepared under Ar and H_2 atmosphere had higher photocatalytic activity for oxygen production than that prepared under air atmosphere [19]. Increasing oxygen percent in feed during the calcination process of TiO_2 resulted in high methanation activity of Co/TiO_2 [20]. TiO_2 calcined under vacuum and H_2 resulted in low photocatalytic activity while Ar calcination enhanced visible-light excitation [21]. The treatment with N_2 promoted the photocatalytic activity of MB degradation [22]. Thus, it is aimed to investigate the effect of calcination atmospheres on the properties of TiO_2 sol-gel supported Pt catalysts in the selective hydrogenation of 3-NS.

Supported Pt catalysts are typically prepared by using impregnation method which is a common and simple for preparation of catalysts. Many preparation method such as sol-gel, chemical vapor decomposition electroless plating and colloidal synthesis were investigated. Strong electrostatic adsorption is a special case of wet impregnation, which this method consists of maximizing the electrostatic interactions between the metal precursor and the support by adjusting the pH of the slurry to the adequate value, so as to adsorb the maximum amount of metal at the support surface. The goal

was to obtain maximum metal weight percentage while keeping the highest possible dispersion. Advantages of the strong electrostatic adsorption are the higher dispersion of metal than those prepared via other methods for the same metal loadings [23-25]. In this study, strong electrostatic adsorption was employed for preparation of Pt/TiO_2 catalysts and compared to those prepared by the conventional impregnation method.

The present study shows a simple method to obtain high performance Pt/TiO_2 catalysts in chemoselective hydrogenation of 3-nitrostyrene. The sol-gel derived TiO_2 nanopowder were calcined under different gas flows (H_2, Air, N_2, O_2 and Ar) and used as the supports for preparation of Pt/TiO_2 catalysts by impregnation method and compared to those prepared by strong electrostatic adsorption. The effect of calcination atmospheres of sol-gel TiO_2 and different preparation methods of catalysts on the catalytic properties were investigated by X-ray diffraction (XRD), N_2 physisorption, CO-pulse chemisorption, H_2-temperature-programed reduction (H_2-TPR), electron spin resonance (ESR) and X-ray photon spin resonance (XPS) and correlated with the catalyst performances in terms of NS conversion and VA selectivity.

1.2 Objectives

The objectives of this research are

1. To investigate the effects of calcination atmospheres of sol-gel TiO_2 on the physiochemical and catalytic properties of Pt/TiO_2 catalysts prepared by impregnation in the selective hydrogenation of 3-nitrostyrene.
2. To prepare the Pt/TiO_2 catalysts with selected TiO_2 support by strong electrostatic adsorption and investigate their physiochemical and catalytic properties in the selective hydrogenation of 3-nitrostyrene.

1.3 Research Scope

1. Titanium dioxide supports were prepared using sol-gel method calcined at 350 °C under different atmospheres (H_2, air, N_2, O_2, and Ar) for 2 h.
2. 0.5 wt%Pt/TiO_2 catalysts were prepared by using incipient wetness impregnation method with sol gel TiO_2 calcined under H_2, air, N_2, O_2, and Ar and by strong electrostatic adsorption method with sol gel TiO_2 prepared under selected calcination atmospheres.
3. The catalysts were prepared by impregnation calcined in air at 400 °C for 4 h and followed by reduction under H_2 flow (30 cm^3/min) at 200 °C and 500 °C for 2 h.
4. The catalysts were prepared by SEA method and reduced in H_2 at 200 °C for 2 h.
5. The catalysts were characterized by using X-ray diffraction (XRD), BET surface area, electron spin resonance (ESR), X-ray photoelectron spectroscopy (XPS), CO pulse chemisorption, and H_2 temperature programmed reduction (H_2-TPR).
6. The catalyst performances were tested in the selective hydrogenation of 3-nitrostyrene at 40 °C and 2 MPa hydrogen pressure for 10, 20, 40, 80, and 100 min.

1.4 Benefits

1. To obtain suitable calcination atmosphere of sol-gel TiO_2 for preparation of Pt/TiO_2 in selective hydrogenation of 3-nitrostyrene.
2. To obtain suitable method for preparation of Pt/TiO_2 in selective hydrogenation of 3-nitrostyrene.

CHARPTER II

BACKGROUND AND LITERATURE REVIEWS

2.1 Hydrogenation reaction with heterogeneous catalysts.

Hydrogenation is an important chemical reaction for a variety of industrial applications. For example, catalytic hydrotreating or hydroprocessing is one of the important processes in the petroleum refining industry where the reactions with hydrogen atoms. The catalysts used for hydrogenation can either be heterogeneous or homogeneous. Hydrogenation is usually performed using heterogeneous catalysts whereby the solids form a distinct phase in the gas or liquid reaction environment. On the other hand, homogeneous catalysts dissolve and form a single phase with the reaction mixture [26].

The heterogeneous catalysts can further be classified as supported or unsupported. Due to their versatility, easy separation from the product, facilitate recyclability and thermal stability, heterogeneous catalysts are preferred in industry rather than their homogeneous catalysts [26]. Heterogeneous catalyst required properties such as high activity, high selectivity, fast filtration rate, and recycle capability. Activity and selectivity depend on the selection of metal. The most frequently used metals in heterogeneous catalytic hydrogenation are palladium, platinum, rhodium, nickel, cobalt and ruthenium. Heterogeneous catalysts can be unsupported or supported, in the supported catalysts: the metal is deposited on inert material such as carbon, graphite, alumina or inorganic salts which the large range of applications according to the metal used. The advantages of the support catalysts such as easy separation from the reaction medium and more effective use of metal surface which the metal interacted with the support can influence the properties of the catalysts. The metal can be decorated on the surface of the support or it can be loaded into inside of the micropores depending on the mode of distribution. The metal can be shown in oxide or reduced form, depending on the preparation method of catalyst and reaction studied.

Heterogeneous catalytic hydrogenations are important reactions with wide industrial applications in the production of pharmaceuticals, agrochemicals, fine chemicals, flavours, fragrance and dietary supplements. The reactions are generally highly selective and easy to work up, the catalyst can often be recovered and recycled. Thus, reactions used to produce chemicals today between 10-20% are catalytic hydrogenations. Many processes that involve the exchange of material, energy or even information happen through surfaces. The adsorption of chemicals onto the catalyst surface takes place in two stages: physisorption and chemisorption. Physisorption characterized by weak forces (van der waals) and chemisorption that involves the formation of chemical bonds [27]. Catalysts influence on activity, selectivity and stability of chemical reactions, catalysts for producing the desired products become interestingly important.

2.2 Properties of platinum

The most studied nanoparticle catalysts are the noble metals including Ru, Rh, Pd, Pt, and Au. However because of costs, transition metal alternatives are now being investigated, including Co, Ni, and Fe. Transition metal nanoparticles have been used as catalysts due to a number of inherent advantages: they mimic metal surface activation and catalysis, exhibit selectivity and efficiency [26].

Platinum is a chemical element with symbol Pt and atomic number 78. It is a dense, malleable, ductile, highly unreactive, precious, gray-white transition metal. Its name is derived from the Spanish term platina. Platinum is a member of the platinum group of elements and group 10 of the periodic table of elements and it has six naturally occurring isotopes. Platinum is the least reactive metal and It has remarkable resistance to corrosion, even at high temperatures, therefore considered a noble metals. Platinum is used in catalytic converters, laboratory equipment, electrical contacts and electrodes, platinum resistance thermometers, dentistry equipment, and jewelry.

Platinum has widely been used as catalysts and used as hydrogenation catalysts. Platinum catalyst has been favorably used in liquid phase hydrogenation due to it is active under mild condition and has a good characteristic feature. Platinum metal catalysts are widely used in both supported and non-supported form. On a weight of metal basis, a properly supported catalyst invariably shows a higher activity than a non-supported catalyst, and the use of a support is recommended to obtain maximum efficiency of the metal. In addition, supported catalysts usually show a greater resistance to poisoning [28].

2.3 Synthesis and applications of TiO_2 nanoparticles.

2.3.1 Basic properties of TiO_2

Titanium dioxide, known as titanium (IV) oxide or titania is a naturally occurring oxide of the metal titanium with a chemical formular of TiO_2. Titanium dioxide exists in both crystalline and amorphous forms and mainly exists in three crystalline, namely, anatase, rutile and brookite. Anatase type TiO_2 has a crystalline structure that corresponds to the tetragonal system (with dipyramidal habit) and is used mainly as a photocatalyst under UV irradiation. Rutile type TiO_2 also has a tetragonal crystal structure (with prismatic habit) and is used as white pigment in paint. Brookite type TiO_2 has an orthorhombic crystalline structure. Anatase is considered the most important phase of titanium dioxide in terms of trade and rarely exists in nature in pure form. This phase is stable at temperatures less than 600 ℃ and changes to rutile phase at temperature higher than 600 ℃. TiO_2 is a versatile material that has applications in various products [8]. Titanium dioxide (TiO_2) shows unique characteristics such as non- toxicity, low cost, easy handling, strong oxidizing power, long term stability and resistance to photochemical and chemical erosion. The physical and chemical characteristics of TiO_2 can be controlled by its particle size, morphology, and crystalline phase.

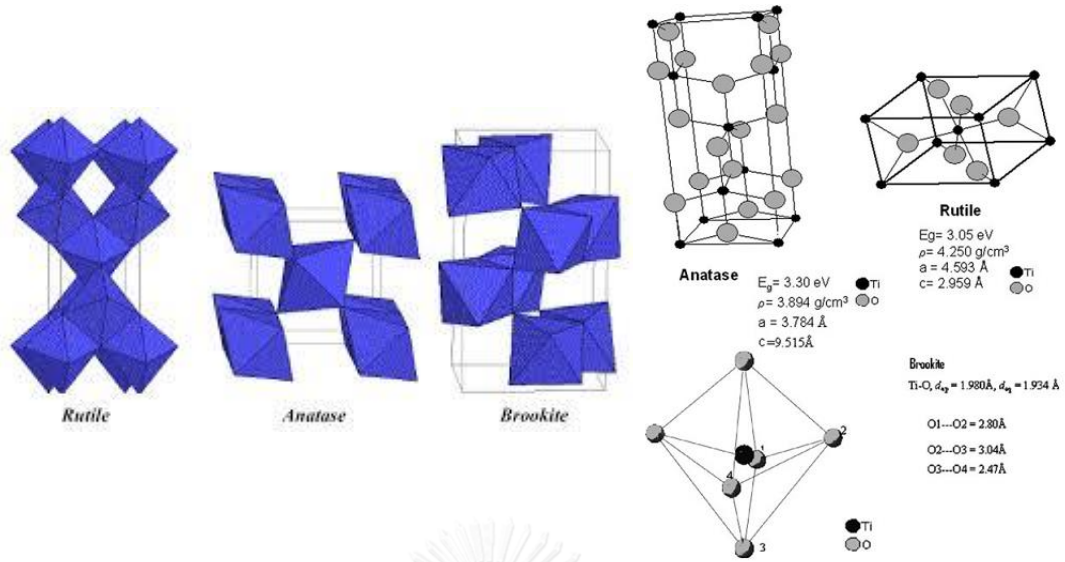

Figure 2.1 Different forms of TiO_2 [8].

Table 2.1 Bulk properties of TiO_2 [29].

Properties	Anatase	Brookite	Rutile
Crystal structure	Tetragonal	Orthorhombic	Tetragonal
Density, kg/m^3	3830	4170	4240
Unit cell	D4a19.4TiO2	D2h15.8TiO2	D4h12.3TiO2
Dimension, nm			
a	0.3733	0.5436	0.4584
b	-	0.9166	-
c	0.9370	0.5135	0.2953

2.3.2 Preparation and applications of TiO_2

Titanium dioxide (TiO_2) is an inorganic metal oxide and it is a versatile material that has applications in various products [8]. Titanium dioxide (TiO_2) is a very useful semiconducting transition metal oxide material and shows unique characteristics such as non- toxicity, low cost, easy handling, strong oxidizing power, long term stability and resistance to photochemical and chemical erosion, thus shows the advantages of these TiO_2 material in solar cells, chemical sensor, photocatalytic applications, medical applications, self-cleaning surface and environmental purification applications [30].

Titanium dioxide is applied as pigments, adsorbents, used in the production of paints, paper, plastics, welding rod-coating material, cosmetics and catalytic supports which the size of the titanium dioxide particle is an importance factor affecting the performance of the materials [31, 32].

The oxide nanoparticles are useful due to their good electrical and optical properties [30]. Titania can be synthesized by several different methods such as microemulsion, sol-gel, flame synthesis, oxidation hydrothermal synthesis, ultrasonic irradiation and hydrolysis precipitation. Different method of preparation resulted in different properties of TiO_2, or the same method of preparation but using different amounts of the starting materials resulting in different powder size [31].

TiO_2 has been used as catalyst support in heterogeneous catalysis, particularly anatase TiO_2. It exhibits a large number of attractive characteristic such as chemical stability, non-toxicity, low cost and high oxidation rate. Heterogeneous catalysts consist of small metal clusters on the oxide support, thus metal on TiO_2 were studied in many research to improve of catalytic properties.

2.4 Strong metal support interaction

The SMSI account for the changes in catalytic activity when the group VIII metals supported on reducible oxide supports were reduced at high temperatures, the so-called strong metal-support interaction (SMSI) effect. Tauster, S. J. et al. [33] studied the catalysts by impregnation TiO_2 with metal salt solution (group VIII noble metal). The reduction of noble metals supported on TiO_2 at low temperatures (200 °C) produces well-dispersed metals which exhibit the capacity to sorb both hydrogen and carbon monoxide. But, when reduction at 500 °C hydrogen and carbon monoxide sorption decreased to near zero. Electron microscope and x-ray diffraction showed that the loss of this sorption capacity was not due to metal agglomeration. This effect for well-dispersed metals is evidenced for a chemical interaction between the noble metal and the support.

The nature of the interaction is explained in terms of metal- metal bonding between the noble metal and titanium cations. Colmenares, J. C. et al. [34] studied two different catalysts consisting of Pt/TiO_2 and Pd/TiO_2 after oxidative and reductive calcination treatment. The XPS characterization showed that thermal treatment at 850 °C resulted in electron transfer from titania to metal particles with so-called strong metal-support interaction (SMSI) effect. The greater the SMSI effect, the better the catalytic performance. The SMSI effect would prevent electron–hole recombination which could explain that, even though oxidation/reduction treatment at 850 °C had led to a decrease in surface area and transformation of anatase to rutile, an improvement in photocatalytic activity.

The activity of a supported catalyst has a close relationship with conditions in the post-treatment. For example, after being prepared, Pt/TiO_2 catalyst needs oxidation or reduction treatment under a proper temperature. Pt atom is diffused into the lattice of TiO_2 during the heating process, while Ti^{4+} in the lattice is replaced by Pt^{2+} generating a Pt-O bond, the so-called strong metal–support interaction of Pt/TiO_2 under oxidizing atmosphere. There are differences between the mechanism of strong metal–support interaction of Pt/TiO_2 under reducing atmosphere such as high-temperature H_2. Many researchs conducted on the SMSI-reducing mechanism of transition metal such as Pt, Rh, and Pd with reducible oxides such as TiO_2, V_2O_3, Nb_2O_5, and Fe_3O_4 on the exhibition of adsorption of H_2 and CO. Zhang, J. et al. [35] studied the Pt/TiO_2 catalysts prepared by sol–gel method and drop-coated with a Pt sol and reduced by H_2 at elevated temperature. It is shown that titanium oxide of low-valence is transferred onto the surface of Pt particulates to encapsulate the surface via a strong metal–support interaction under reducing atmosphere. It was found that Pt atoms were diffused into the lattice of TiO_2 to occupy the oxygen vacancy and accept one electron from adjacent Ti^{3+} forming a $Pt–Ti^{4+}$ bond. When Pt/TiO_2 was treated at 400 °C in air (under oxidizing atmosphere), the Pt atom was diffused into the lattice of TiO_2 to generate Pt of a high valence, it replaced Ti atom and forms a Pt^{2+}-O^{2-} bond.

2.5 Synthesis and properties of sol-gel TiO_2 nanoparticles

Sol-gel method is a good method to synthesize ultra-fine metallic oxide and has widely employed for the preparation of nanocrystalline TiO_2. The physicochemical and electrochemical properties of TiO_2 can be modified to improve efficiency. This method is carried out in solution, improvement of certain desired structure characteristics such as composition homogeneity, grain size, particle morphology and porosity is possible [36]. This method is of interest in preparation of materials due to its mild conditions such as low temperature and pressure requirements and does not require complicated set-up. The advantage of sol-gel method is that it facilitates the synthesis of nanometer sized crystallized TiO_2 powder of high purity at relatively low temperature, homogeneity, felicity and flexibility. But the commonly problem is that these methods are the precipitates derived by sol-gel are amorphous in nature or low crystallinity products, in order to obtain crystalline products, further heat treatment at high temperature is required. This calcination process resulted in the grain growth and reduction in specific surface area of particles and induce phase transformation [37].

The sol-gel process involves the evolution of inorganic networks through the formation of a colloidal suspension (sol) and gelation of the sol to form a network in a continuous liquid phase (gel). A sol is a dispersion of the solid particles in a liquid where only the Brownian motions kept particles in suspension. While a gel is a state where both liquid and solid are dispersed in each other, which presents a solid network filled with liquid components. Sol is formed from the hydrolysis and polymerization reactions of the precursors, which are usually inorganic metal salts or metal organic compounds such as metal alkoxides, which metal alkoxides are most popular because they react readily with water. Complete polymerization and loss of solvent leads to the transition from the liquid sol into a solid gel phase [38]. Three main reactions that occur during the sol-gel process are hydrolysis, alcohol condensation, and water condensation.

The reaction is as follows

$Ti\text{-}OR + H_2O \Rightarrow Ti\text{-}OH + R\text{-}OH$ Hydrolysis

$Ti\text{-}OH + RO\text{-}Ti \Rightarrow Ti\text{-}O\text{-}Ti + R\text{-}OH$ Alcohol condensation

$Ti\text{-}OH + HO\text{-}Ti \Rightarrow Ti\text{-}O\text{-}Ti + H_2O$ Water condensation [39]

The properties of sol-gel TiO_2 depend on several factors. Factors affecting the sol gel process are the reactivity of metal alkoxides, pH of the reaction medium, water:alkoxide ratio, reaction temperature, and nature of solvent and additive. By varying these processing parameters, materials with different microstructure and surface chemistry can be obtained. The calcination process frequently gives rise to particle agglomeration and grain growth and may induce phase transformation. Hydrothermal treatment represents an alternative to calcination for promoting crystallization under milder temperatures. In the hydrothermal treatment, grain size, particle morphology, crystalline phase, and surface chemistry can be controlled via processing variables such as sol composition and pH, reaction temperature and pressure, aging time, and nature of solvent and additive [40]. The studies on the synthesis of TiO_2 by sol-gel method are summarized in Table 2.2.

Table 2.2 Summary of the research of the synthesis of sol-gel TiO_2

Researchers	Studies	Properties of TiO_2	Results
Li, B. et el. (2003) [31]	Studied the different preparation conditions (concentration, pH value, calcination time and calcination temperature) on properties of nano-TiO_2 powders as prepared by a sol-gel method.	-Calcined at 350 ℃ obtained 6 nm nano-TiO_2 powders, 13 nm at 500 ℃, 36 nm at 600 ℃. -Calcined at below 600 ℃, phase structure is mainly of anatase. -The phase transformation from anstase to rutile at about 600 ℃ and completed at about 800 ℃.	The effects of calcination temperature and pH value on the grain size and microstructure were founded that more effective compared with the calcination time and concentration.
Karami, A. et al. (2010) [41]	Studied the preparation of titanium dioxide nanopowder by the simple sol-gel method and various pH values of 3, 7, and 9 were investigated on properties of the TiO_2 (crystalline phase and particle size)	pH equal 3 has the smallest particle sizes, larger specific surface area and pure anatase phase was obtained.	-Titanium dioxide was synthesized in the pure anatase phase by adjusting the gelling pH, which in tgree value of gelling pH resulted in particle sizes between 10-20 nm. -TiO_2 prepared in pH 3 has a lowest particle size, the highest reactivity for photocatalytic reduction of nitric oxide.

Researchers	Studies	Properties of TiO_2	Results
S, Music et al. (1997) [42]	Studied the preparation of nanosized TiO_2 powders by sol-gel method with improved properties of TiO_2.	-Calcined up to 500 °C leading to a mixture of anatase and brookite phase while calcined at 850 °C and more showed single phase is a rutile. -The average crystallite size increased from 6 to 9 nm with increasing of the temperature up to 300 °C.	-The selected colloidal suspensions were stabilized with polyethylene glycol, prevented sintering of TiO_2 nanoparticles during the calcination.
Hossain et al. (2011) [30]	Studied the preparation of TiO_2 nanopowder by a sol-gel method at room temperature using $TiCl_4$ as a precursor with ethanol solution and investigated the size and morphology of TiO_2 nanoparticle with changing the synthesis parameters.	-Calcination temperature increased from 120 to 600 °C led to the average crystallite sizes changed from 4.1 to 28.06 nm and gelatinizing time from 24 to 120 h. -Calcination temperature at 500 °C exhibited anatase phase and phase transformation from anatase to rutile when calcined in after 500 °C.	- Decreasing of the gelatinizing time and using ultrasound waves can be promote the size of anatase TiO_2. -Diameter of anatase TiO_2 nanoparticles increased with increasing calcination temperature and gelatinization time.

Li, B. et al. (2003) [31] studied the different preparation conditions (concentration, pH value, calcination time and calcination temperature) on properties of nano-TiO_2 powders as prepared by a sol-gel method. The grain size tends to increase with increasing temperature and the increase in pH value. Controlling the conditions properly resulted in nano-TiO_2 powders with the grain size less than 6 nm nano-TiO_2 powder were obtained. From experimental, calcined at 350 ℃ obtained about 6 nm nano-TiO_2 powders. The effects of calcination temperature and pH value on the grain size and microstructure were founded that more effective compared with the calcination time and concentration.

Karami, A. et al. (2010) [41] studied the preparation of titanium dioxide nanopowder by the simple sol-gel method and various pH values of 3, 7, and 9 were investigated on properties of the TiO_2 (crystalline phase and particle size). The larger surface areas were obtained at pH equal 3 about of 80 m^2/g which 50% higher than that of the reference TiO_2 and it was possible to synthesize pure anatase phase of titania. In three value of gelling pH resulted in particle sizes between 10-20 nm. From pH value at 7 and 9 of synthesis TiO_2 showed surface area that smaller than of reference TiO_2 (P25) and agglomerates of small particles leading to the bigger than of the pH equal 3. Preliminary result on the photocatalytic activity of the synthesized in the reduction of nitric oxide showed that TiO_2 prepared in pH 3 with lowest particle size has the highest reactivity for photocatalytic reduction of nitric oxide.

S, Music et al. (1997) [42] studied the preparation of nanosized TiO_2 powders by sol-gel method with improved properties of TiO_2. The selected colloidal suspensions were stabilized with polyethylene glycol (PEG), prevented sintering of TiO_2 nanoparticles during the calcination due to stabilization of TiO_2 colloids can be obtained with polymer. From this research, showed that the samples calcined up to 500 ℃ leading to a mixture of anatase and brookite phase while calcined at 850 ℃ and more temperature showed single phase is a rutile. The average crystallite size increased from 6 to 9 nm with increasing of the temperature up to 300 ℃. From results of thermal analysis, the transition to rutile started at 610 ℃, accelerated at 730 ℃ and completed at 915 ℃.

Hossain et al. (2011) [30] studied the preparation of TiO_2 nanopowder by a sol-gel method at room temperature using $TiCl_4$ as a precursor with ethanol solution and investigated the size and morphology of TiO_2 nanoparticle with changing the synthesis parameters. Decreasing of the gelatinizing time and using ultrasound waves can be promote the size of anatase TiO_2 nanoparticles. The average grain size of anatase TiO_2 was obtained in the range 4-32 nm. The sol-gel dried and calcined in different temperatures results in the diameter of anatase TiO_2 nanoparticles increased with increasing calcination temperature and gelatinization time. The single phase is a anatase phase was obtained in titanium as calcined up to 500 ℃, when the calcination temperature increased in the after 500 ℃ showed phase transformation from anatase to rutile. From TEM analysis, the shape, crystallinity and spherical morphology of TiO_2 were strongly depened on the calcination temperature. The dispersivity and homogeneity were improved with the increase of the calcination temperature to 500 ℃ and size of nanoparticles were quite uniform.

2.6 Pretreatment gas in calcination process

The calcination process resulted in the grain growth and reduction in specific surface area of particles and induce phase transformation. The studies on the synthesis of sol-gel TiO_2 by different calcination atmospheress are summarized in Table 2.3

Table 2.3 summary of the research of the synthesis of sol-gel TiO_2 and calcined under different atmospheres.

Researchers	Studies	Characterizations	Properties of TiO_2	Results
Wu, N. et al. (2004) [21]	The effect of calcination atmospheres of TiO_2 in H_2 production from methanol/water.	-XPS and UV-Vis were used for showing the relation between the reactivity and the surface and bulk electronic properties.	-Crystallite sizes in the range of 9.0-10.0 nm. -Similar BET surface area of 110 m^2/g.	-Calcination under H_2 and vacuum resulted in low activity -Calcination under Ar, leading to high activity.

Researchers	Studies	Characterizations	Properties of TiO_2	Results
Suriye, K. et al. (2005) [20]	Studied the defect structure in titania support by calcined under N_2 plus increasing the amount of O_2 feed during the calcination on characteristics and activity of the Co/TiO_2 catalyst.	-CO_2-TPD and ESR used for showing the defect site in the surface of titania. -SEM-EDX and XRD used showing the morphology, element distribution and crystallite size. -TPR and H_2-chemisorption.	-Surface area of titania was decreased with increasing amount of O_2 during calcinations of titania while crystallite size was constant about of 7 nm.	-Surface defect of titania increased with increasing the O_2 percent in feed during the calcination. -Ti^{3+} in titania resulted in enhance conversion of CO on methanation
Riyapan, S. et al. (2014) [18]	Studied the performance of Pd/TiO_2 in the selective hydrogenation of acetylene by thermal treatment in air and H_2 of preparations of TiO_2 by a sol-gel method.	-XRD -TEM -ESR -CO-IR	-No change in the average crystalline size ≈ 4 nm, surface area ≈ 187-198 m^2/g, pore diameter ≈ 4.7-4.8 nm, and pore volume ≈ 0.3 cm^3/g -Mixture of anatase/brookite at 350 °C	-H_2-treated sol–gel derived TiO_2 resulted in higher Pd dispersion and improved catalytic performance of Pd/TiO_2 catalys, compared to the TiO_2 calcined in air.

Researchers	Studies	Characterizations	Properties of TiO_2	Results
Riyapan, S. et al. (2015) [43]	Studied the effects of calcination atmospheres (N_2 and O_2) and the preparation methods on the catalytic properties of Pd/TiO_2 catalysts in the selective hydrogenation of acetylene.	-XRD -TEM -ESR -CO-IR -H2-TPR -XPS	-TiO_2 supports calcined under N_2 and O_2 had similar average crystalline size ≈ 6 nm, BET surface area ≈ 208-210 m^2/g, pore volume ≈ 0.3 cm^3/g and average pore diameter ≈ 4.3 nm.	The presence of more surface Ti^{3+} on the TiO_2 under N_2 resulted in higher dispersion of Pd metal and metal-support interaction, leading to modification of catalytic performances.
Klaysri, R. et al. (2015) [22]	Studied impact of calcination atmospheres (O_2, air and N_2) of nanocrystalline TiO_2 and Si-doped TiO_2 on the photocatalytic properties.	-XRD -UV-vis -ESR -XPS -TEM	-The TiO_2 were calcined in O_2, air and N_2 at 450 °C exhibited in anatase and rutile phase -Calcination atmosphere did not the effect in the phase structure and the crystalline size of the catalysts.	-Calcination in N_2 increased the formation of Ti^{3+} defect sites on the TiO_2 surface. -Photocatalytic activity of MB was improved in N_2-treated TiO_2 and Si-doped TiO_2 due to increasing of anatase phase stability and the formation of Ti^{3+}sites.

Wu, N. et al. (2004) [21] studied the effect of calcination atmospheres (Ar, air, N_2, H_2, and vacuum) on properties of TiO_2 in hydrogen production from methanol/water solution. TiO_2 was prepared by a sol-gel method and calcination at 400 °C in Ar, air, N_2, H_2 (3% in N_2), and vacuum. Calcination atmospheres have significant effect on activity of TiO_2 in hydrogen production from methanol/water solution. Calcination under H_2 and vacuum resulted in low activity because of high defect density and low surface hydroxyl coverage. Calcination under Ar, enhances visible-light excitation and high hydroxyl coverage, leading to high activity.

Suriye, K. et al. (2005) [20] studied effect of the defect structure present in titania support on characteristics and activity of the Co/TiO_2 catalyst. Titania supports were prepared by sol-gel method and calcined under N_2 plus increasing the amount of O_2 to change the surface defect concentration. The surface defect (Ti^{3+}) of titania support was increased with increasing the oxygen percent in feed during the calcination. Dispersion of cobalt and reducibility increased with the amount of Ti^{3+} present in titania support. The Co/TiO_2 catalysts were tested in methanation founded that strong interaction increased with the present of Ti^{3+} in titania resulted in enhance conversion of CO on methanation without changing CH_4 selectivity.

Riyapan, S. et al. (2014) [18] studied the performance of Pd/TiO_2 in the selective hydrogenation of acetylene by using a thermal treatment under air and H_2 atmospheres of preparations of nanocrystalline TiO_2 by a sol-gel method. Calcination under H_2 atmosphere led to more surface Ti^{3+}defects on the TiO_2, compare to air. The presence of Ti^{3+} resulted in higher Pd dispersion and promoted the formation of isolated adsorption sites. The use of H_2-treated sol–gel derived TiO_2 resulted in higher Pd dispersion and improved catalytic performance of Pd/TiO_2 catalysts in the selective hydrogenation of acetylene, compared to the TiO_2 calcined in air. For the effects of preparation method, the catalysts were prepared by electroless deposition method resulted in higher Pd dispersion, compared to conventional impregnation.

Riyapan, S. et al. (2015) [43] studied the effects of calcination atmospheres and the preparation methods on the catalytic properties of Pd/TiO_2 catalysts in the selective hydrogenation of acetylene. Preparation of TiO_2 supports by a sol-gel method and calcined under O_2 and N_2 at 350 °C. The amount of surface Ti^{3+} was higher on the

TiO_2 calcined under N_2, compared to the TiO_2 calcined under O_2. The presence of Ti^{3+} on the TiO_2 surface resulted in higher dispersion of Pd metal and metal-support interaction, leading to modification of catalytic performances in the selective hydrogenation of acetylene. For the effects of preparation method, the 1% Pd/TiO_2-N_2 catalyst prepared by electroless deposition method resulted in high ethylene selectivity≈ 92% at complete acetylene conversion.

Klaysri, R. et al. (2015) [22] studied impact of calcination atmospheres of nanocrystalline TiO_2 and Si-doped TiO_2 on the photocatalytic properties. TiO_2 and Si-doped TiO_2 catalysts were prepared by solvothermal and a sol-gel methods and then catalysts were calcined under O_2, air and N_2 atmospheres. Calcination atmospheres resulted in distribution concentration of surface and interface species in TiO_2 and Si-doped TiO_2, such as surface oxygen and Ti^{3+} sites. Calcination under the N_2 atmosphere increased the formation of Ti^{3+} defect sites on the TiO_2 surface. Photocatalytic activity of MB degradation was improved in N_2-treated TiO_2 nanocatalyst and Si-doped TiO_2 due to increasing of anatase phase stability and the formation of Ti^{3+}sites on surface TiO_2. Preparation of TiO_2 catalysts by solvothermal method and calcined under N_2 atmosphere showed the highest photocatalytic activity under both UV and visible light irradiation.

2.7 Hydrogenation of nitrostyrene over heterogeneous catalysts

The selective hydrogenation of NS to VA is an important reaction, functionalized anilines such as VA are high value chemicals and are industrially important intermediates for pharmaceuticals, polymers, herbicides, and other fine chemicals. They are conventionally produced by selective hydrogenation of nitroaromatics (e.g.nitrostyrenes, NS) which the compound consists of two functional group a c=c double bond and a nitro group [1]. As shown in Figure 2.2, nitrostyrene hydrogenation is quite a complex reaction, which involves a nitro group reduction towards 3-vinylaniline, which can be further transformed to the undesired 3-ethylaniline and 3-ethylnitrobenzene which can be further converted to 3-ethylaniline. Nitrostyrene can be hydrogenated to be vinylaniline and ethylnitrobenzene, it is a

difficult to achieve high selectivity for either compound with high conversion. There are many attempts to solve this problem with using different metals, supports and solvents.

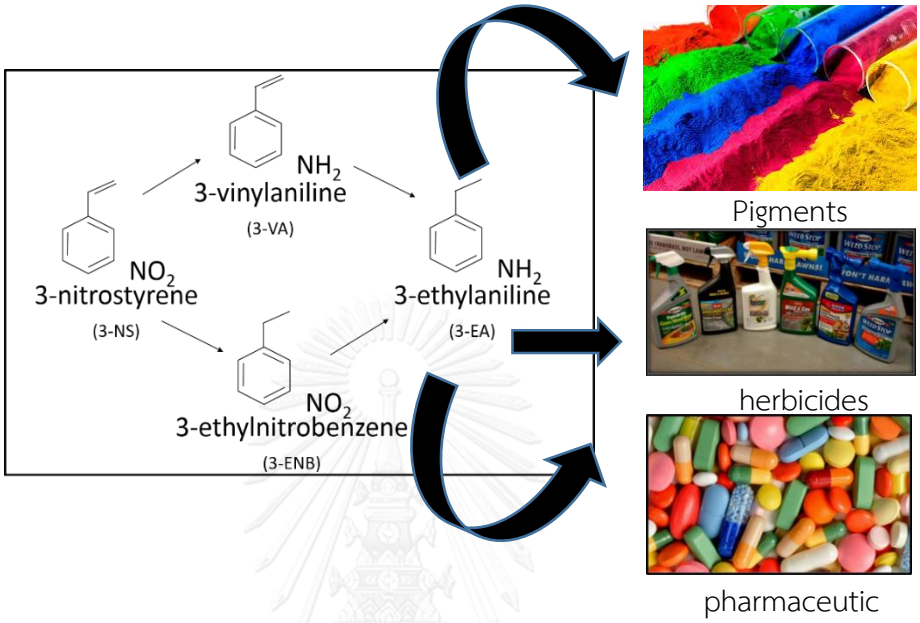

Figure 2.2 Simplified reaction scheme of the hydrogenation of 3NS.

Metal catalysts (noble and non-noble) were used in the hydrogenation of nitrostyrene such as Au, Ag, Pt, Pd, Ni, Ru and Mo and were supported on various materials such as CNT, SiO_2, Al_2O_3 and TiO_2. Highly selective catalysts including Au, Ag, and Mo were developed in NS hydrogenation, but they showed low activity [3-6]. Pt-based catalysts are used in the hydrogenation of NS because of their high catalytic activity but the catalysts simultaneously hydrogenate both functional groups, leading to undesired products. There are many research studied hydrogenation of nitrostyrene over various catalysts and condition reactions. It was suggested that the proper selection of the support could improve selectivity through a cooperative effect between the support (TiO_2) and the metal, avoiding the formation of hydroxylamine derivatives. To increase the selectivity of vinylaniline should be reduced the fraction of the Pt atoms in terraces and increase the Pt-Ti interface sites. Corma, A. et al. [3] studied the Pt/TiO_2 samples prepared by impregnation method with various reduction temperatures from 473 to 723 K, the results showed that the high reduction

temperatures of Pt/TiO_2 catalysts produced a decoration of the Pt crystal terraces with TiO_2, decreasing the number of Pt atoms exposed on terraces as well as increasing the number of Pt-Ti sites. Therefore, the catalyst was reduced at 723 K instead of 473 K, and was characterized by IR spectroscopy of adsorbed CO to confirm the results. This results is in agreement with Fujita, S. et al. work [15] that studied the Pt/TiO_2 prepared by the H_2 reduction at different temperatures. The relative activities of the nitro and the vinyl groups depended on the catalyst reduction temperature. It can be concluded that the reduction at higher temperature makes the catalyst more selective for the hydrogenation of the nitro group of NS. The FTIR measurements of adsorbed CO over the catalysts suggested that the presence of less-coordinated Pt atoms on edge, corner and kink sites was significant for the selective hydrogenation of NS to AS. The hydrogenation of the nitro group would preferentially proceed on less-coordinated Pt sites as edge, corner, and kink, whereas that of the vinyl group would occur on the terrace sites. It was suggested that Pt content on catalysts resulted in catalytic performance of catalyst.

Corma, A. et al. [3] studied the effect of Pt loading on Al_2O_3 catalysts in selective hydrogenation of nitrostyrene to vinylaniline. The characterized by FTIR measurement to determine Pt species site and reaction study indicated that the chemoselective reduction of 3-nitrostyrene to 3-aminostyrene will increase when the crystallite size of Pt is decreased. Decreasing of the metal crystalline size by preparing a catalysts at low Pt loading. This results is in agreement with Fujita, S.' work [15] who studied the effect of Pt content by varying from 0.5 to 2.0 wt% on TiO_2 in hydrogenation of nitrostyrene. It was found that increasing the Pt loading, the Pt crystallite size was slightly increased and the activity of the catalyst was enhanced. The catalyst with higher Pt loading showed lower AS selectivity. This results can be concluded that the increase in the Pt loading caused the decrease in the relative quantity of Pt atoms on edge and corner sites over Pt/TiO_2 catalysts. The higher selectivity of AS on 0.5 wt.% Pt/TiO_2 resulted from the larger relative quantity of less-coordinated Pt atoms on edge, corner and kink sites. This section showed the performance of different metals catalysts and condition reactions (temperature and pressure) in hydrogenation of nitrostyrene.

Table 2.4 summary of the research of selective hydrogenation of nitrostyrene on various catalysts and reaction conditions.

Researchers	Studies	Catalyst and preparation method	Reaction condition	Results
Wei, H. et al. (2015) [44]	Studied the catalytic performance of AU-Ni alloy supported on silica with different Au/Ni ratios in the chemoselective hydrogenation of a variety of substituted nitroaromatics.	-Au/SiO_2, Ni/SiO_2, Au-Nix/SiO_2 - Ni/SiO_2 was prepared by incipient wetness impregnation.	T=50 ℃ P_{H2}=300 kPa	-The best performance was achieved in Au-Ni3 (3 referes to the atomic ratio of Au to Ni)/SiO_2 with a selectivity of 93 % at 90.8% conversion for 3-nitrostyrene hydrogenation.
Xu, G. et al. (2016) [45]	Studied the performance of a pseudo-single-atom-catalyst Pt/FeO_x in supercritical CO_2 and CO_2-expanded toluene for the chemoselective hydrogenation of 3-NS.	-Pt/FeO_x, Pt/TiO_2, Pt/SiO_2 Pt/Al_2O_3 -FeO_x support prepared by precipitation. -Pt colloids prepared by a polyol reduction. -The Pt/FeO_x-T prepared by a colloid deposition.	T=50 ℃ P_{H2}=3 MPa	-For supercritical CO_2, excellent selectivity but low reactivity -Conversion of 3-NS and the selectivity of 3-VA reached exceed 95 % for reaction in CO_2 expanded toluene while toluene solvent was decreased by 90 %

Researchers	Studies	Catalyst and preparation method	Reaction condition	Results
Fujita, S. et al. (2011) [15]	The effects of CO_2 pressurization on the hydrogenation of nitrostyrene by using Pt/TiO_2 catalyst and studied the catalyst preparation conditions (Pt loading and the catalyst reduction temperature).	-Pt/TiO_2 -Impregnation method.	T=323 K P_{H2}=4 MPa.	-Lower Pt loadings and higher reduction temperature gave Pt/TiO_2 more selective for the AS formation. -Pressurized CO_2 increased the overall reaction rate, the selectivity to AS under CXL conditions.
Yoshida, H. et al. (2014) [32]	The effects of TiO_2 crystallite size on the catalytic performance of TiO_2-supported metal catalysts in liquid-phase selective hydrogenation of 3-NS, NB and styrene.	-Pt/TiO_2 -Difference in crystallite size of TiO_2 prepared by solvothermal method. -catalysts prepared by impregnation.	T=50 ℃ P_{H2}=4 MPa.	-Pt on smaller TiO_2 crystallite size was improved in hydrogenation of 3-NS. -Selectivity to AS was promoted in the hydrogenation of mixture of NB and styrene.
Yarulin, A. et al. (2015) [46]	The effect of Zn on Pt-based catalysts in liquid-phase hydrogenation of 3-nitrostyrene.	-Pt/HPS, Pt-Zn/HPS - Incipient wetness impregnation	T=348 K, P_{H2}=10 bar	Pt-Zn/HPS catalyst showed an increased yield of 3-VA (97%) compared to those Pt/HPS (16%)

Researchers	Studies	Catalyst and preparation method	Reaction condition	Results
Pisduangdaw, S. (2015) et el. [1]	The effects of preparation methods and reduction temperature of Pt/TiO_2 catalysts in selective hydrogenation of 3-NS.	-I-Pt/TiO_2, F-Pt/TiO_2 -Single-step flame spray pyrolysis method and impregnation method.	T=323 K P_{H2}= 4 MPa.	-The F-Pt/TiO_2 were improved in terms of NS conversion and VA selectivity. -Reduction at high temperature, higher dispersion, activities and VA selectivity.
Serna, P. et al. (2011) [47]	Studied the increasing the activity of the Au/TiO_2 catalyst and to improve the selectivity of traditional Pt catalysts.	-Au/TiO_2, Pt/ γ-Al_2O_3, Pt/TiO_2 -Deposition-precipitation -incipient wetness impregnation.	T=120 ℃ P_{H2}=9 bar	-Improve the catalytic activity, increase the concentration of low coordinate Au. -For Pt/TiO_2, the selectivity is governed by the T used for catalyst activation.
Furukawa, S. et al. (2014) [48]	Studied the series of Pd- and Rh-based intermetallic compounds supported on silica and investigated catalytic properties in the NB and NS reactions.	-Pd/SiO_2, Rh/SiO_2, Pd-M/SiO_2 (M=Pb, Ga, Fe, Zn, Sn and Bi) Rh-M/ SiO2 (Pb, Bi, Sn, Fe, Sb and Ti) -impregnation.	T=343 K	-Pd-Pb, highest chemoselective in the conversion of NS to AS (92%) -Rh-Pd, high selectivity to AS (93%) and the highest NS conversion (94%).

Researchers	Studies	Catalyst and preparation method	Reaction condition	Results
Yarulin, A. et al. (2015) [49]	Studied the promoting effect of Zn on Pt-based catalyst for the liquid phase hydrogenation of 3 NS.	-Pt/ZnO -Ion exchange method.	T=313-393 K P_{H2}=1-15 bar	The monodisperdes Pt supported on ZnO catalyzed the target 3-VA formation by Pt-Zn intermetallic phase by alloying via reactive metal-support interactions.
Yoshida,H. et al. (2011) [50]	Studied the effects of CO_2 pressure and organic solvents in hydrogenation of nitrostyrene by using Pt/TiO_2 catalyst.	-Pt/TiO_2 -Impregnation method.	T=323 K P_{H2}=4 MPa	-The conversion decreases with CO_2 P in both solvents. -In toluene, VA selectivity decreases with CO_2 P while ENB increases.
Makosch, M. et al. (2012) [51]	Studied the simple modification method to control chemoselectivity over Pt/TiO_2 employing organic thiols as surface modifiers for the hydrogenation of 4-NS	-Pt/TiO_2 -Incipient wetness impregnation method	T=80 ℃ P_{H2}=10 bar	-The modifiers containing polar groups yielded 100% selectivity to 4-AS, un-polar modifier yielded 88% selectivity at conversion close to 100 %.

Researchers	Studies	Catalyst and preparation method	Reaction condition	Results
Pisduangdaw, S et al. (2015) [1]	The properties of Pt-Co/TiO_2 catalysts by using FSP method in selective hydrogenation of 3-nitrostyrene.	-Pt/TiO_2, Pt-Co/TiO_2 -Single step flame spray pyrolysis.	T=323 K, P_{H2}=40 bar	Reduced at 200 °C, NS conversion and VA selectivity of Pt-Co/TiO_2 increased. ENB selectivity increased with the maximum Co at 0.2 wt%.
Beier, M. et al. 2012 [7]	Studied the influenced of the presence of an ionic liquid, the reaction medium (acidic or basic), and the type of support on the catalytic behavior for the chemoselective hydrogenation of 3-nitrostyrene.	-Pt/SiO_2, Pt/TiO_2, Pt/Al_2O_3, Pt/CNTs	P_{H2}=1 bar	- Supports such as Al_2O_3, TiO_2, and CNTs gave low selectivities for ENB. - Solvent was crucial for the catalyst's selectivity, EtOA can be both good selectivity for ENB and good activity -The yield exceeding 90 % to 3-aminostyrene under basic condition

Wei, H. et al. (2015) [44] studied the catalytic performance of AU-Ni alloy nanoparticles supported on silica with different Au/Ni ratios, which prepared with a modified two-step method in the chemoselective hydrogenation of a variety of substituted nitroaromatics. In the first step, Au nanoparticles were deposited on an APTES-functionalized silica surface and the second step, Ni was deposited on the Au surface using a weak reducing agent (tert-butylamine borane). Au@Ni core-shell structure was transformed to Au-Ni alloys nano-phase by reduction in H_2 at elevated temperature. The Au-Ni alloy nanocatalysts exhibited highly active for the hydrogenation of substituted nitroarenes to the coresponding anilines. The best performance was achieved in Au-Ni3 (3 referes to the atomic ratio of Au to Ni) /SiO_2 catalysts with a chemoselectivity of 93 % at 90.8% conversion for 3-nitrostyrene hydrogenation.

Xu, G. et al. (2016) [45] studied the performance of a pseudo-single-atom-catalyst Pt/FeO_x in supercritical CO_2 and CO_2-expanded toluene for the chemoselective hydrogenation of 3-NS. For supercritical CO_2, resulted in excellent selectivity but low reactivity due to the limited substrate solubility in the reaction medium. Both the conversion of 3-NS and the selectivity of 3-VA reached exceed 95 % were obtained for reaction in CO_2 expanded toluene under optimum conditions while toluene solvent amount was decreased by 90 % compared to as without CO_2. Thus, demonstrating a green synthesis approach to functionalized anilines.

Fujita, S. et al. (2011) [15] studied the effect of CO_2 pressurization in the hydrogenation of nitrostyrene by using Pt/TiO_2 catalyst. Phase behavior was an important factor for the reaction system, pressurized CO_2 increased the overall reaction rate and the selectivity to AS under CXL conditions at any conversion level. But under the condition where all NS was dissolved in scCO_2 leading to lower selectivity to AS because of strong interaction between CO_2 molecule and the nitro group of NS. Lower Pt loadings and higher catalyst reduction temperature gave Pt/TiO_2 catalysts more selective for the AS formation. Competitive adsorption of nitro and vinyl group was suggested to determine the product selectivity

Yoshida, H. et al. (2014) [32] studied the effects of TiO_2 crystallite size on the catalytic performance of TiO_2-supported metal catalysts in liquid-phase selective hydrogenation of 3-NS, nitrobenzene, and styrene. The crystallite size of TiO_2 supports is an important factor for controlling and improving the performance of dispersed Pt. Pt on smaller TiO_2 crystallites can improve selectivity to vinylaniline for the hydrogenation of 3-NS and the selectivity to aniline was promoted in the hydrogenation of a mixture of nitrobenzene and styrene. Low coordinated Pt sites should be formed on the surface of nanocrystal TiO_2 supports, which more active for the hydrogenation of nitro group than vinyl group and this sites is decreased with an increase in the crystallite size of TiO_2 support.

Yarulin, A. et al. (2015) [46] studied the effect of Zn on Pt-based catalysts in liquid-phase hydrogenation of 3-nitrostyrene. The modification of Pt surface and electronic structure invoked by Zn incorporation, resulted in the Pt-Zn/HPS catalyst showed an increased yield of 3-VA (97%) compared to those of Pt/HPS catalyst (16%). The formation of mono- (Pt) and bi-metallic (Pt-Zn) with diameter controlled by the pore size of the HPS support. Pt-Zn/HPS exhibited high performance under repeated reaction runs by without catalyst deactivation.

Pisduangdaw, S. et al. (2015) [1] studied the effects of preparation methods and reduction temperature of Pt/TiO_2 catalysts in selective hydrogenation of 3-NS. FSP-made catalysts improved of both hydrogenation activity and selectivity to vinylaniline by reduction at high temperature. Pt/TiO_2 was prepared by impregnation method on a sol-gel TiO_2 showed higher amount of rutile phase than Pt/TiO_2 obtained by FSP and exhibited lower Pt dispersion and hydrogenation activity. Rutile phase occurred after reduction at 600 °C and 700 °C for the I-Pt/TiO_2 and F-Pt/TiO_2, respectively, leading to excessive decoration of Pt by the reducible TiO_x species and poor catalytic performances. Reduction at high temperature showed in higher Pt dispersion, resulted in higher hydrogenation activity and selectivity to VA.

Serna, P. et al. (2011) [47] studied gold catalyst on TiO_2 was synthesized by a deposition-precipitation in the hydrogenation of 3 NS. From relationship between the activity of Au/TiO_2 catalysts and the concentration of low coordinated Au sites, leading to the catalytic activity was improved when increase the concentration of low

coordinate Au site. The highest yields were obtained on small particles size of 3.8 and 5.8 nm and the particles larger than 8.5 nm show the activity decreases, then it suggesting that particle shape may be playing an important role. The difficulties to substantially increase hydrogenation activity of gold catalysts. Selectivity to 3 VA were increase for smaller Pt crystallites, selection of a support with higher specific surface area. Pt nanoparticle support on TiO_2 can be easily decorated with TiO_x species by treatment the catalyst with H_2 at temperature above 400 C enhances the selectivity of the nitro group in NS. For Pt/Al_2O_3, influence of metal content and particle size is less critical than the effect of temperature used for catalyst activation.

Furukawa, S. et al. (2014) [48] studied the series of Pd- and Rh-based intermetallic compounds supported on silica and investigated their catalytic properties in the reaction of nitrobenzene and nitrostyrene. The formation of the intermetallic compounds made the platform for the chemoselective hydrogenation of NS: two metal elements are coadjacent at the atomic level on the surface of the nanoparticles. An increase in the electronegativity of the second metal provides polar sites and enhances the activation of methanol as a hydrogen donor, which accelerates the hydrogenation of the nitro group of NS leading to improves the yield of AS. PdPb exhibits the highest chemoselective in the conversion of NS to AS (92%) among the Pd-based catalysts and RhPd exhibits high selectivity to AS (93%) and the highest NS conversion (94%) among the Rh-based catalysts. Thus, intermetallics that contain Pb in this study, afforded good catalytic performance for the chemoselective hydrogenation of NS.

Yarulin, A. et al. (2015) [49] studied the promoting effect of Zn on Pt-based catalyst for the liquid phase hydrogenation of 3 NS. The monodispersed Pt supported on ZnO catalyzed the target 3-VA (3-VA=97% at conversion=100%) formation by Pt-Zn intermetallic phase was formed by alloying via reactive metal-support interactions. The effects of solvent found that ethanol is the best solvent in optimal reaction conditions for 3-NS hydrogenation and resulted in the highest activity and 3-VA selectivity. H_2 partial pressure had no effect on the products distribution. Increase in reaction temperature would have the effect on C=C group activation resulted in a greater formation of the 3-EA and lower 3-VA. Thus, reaction conditions (solvent, reaction

temperature and H_2 partial pressure) is crucial for a process development in reaction system.

Yoshida, H. et al. (2011) [50] studied the effects of CO_2 pressure and organic solvents in hydrogenation of nitrostyrene by using Pt/TiO_2 catalyst. The conversion decreases with CO_2 pressure in both of solvents (ethanol and toluene). The effect of CO_2 pressure changes the product distribution in the toluene as a nonpolar solvent but not in ethanol as a polar solvent. In toluene solvents, selectivity to VA decreases with CO_2 pressure while that to ENB increases due to the reactivity of the nitro group of NS were decreased by interactions with the dissolved CO_2 molecules in toluene. Interactions of nitro group with CO_2 molecules changes the product distribution by depending on CO_2 pressure and the suitable selection of solvent.

Makosch, M. et al. (2012) [51] studied the simple modification method to control the chemoselectivity over Pt/TiO_2 catalysts employing organic thiols as surface modifiers for the liquid phase selective hydrogenation of 4-nitrostyrene. The modifier structure affected to the selectivity by the modifiers containing polar groups yielded 100% selectivity to 4-aminostyrene while an un polar modifier yielded 88% selectivity at conversion close to 100 %. The variation of the modifier showed that a polar group adjadcent to the chain of the organic thiol revealed higher selectivities, 1, 6-dithiolhexane modified Pt/TiO_2 is the best result. The complete switch of selectivity to 4-aminostyrene was obtained by the surface modification. The rate of the unmodified Pt/TiO_2 catalyst at 40% conversion was the highest for all the catalysts due to tiols block part of the surface of the Pt nanoparticles and active sites.

Pisduangdaw, S. et al. (2015) [1] studied the preparation of $Pt\text{-}Co/TiO_2$ by single step flame spay pyrolysis in selective hydrogenation of 3-NS. Co loading varying at 0-0.5wt% with Pt at 0.5 wt%. The effect of Co addition, catalysts were reduced at 200 °C resulted in the ENB selectivity increased. The positive effect of Co addition when the catalysts were reduced at 500 °C. The $Pt\text{-}Co/TiO_2$ increased in the activity and VA selectivity compared to monometallic Pt/TiO_2 due to the strong interaction between Pt/Co.

Beier, M. et al. (2012) [7] studied the influenced of the presence of an ionic liquid, the reaction medium (acidic or basic), and the type of support on the catalytic

behavior for the chemoselective hydrogenation of 3-nitrostyrene. The selectivity of C=C or NO_2 group hydrogenation can be controlled by basic or acidic conditions. The yields of 3-ethylnitrobenzene above 90 % were obtained by using trifluoroacetic acid as an additive and yield exceeding 90 % to 3-aminostyrene under basic condition. Supports such as Al_2O_3, TiO_2, and CNTs gave low selectivities for ENB and led to considerable hydrogenation of the NO_2 group to the amine due to interact strong with the metal. The effect of the solvent such as toluene, tetrahydrofuran (THF), EtOA, $CHCl_3$, and 1, 2-Dichlorobenzene (DCB) on the catalytic behavior were investigated. Solvent was crucial for the catalyst's selectivity, EtOA can be both good selectivity for ENB and good activity.

2.8 Preparation of catalysts

The objectives of studies in the synthesis procedure, were to keep it as simple and inexpensive as possible. Methods available to prepare metal-supported catalysts, impregnation is the simplest, least expensive, and most prevalent method, in which a high surface area oxide or carbon support is contacted with a liquid solution containing precursor dissolved metal ions or coordination complexes. The metal deposition was first performed by simple wet impregnation, followed by reduction under hydrogen, the excellent metal dispersion obtained at low Pt loading and could not be maintained at a high metal weight percentage [52]. Impregnation can be termed wet or dry, depending on the volume of impregnating solution is greater than or equal to the pore volume of the support. In wet impregnation (WI), the support is contacted with an excess of a solution containing the metal precursor, the metal precursor species may not diffuse into the pore system of the solid during the equilibration period. Dry impregnation is often termed "incipient wetness impregnation (IWI)" or "pore filling", an amount of solution that corresponds to the total pore volume of the support material is mixed with support and capillary action provides the driving force for the imbibition of the impregnation solution into the porous solid. However, a non-uniform metal precursor distribution may develop as the metal complex remains in solution and is carried to the surface during drying. When pH is not controlled, the pH of the

impregnating solution can vary quite dramatically and often ends up near the support point of zero charge (PZC), at which point no metal precursor–support interaction occurs [53]. If pH of the metal solution is adjusted before contact to promote metal sorption onto the support, this is the concept of "strong electrostatic adsorption (SEA) method". To design new procedures allowing for high Pt dispersion and high Pt weight percentage with attention to the metal precursor-support interactions. Rational synthesis techniques were then developed by Regalbuto et al. The technique is quite versatile: it was adapted to various supports, like silica [25], alumina and carbon [54], and can be extended to other metals and to bimetallic nanoparticles.

2.8.1 Strong electrostatic adsorption method (SEA)

2.8.1.1 Theory

SEA is a simple, rational approach to synthesize highly dispersed supported metal catalysts. The method is based on an electrostatic mechanism in which the (typically hydroxyl) functional groups on the support surface can be protonated and deprotonated and so positively or negatively charged as a function of pH relative to the point of zero charge (PZC) [23]. The point of zero charge (PZC) of a support corresponds to the pH value at which the electric charge density on the support surface is zero (neutral surface), which can be measured by the method of Park and Regalbuto. The hydroxyl groups that populate oxide surfaces become protonated and thus positively charged below a characteristic pH value or become deprotonated and thus negatively charged above the characteristic pH value. Brunelle explained that oxides placed in solutions at pH values below their PZC would adsorb anions such as hexachloroplatinate $[PtCl_6]^{2-}$; at pH values above their PZC, the same support would adsorb cations such as platinum tetraammine $[Pt(NH_3)_4]^{2+}$ [24]. This method consists of maximizing the electrostatic interactions between the metal precursor and the support by adjusting the pH of the slurry to the adequate value, so as to adsorb the maximum amount of metal at the support surface. The latter depends on the surface chemistry of the support and on the chemical nature of the metal precursor (anion or

cation, size, etc.). The goal was to obtain maximum metal weight percentage while keeping the highest possible dispersion [54].

The first step in the SEA method is to determine the PZC of the support, which is easily determined by measuring final pH versus initial pH at high surface loading. Surface loading (SL) is defined at the amount of support surface per liter of solution, and can be calculated by equation

Surface loading (m^2/L) = Surface Area of support (m^2/g) * grams of support (g) / Volume of Precursor Solution (L)

The second step of SEA is to perform an uptake-pH survey to determine the pH of strongest interaction.

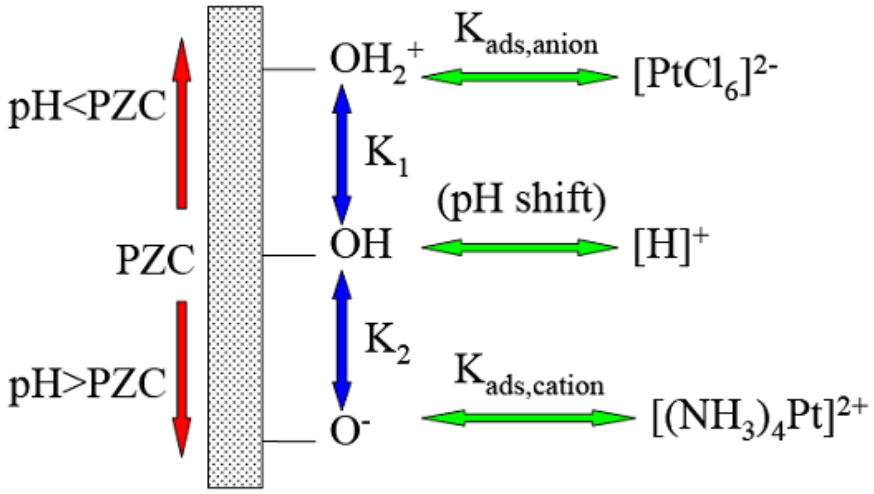

Figure 2.3 Electrostatic adsorption mechanism [53].

2.8.1.2 Synthesis of Pt based catalysts by strong electrostatic adsorption method

Strong electrostatic adsorption of Pt onto support can be used with hexachloroplatinate $[PtCl_6]^{2-}$ or CPA at low pH and tetraammine $[Pt(NH_3)_4]^{2+}$ or PTA at high pH to achieve a monolayer or submonolayers of Pt precursors that retain their high dispersion with a simple reduction in hydrogen [23]. Both physicochemical and electrochemical characterization show that the use of H_2PtCl_6, which is a very classical impregnation precursor leading to Pt catalysts poisoned with chlorine, especially if they were reduced at low temperature. Chlorine coming from the metal precursor decomposition appears difficult to remove completely and the presence of chlorine on the Pt particles leads to decreasing the active Pt surface. Preparation with PTA avoids the problem of residual chloride which can hinder activity for certain reactions [23, 54]. This study demonstrates that the SEA method allows the fine control of the structure and the morphology of the metal nanoparticles (average particle size, size distribution, degree of agglomeration) [54]. SEA is a special case of wet impregnation in which the final pH is targeted to the pH range in which the electrostatic interaction is strongest. It also was demonstrated that catalysts prepared via SEA had a higher dispersion of metal than those prepared via another method at the same metal loadings. The hypothesis behind the SEA approach to catalyst preparation is that monolayer adsorption of metal complexes via strong electrostatic adsorption can lead to small metal particles when the complexes are reduced [53]. The studies on the synthesis of Pt/TiO_2 catalysts by SEA method are summarized in Table 2.5

Table 2.5 summary of the research of the synthesis of Pt onto support by strong electrostatic adsorption

Researchers	studied	results
Jiao, L. et al. (2008) [53]	Studied the preparation of silica-supported noble and base metal catalysts by strong electrostatic adsorption (SEA) method and compared with traditional dry impregnation method.	-Ammine complex were used as metal precursor and it appears that the high dispersion of electrostatically adsorbed ammine metal precursor is retained during reduction. -SEA showed a much higher dispersion than DI.
Lambert, S. et al. (2009) [24]	Studied the preparation of highly dispersed Pt/carbon xerogel catalysts by strong electrostatic adsorption method using hexachloroplatinic acid to carbon xerogels and platinum tetraammine chloride to oxidized carbon xerogels.	-Platinum loading of Pt/C catalysts up to about 8-10wt% of unoxidized carbon xerogel and about 1-5 wt% for oxidized carbon xerogels. -All Pt/Carbon xerogel catalysts showed a high dispersion and very small platinum particles (1.1-1.3 nm) and very active in the hydrogenation of benzene into cyclohexane.
Hao, X.et al. (2011) [23]	Studied the preparation of carbon-supported Pt catalysts by strong electrostatic adsorption (SEA) by using different type of carbons (activated, black and graphitic) with different surface areas.	-The SEA method gives smaller particle sizes with narrower particle size distributions than by other method, at high metal loadings. -Preparation with platinum (II) tetraammine chloride to avoids the problem of residual chloride which can hinder activity for certain reactions.

Researchers	studied	results
Jiao, L. et al. (2008) [25]	Studied the synthesis method of mesoporous silica SBA-15 with metal ammines (Pt, Pd, Cu, Co, Ru) by strong electrostatic adsorption method (SEA) and compared to the traditional dry impregnation method.	- Low-temperature-reducing metals such as Pt and Pd, form very well dispersed nanoparticles after reduction. -Co particles were large due to the higher temperature required for reduction of the adsorbed cobalt ammine complex led to metal sintering, but Co particles were still smaller than the preparation by DI.
Job, N. et al. (2010) [54]	Studied the preparation of Pt/carbon xerogel catalysts with the high metal weight percentages by impregnation with H_2PtCl_6 in SEA method	-The catalysts were reduced at 200 °C in H_2 for 1 h showed a poorly accessible Pt surface area due to Pt poisoning in residues from the synthesis procedure. -The presence of chlorine from metal precursor was suspected to poison the Pt catalysts.

Jiao, L. et al. (2008) [53] studied the preparation of silica-supported noble and base metal catalysts by strong electrostatic adsorption (SEA) method and compared with traditional dry impregnation method. Correlation between strong electrostatic interaction during impregnation and the high dispersion of reduced metals were investigated. SEA is a special case of wet impregnation in which the final pH is targeted to the pH range in which the electrostatic interaction is strongest. The SEA method showed rational procedure for the cheap, simple, and scalable preparation of highly dispersed supported catalysts, even at relatively high metal loadings. Ammine complex $[Pd(NH_3)_4]^{+2}$, $[Cu(NH_3)_4]^{+2}$, $[Co(NH_3)_6]^{+3}$, $[Ru(NH_3)_6]^{+2}$, $[Ru(NH_3)_6]^{+3}$, and $[Ni(NH_3)_6]^{+2}$ were used as metal precursor and it appears that the high dispersion of electrostatically adsorbed ammine metal precursor is retained during reduction. It was found that strong correlation between adsorption and high metal dispersion. Compares the metal

dispersion, catalysts synthesized by SEA and DI methods: SEA showed a much higher dispersion than DI.

Lambert, S. et al. (2009) [24] studied the preparation of highly dispersed Pt/carbon xerogel catalysts by strong electrostatic adsorption method using hexachloroplatinic acid to carbon xerogels (PZC=9.4) and platinum tetraammine chloride to oxidized carbon xerogels (PZC=2.4). This research showed the developement a simple and effective method to synthesize highly loaded and highly dispersed Pt/carbon that can used as electrocatalysts in PEM fuel cells. Four supports with various maximal pore sizes (18, 32, 68, and 90 nm) were used and PZC was determined equal 9.4. Carbon xerogels were oxidized in nitric acid in order to alter irreversibly surface and to increase the number of surface acidic groups and PZC was 2.4. Unoxidized carbon xerogel carried out in solution at pH below their PZC and adsorb platinum anions, while oxidized carbon xerogels carried out in solutions at pH above their PZC and adsorb platinum cations. Platinum uptake curve, platinum loading of Pt/C catalysts about 8-10wt% of unoxidized carbon xerogel and about 1-5 wt% for oxidized carbon xerogels. All Pt/Carbon xerogel catalysts showed a high dispersion and very small platinum particles (1.1-1.3 nm) and very active in the hydrogenation of benzene into cyclohexane which this method was used for heterogeneous catalysis to obtained Pt loading up to 20 wt% while the Pt particle size below 3 nm.

Hao, X. et al. (2011) [23] studied the preparation of carbon-supported Pt catalysts by strong electrostatic adsorption (SEA) by using different type of carbons (activated, black and graphitic) with different surface areas. Strong electrostatic adsorption of Pt onto carbon used with hexachloroplatinic acid at low pH and platinum (II) tetraammine chloride at high pH to achieve a monolayer or submonolayers of Pt precursors that retain high dispersion with a simple reduction in hydrogen. The SEA method gives smaller particle sizes with narrower particle size distributions than by other method, at high metal loadings. Preparation with platinum (II) tetraammine chloride to avoids the problem of residual chloride which can hinder activity for certain reactions, but drawback to platinum (II) tetraammine chloride preparation is the exclusion of the large precursor complex which retains two hydration sheaths. Platinum (II) tetraammine chloride will not adsorb over high-PZC carbons, it can be

solved by lowering the PZC of the carbon by surface oxidation. At high of metal loading, the adsorptive reduction reaction plays a significant role in the dispersion of the hexachloroplatinic acid precursor during dry impregnation.

Jiao, L. et al. (2008) [25] studied the synthesis method of mesoporous silica SBA-15 with metal ammines (Pt, Pd, Cu, Co, Ru) by strong electrostatic adsorption method (SEA) and compared to the traditional dry impregnation method. From this research, the SEA method showed that a rational procedure for the cheap, simple and scalable preparation of highly dispersed supports catalysts for all ammine complexes. Adsorption surveys carried out to determine the pH of maximum uptake and synthesized at the optimal pH. The results showed that the adsorption mechanism of all metal ammines is largely electrostatic and the adsorption can approach equilibrium in a short time. Low-temperature-reducing metals such as Pt and Pd, form very well dispersed nanoparticles after reduction. Cobalt particles were large due to the higher temperature required for reduction of the adsorbed cobalt ammine complex led to metal sintering, but Co particles were still smaller than the preparation by DI method.

Job, N. et al. (2010) [54] studied the preparation of Pt/carbon xerogel catalysts with the high metal weight percentages by impregnation with H_2PtCl_6 in SEA method. This research demonstrates that the SEA method allows the control of the structure and the morphology of the metal (average particle size, size distribution, degree of agglomeration). In order to increase the Pt weight percentage, impregnation-drying-reduction cycles were performed: the final metal content at 22.3wt% in three cycles. The aim of this study is I) to studied the Pt/carbon xerogel prepared by SEA method II) high metal dispersion III) high electrochemical activity. When the catalysts were reduced at 200 °C in H_2 for 1 h showed a poorly accessible Pt surface area and used as cathodic catalysts in a Proton Exchange Membrane (PEM) fuel cell showed a low performance due to Pt poisoning in residues from the synthesis procedure. The reduction temperature and duration were increased up to 450 °C and 5 h, increasing in the Membrane-Electrode Assembly (MEA) performance: attributed to the development of the active Pt surface area. The presence of chlorine from metal precursor was suspected to poison the Pt catalysts. In the future studied, the SEA method replaced of H_2PtCl_6 by another Pt precursor.

CHARPTER III
MATERIALS AND METHODS

This chapter describes the chemicals used for the synthesis of the catalysts and the details of experimental procedure of this research which are divided into three parts. Part 3.1 describes the preparation of Pt supported TiO_2 catalysts by incipient wetness impregnation and strong electrostatic adsorption method. Part 3.2 provides the characterization techniques used to investigate the properties of catalysts such as X-ray diffraction (XRD), N_2 physisorption, CO-pulse chemisorption, H_2-temperature programmed reduction (H_2-TPR), electron spin resonance (ESR) and X-ray photron spin resonance (XPS). And finally, the reaction study in the liquid phase hydrogenation of 3-nitrosstyrene is described in part 3.3.

3.1 Catalysts preparation

3.1.1 Preparation of TiO_2 support

Titanium dioxide support was prepared by the sol-gel method using titanium isopropoxide as a precursor. At first 7.33 cm^3 of 70 vol% nitric acid was added to 1000 cm^3 of de-ionized (DI) water under continuous stirring. While the mixture was stirred, 83.5 cm^3 of titanium isopropoxide was added slowly. The mixture was stirred continuously at room temperature for about 3 days until clear sol was obtained. After that, the clear sol was placed in dialysis tubing, which was submerged in DI water. The water was changed daily for 3-4 days until the pH of the water reached 3.5. The dialyzed sol was dried at 110 ºC overnight to remove the solvent. The resulting materials were calcined in different gas flows including H_2, Air, N_2, O_2, and Ar at 350 ºC for 2 h with the heating rate of 10 ºC/min. The prepared TiO_2 are referred to as TiO_2-H_2, TiO_2-Air, TiO_2-N_2, TiO_2-O_2 and TiO_2-Ar for those calcined in hydrogen, air, nitrogen, oxygen and argon, respectively.

Table 3.1 Chemical used for prepared TiO_2 by sol-gel method.

Chemicals	Formula	Suppliers
Titanium isopropoxide	$Ti[OCH(CH_3)_2]_4$	Aldrich Chemical Ltd.
70% nitric acid	HNO_3	Asia Pacific Specialty Chemical Limited.

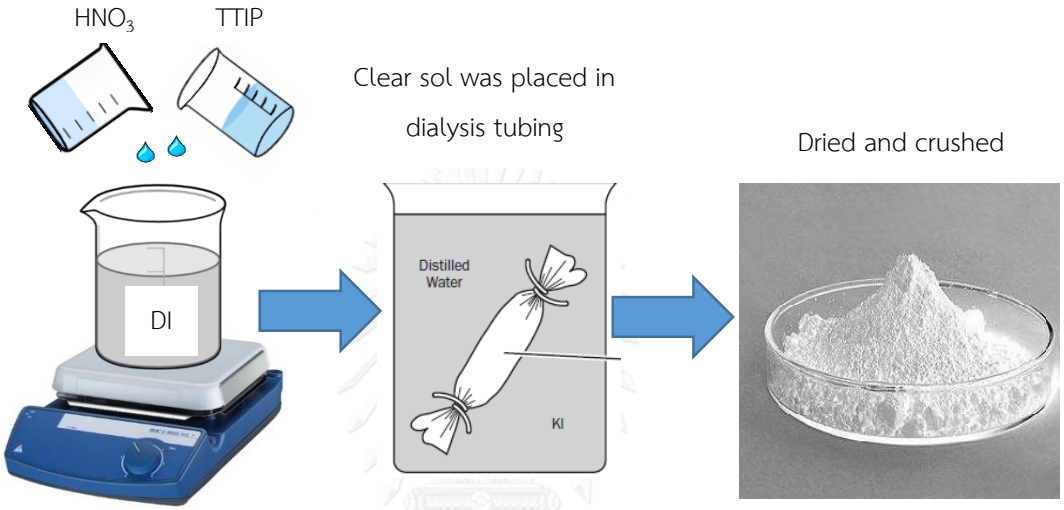

Figure 3.1 Diagram of TiO_2 catalysts preparation by sol-gel method.

3.1.2 Preparation of Pt/TiO_2 catalysts by incipient wetness impregnation method.

The 0.5 wt% Pt/TiO_2 catalysts were prepared by impregnation method, chloroplatinic acid hexahydrate was used as the Pt precursor. A desired amount of chloroplatinic acid hexahydrate was dissolved in deionized water which the volume equal to pore volumn of TiO_2 support. The TiO_2 supports were impregnated with aqueous solutions of H_2PtCl_6. The Pt/TiO_2 was left to stand for 6 h to assure adequate distribution of metal complex and subsequently dried at 110 °C overnight in air. Then, the catalysts were calcined in air at 400 °C for 4 h.

Table 3.2 Chemical used for prepared Pt/TiO_2 by impregnation method.

Chemicals	formula	Suppliers
Chloroplatinic acid hexahydrate	H_2PtCl_6•6H20, 37.50%	Aldrich Chemical Ltd.

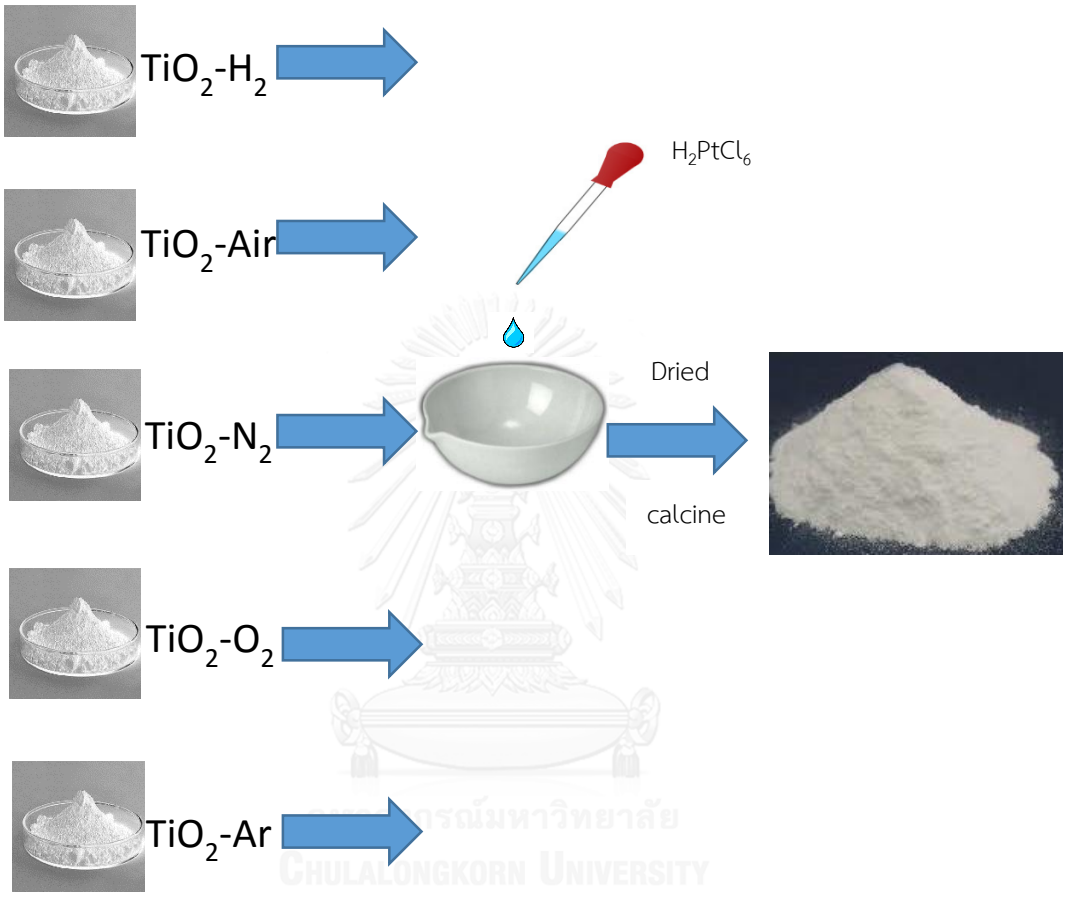

Figure 3.2 Diagram of Pt/TiO_2 catalysts preparation by impregnation method

3.1.3 Preparation of Pt/TiO_2 catalysts by strong electrostatic adsorption method.

3.1.3.1 Determination of the point of zero charge (PZC) of TiO_2 support.

In the SEA method, it is important to know the PZC of the support. The PZC is the pH value which the electrical charge density on the support surface is zero. TiO_2 supports with different surface areas, the mass of the two nanocrystalline TiO_2-H_2, and TiO_2-Air were adjusted to obtain same surface loading of 10^3 m^2/L for 10 ml of water

solutions in all case. Water solution were made up at various initial pHs values using HCl or NaOH in the pHs range of 1-13. The TiO_2 support was added to the 10 ml of each solution and shaken for 1 h at 150 rpm. Then, final pH is measured again and the plateau of the final pH vs the initial pH plot corresponds to the PZC of the solid support.

3.1.3.2 Determination of the optimal adsorption pH.

The Pt/TiO_2 catalyst was prepared by SEA. The titanium dioxide support was obtained from synthesis of TiO_2 by sol-gel method and calcined under H_2 and air atmosphere. Tetraammineplatinum (II) chloride hydrate from Sigma Aldrich was used as metal precursor on TiO_2 support. The surface area of the titanium dioxide was measured by the BET method about of 130 m^2/g for TiO_2-H_2 and 150 m^2/g for TiO_2-air. Differences in the specific surface area of each titanium dioxide support, the mass of the both TiO_2-H_2 and TiO_2-air were adjusted so that same surface loading. In order to determine the optimal pH leading to required metal loading (0.5 wt%Pt), adsorption experiments were conducted 10 ml of 200 ppm metal solutions and the pH values of all these solutions were adjusted using HCl or NaOH between pH 9 and 12.5, according to the PZC value of the supports. Metal concentrations were measured by ICP before and after contact with TiO_2 to determine the metal uptake. For the mass of the TiO_2-H_2 (0.0769 g) and the TiO_2-air (0.0670 g) were adjusted so that surface loading = 10^3 m^2/L in 13 ml (3 ml for measured initial concentration of metal by ICP) of solution of Pt and contacted slurries were placed on a rotary shaker for 1 h at 150 rpm. After final pH is measured again and 3 ml of the contacted slurries was with drawn and filtered. The remaining concentration of Pt in the solution was determined by inductively coupled plasma (ICP). Pt uptakes from pH 9 to 12.5 were determined from the difference in Pt concentration between the precontacted and postcontacted solutions.

3.1.3.3 Synthesis of Pt/TiO2 catalysts by SEA

The required Pt uptake at a initial pH followed to above section, leading to metal loading around 0.5 wt%. The Pt/TiO_2 catalyst was prepared by adjusting the initial pH of metal solution to this value with HCl or NaOH. Three gram of TiO_2-H_2 and TiO_2-air support were soaked in Pt solution at surface loading = 10^3 m^2/L. After 1 h at 150 rpm under shaker, the slurry was filtered and measured metal loading by ICP. The solution is trapped by the vacuum filter and the liquid is drawn through the funnel into the flask below and dried for 24 h at room temperature. Then, the Pt/TiO_2 catalyst was reduced with H_2 at 200 °C for 2 h.

Table 3.3 Chemicals used for prepared Pt/TiO_2 by strong electrostatic adsorption (SEA)

Chemicals	formula	Suppliers
Tetraammineplatinum (II) chloride hydrate	$Pt(NH_3)_4Cl_2 \cdot xH_2O$, 98%	Aldrich Chemical Ltd.
Sodium hidroxide	NaOH	Aldrich Chemical Ltd.

3.2 Catalyst Characterization

3.2.1 X-ray diffraction (XRD)

The XRD patterns of TiO_2 supports and Pt/TiO_2 catalysts were obtained using a SIEMENS XRD D5000 X-ray diffractometer with CuK_α radiation in scanning range from 20 to 80 degrees of 2theta. The average crystallite size (d_{XRD}) of TiO_2 was calculated using the Scherrer's equation.

3.2.2 BET surface area

Surface area was a physical adsorption of nitrogen gas on the surface of catalyst to find the total surface area. The BET surface areas of the TiO_2 supports, average pore size distribution and average pore size diameter were measured by N_2 physisorption using a BEL-SORP automated system.

3.2.3 CO-pulse experiment

Metal active sites were measured by using CO chemisorption technique. The amounts of CO-chemisorbed on the Pt/TiO_2 catalysts were measured at room temperature by using CO-pulse chemisorption technique using MicromeriticsChemiSorb 2750 (pulse chemisorption system). 0.05 g of catalyst was packed in a glass tube. Prior to the measurement, He gas was introduced into the sample cell (30 cm^3/min) in order to remove the remaining air. Then, catalysts were reduced with hydrogen at 500 ℃ for 2 h with a heating rate of 10 ºC/min and cooled down to the room temperature in a He flow. After that, 20 µl of carbon monoxide was injected into catalysts to adsorb on the metal surface of catalyst and repeated until the sample did not any longer adsorbed carbon monoxide (the desorption peak were constant).

3.2.4 Temperature-programmed reduction (TPR)

The H_2-TPR measurements were carried out in a quartz u-tube reactor to determine the reducibility and reduction temperature of platinum catalysts. Approximately, 0.1 g of catalyst was packed in a quartz U-tube. Prior to the measurements, all the catalyst samples were pretreated with a N_2 flow (30 cm^3/min) at 200 ℃ for 1 h in order to remove any adsorbed and then cooled down to the room temperature. After that, TPR profiles were obtained by flow carrier gas (10%H_2/Ar) through the catalysts samples with 30 cm^3/min and temperature ramping from 30 ºC to 800 ℃ at 10 ºC/min.

3.2.5 Electron spin resonance (ESR)

The surface Ti^{3+} on surface TiO_2 supports were measured by electron spin resonance spectroscopy (ESR) using a Elxys500 at X-band (Bruker). It was performed to monitor the surface Ti^{3+} on the surface of the TiO_2.

3.2.6 X-ray photoelectron spectroscopy (XPS)

The XPS analysis was performed using an AMICUS photoelectron spectrum spectrometer equipped with an MgK_α X-ray as primary excitation and KRATOS VISION2

software. XPS elemental spectra were acquired with 0.1 eV energy step at a pass energy of 75 kV. The C 1s line was taken as an internal standard at 285.0 eV.

3.2.7 Inductively coupled plasma-atomic emission spectrometry (ICP)

The actual Pt loading of the catalysts after impregnation and adsorption were measured by inductively coupled plasma-atomic emission spectrometry (ICP), using an Iris advantage Thermo Jarrel Ash devide.

3.2.8 Infrared spectroscopy of adsorbed CO (CO-IR)

The CO adsorbed species on the Pt/TiO_2 catalysts were measured. He gas was introduced into the sample cell in order to remove the remaining air. The catalysts were reduced with H_2 flow for 2 h. and cooled down to the room temperature in He flow. Then, CO-He mixture was flow over the catalyst for 30 min. After that, CO was purged from the cell with He flow and the IR spectrum of CO adsorbed over the catalyst was recorded.

3.2.9 Transmission electron microscopy (TEM)

The morphology and crystallite sizes of TiO_2 supports were measured by using JEOL-JEM 2010 transmission electron microscope using energy-dispersive X-ray detector operated at 80-200 kV.

3.3 Catalytic hydrogenation

Prior to the catalytic tests, the catalysts were reduced under H_2 flow (30 cm^3/min) at 200 and 500 °C for 2 h. Liquid-phase hydrogenation reaction of 3-nitrostyrene (NS) was carried out in a 50 cm^3 autoclave. The reactor was charged with 0.5 cm^3 of NS (3.6 mmol) and 20 mg of the catalysts. It was purged with H_2 for three times to remove the air and heated in a water bath. The reaction was carried out at 40 °C, 2 MPa of H_2 with a high-pressure liquid pump. The reaction was conducted while stirring the reaction mixture with a magnetic stirrer. After the reaction, the reactor was cooled below room temperature with an ice-water and carefully depressurized. The reaction mixture was then analyzed by a gas chromatograph attached with a flame ionization detector using decane as an internal standard.

Table 3.4 Chemicals used in the liquid-phase hydrogenation of 3-nitrostyrene

Chemicals	formula	Suppliers	density	Molecular weight
3-nitrostyrene 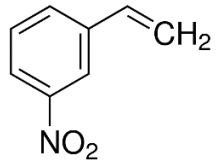	$H_2C=CHC_6H_4NO_2$, 96%	Aldrich Chemical Ltd.	1.07 g/mL at 25 °C (lit.)	149.15
3-Vinylaniline 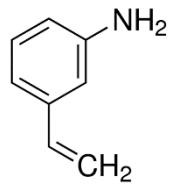	$CH_2=CHC_6H_4NH_2$, 97%	Aldrich Chemical Ltd.	1.051 g/mL at 25 °C (lit.)	119.16
3-Ethylaniline 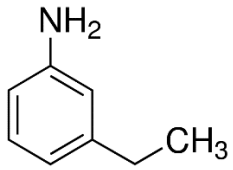	$C_2H_5C_6H_4NH_2$, 98%	Aldrich Chemical Ltd.	0.975 g/mL at 25 °C (lit.)	121.18
Hydrogen gas	H_2(UHP; 99.99vol%)	linde		
Ethanol	C_2H_5OH, 99.5%	Aldrich Chemical Ltd.	0.789 g/mL at 20 °C	46.07

Table 3.5 Operating conditions of gas chromatograph of selective hydrogenation of 3-NS.

Gas chromatograph	Shimadzu GC2014
Detector	FID
Capillary column	Rtx®-5
Carrier gas	Helium (99.99 vol. %)
Make-up gas	Air (99.9 vol. %)
Column temperature	140 °C
Injector temperature	270 °C
Detector temperature	310 °C

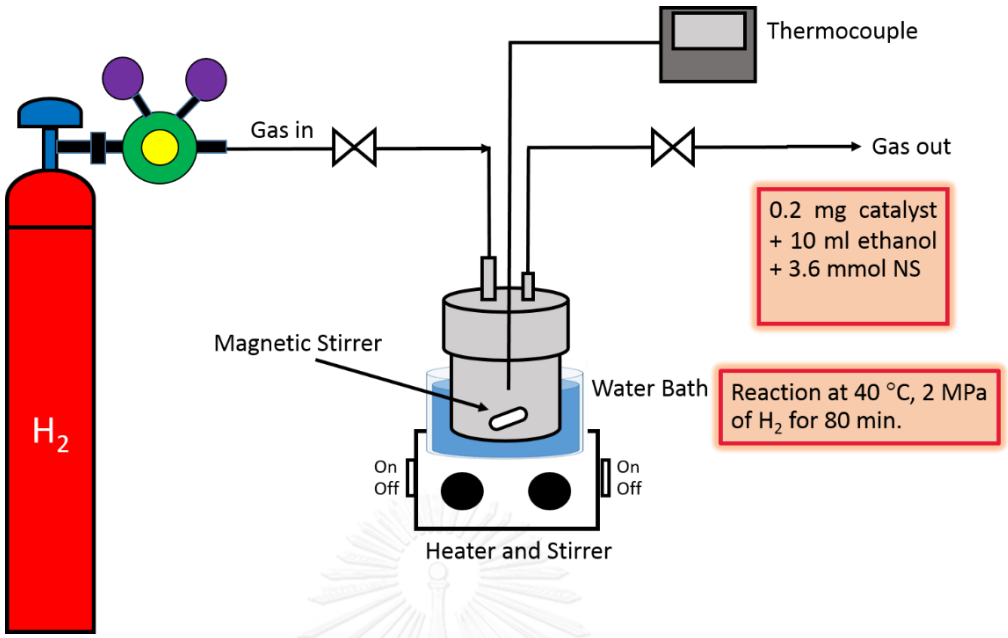

Figure 3.3 Schematic of the liquid-phase hydrogenation of 3-NS

CHARPTER IV

RESEARCH METHODOLOGY AND REDEARCH PLAN

4.1 The research methodology

The research methodology consists of two parts.

Part I. The investigation of the effect of calcination atmospheres of a sol-gel TiO_2 on the catalytic properties of Pt/TiO_2 catalysts by incipient wetness impregnation for liquid-phase hydrogenation of 3-nitrostyrene.

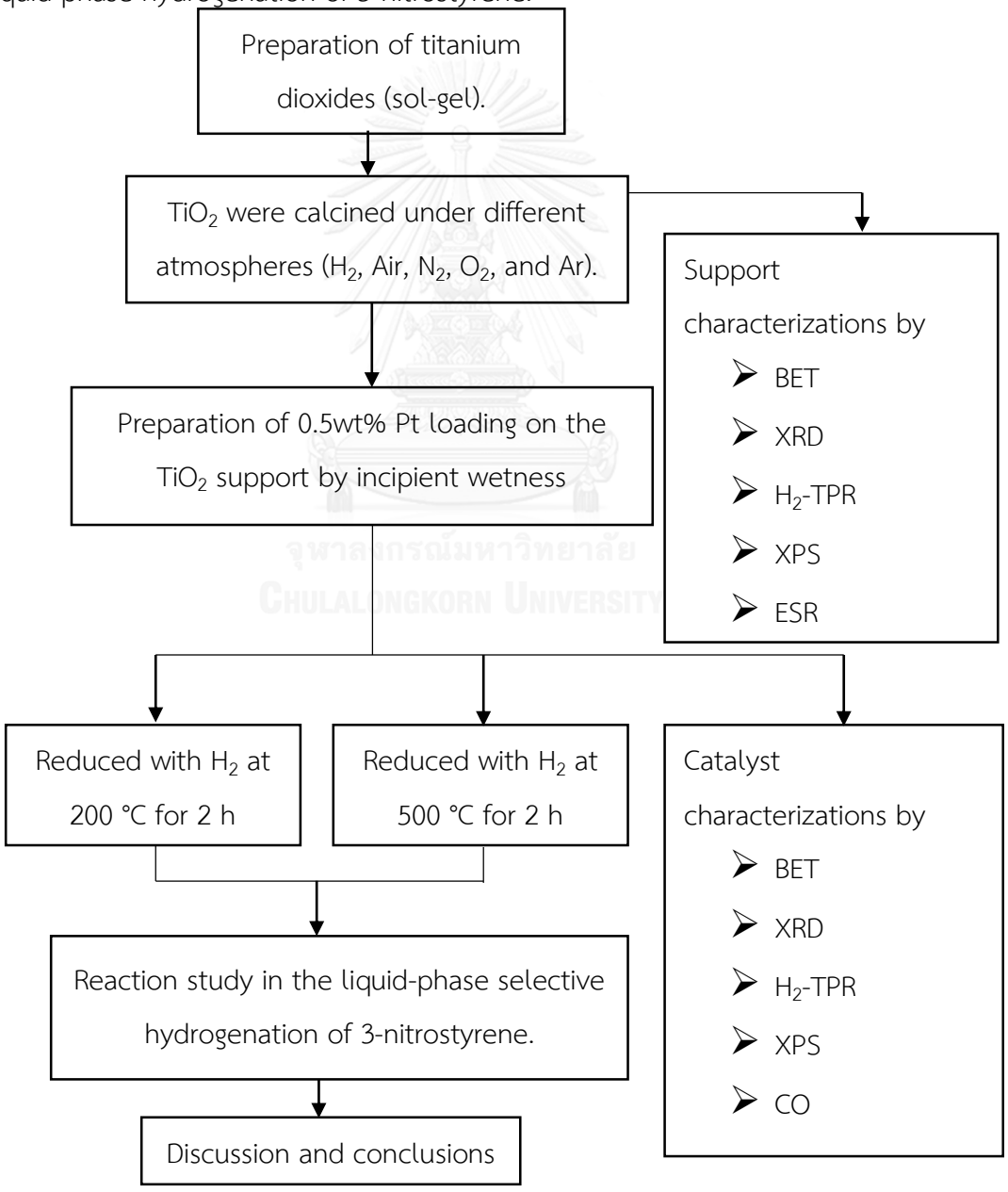

Part II Study the Pt/TiO_2 catalysts prepared by strong electrostatic adsorption method of Pt on the selected sol-gel TiO_2 and compare to those prepared by the incipient wetness impregnation method in the liquid-phase hydrogenation of 3-nitrostyrene.

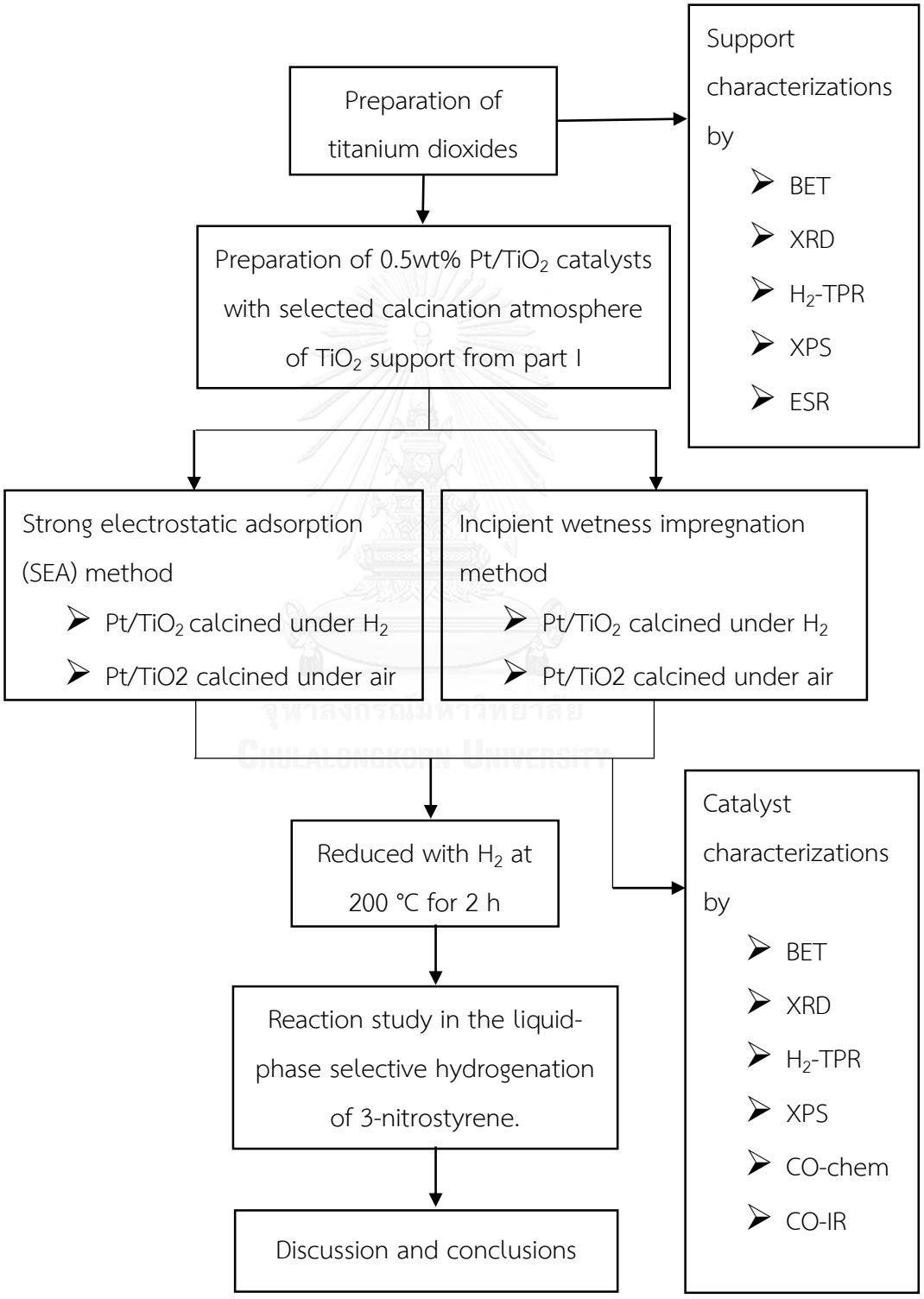

CHARPTER V
RESULTS AND DISCUSSION

In this chapter, the investigation of the physiochemical and catalytic properties over the Pt/TiO_2 prepared by strong electrostatic adsorption and incipient wetness impregnation are discussed. The results and discussion are divided into two parts. In the first part, the effects of calcination atmospheres of the sol-gel TiO_2 on the physiochemical and catalytic properties of Pt/TiO_2 catalysts and influence of reduction temperature in the liquid-phase hydrogenation of 3-nitrostyrene were investigated. The titanium dioxide particles were analyzed by XRD, BET surface areas, ESR, and XPS. The characteristics and catalytic properties of Pt (0.5wt% Pt) prepared by the incipient wetness impregnation method in the selective hydrogenation of 3-nitrostyrene were analyzed by XRD, N_2-physisorption, H_2-temperature programmed reduction (H_2-TPR), infrared spectroscopy of adsorbed CO (CO-IR) and CO-pulses chemisorption. In the second part, the Pt/TiO_2 catalysts prepared by strong electrostatic adsorption method on the selected sol-gel TiO_2 were investigated and compare to those prepared by the incipient wetness impregnation method in the liquid-phase hydrogenation of 3-nitrostyrene. The characterization of the catalyst samples include XRD, ICP, CO chemisorption and H_2-TPR.

Part I

The effects of calcination atmospheres of the sol-gel TiO_2 on the catalytic properties of Pt/TiO_2 catalysts prepared by incipient wetness impregnation and the influence of reduction temperature in the liquid-phase hydrogenation of 3-nitrostyrene.

5.1 The characteristics and properties of a sol-gel TiO_2 calcined under H_2, air and Ar atmosphere.

In this section, the nanocrystalline TiO_2 supports were prepared by the sol-gel method and calcined at 350 ℃ under different atmospheres including reducing, air, and inert atmosphere (H_2, Air and Ar) for 2 h. The properties of the TiO_2 supports were investigated by X-ray diffraction (XRD), BET surface areas, Hydrogen temperature program reduction (H_2-TPR), electron spin resonance (ESR), and X-ray photoelectron spectroscopy (XPS).

5.1.1 X-ray diffraction (XRD)

The sol-gel method is an easy method for preparation of nanosized TiO_2 but the powder obtained is amorphous in nature and further heat treatment is required for crystallization. The XRD patterns of TiO_2 supports prepared by sol-gel method and calcined at different atmospheres are shown in Figure 5.1. The measurements were carried out at the diffraction angles (2θ) between 20° and 80°. From the XRD results, all the TiO_2 synthesized samples exhibited anatase phase TiO_2 at 2θ degrees 25° (major), 37°, 48°, 55°, 56°, 62°, 71° and 75° and the small peak at 30.81° corresponded to brookite phase TiO_2. The average crystallite sizes of anatase phase TiO_2 supports calcined under different atmosphere were calculated by the Scherrer's equation from the full width at half maximum of the XRD peak at 2θ = 25°. The average crystallite size of the anatase phase TiO_2 calcined under H_2, air and Ar atmospheres was similar about 7-8 nm as shown in Table 5.1. According to Riyapan, S. et al. [18] the TiO_2

supports calcined under H_2 and air were similar in structural properties. From the XRD results, it is suggested that the calcination atmosphere of sol-gel TiO_2 supports did not have any influence on the average crystallite size and exhibited similar phase composition.

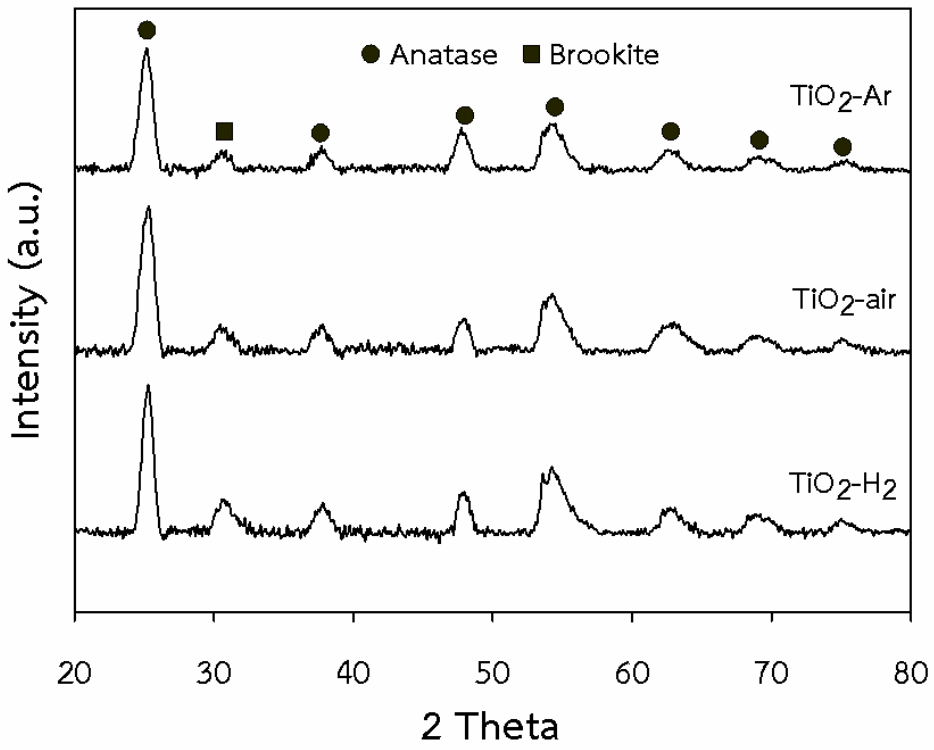

Figure 5.1 The XRD patterns of TiO_2 calcined under H_2, air and Ar atmosphere.

5.1.2 N_2-physisorption

The BET surface area, pore volume, and pore diameter of the sol-gel TiO_2 calcined under different atmospheres are shown in Table 5.1. The pore structures were determined from the Barret-Joyner-Halenda (BJH) desorption metod. The BET surface areas of all the TiO_2 supports were not different ranging between 139-159 m^2/g with pore volume about of 0.3 cm^3/g and average pore diameter about of 4.9 nm. The physisorption isotherms of TiO_2-H_2, TiO_2-air and TiO_2-Ar supports are shown in Figure.5.2 All the TiO_2 supports exhibited type-IV physisorption isotherm with hysteresis loop, corresponding the characteristic of mesoporous materials with pore diameters between 2 and 50 nm. The shape characteristic of hysteresis loop for all TiO_2 supports

as calcined under different atmosphere were type H1, which describes a narrow distribution of relatively uniform pores. It is clearly observed that the titania supports prepared by sol-gel method and calcined under different atmosphere had a uniform pore size distribution in a very narrow range. Thus, the calcination atmosphere did not have any influence on the structural properties of the sol-gel TiO_2. Similar results have been reported by Wu et al. [21] There were no significant differences in the average crystallite size and specific surface area of the TiO_2 synthesized by a sol-gel process and calcined under different atmosphere (H_2(3% in N_2), Ar, Air, N_2 and vacuum).

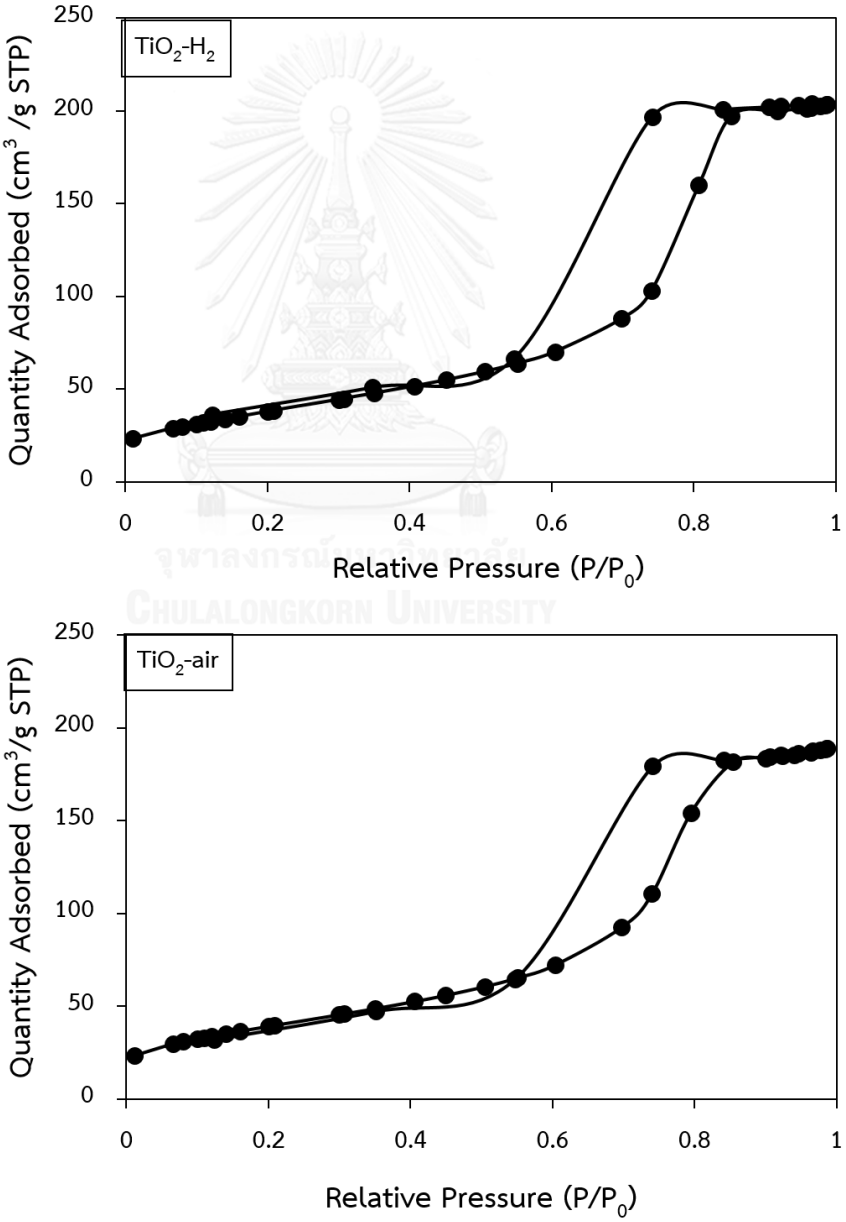

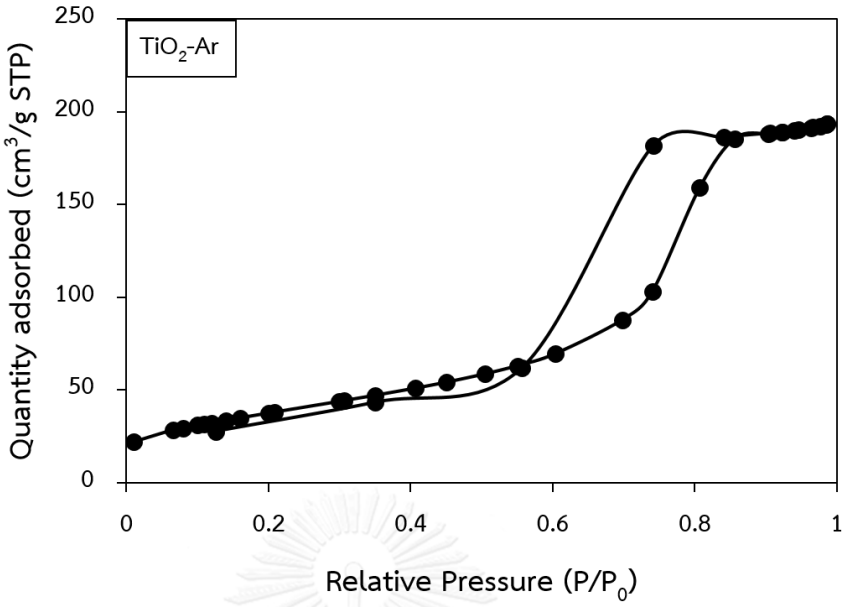

Figure 5.2 N_2 adsorption isotherm of TiO_2 supports calcined under H_2, air and Ar atmosphere

Table 5.1 Physical properties of the TiO_2

Catalysts	Crystallite size[a] of anatase TiO_2 (nm)	BET surface area (m^2/g)	Pore volume[b] (cm^3/g)	Pore diameter[b] (nm)
TiO_2-H_2	7.9	139	0.32	4.92
TiO_2-Air	7.5	159	0.30	4.74
TiO_2-Ar	7.8	134	0.28	4.95

[a] Base on the XRD results.

[b] Determined from the Barret-Joyner-Halenda (BJH) desorption method.

5.1.3 H_2-TPR

The H_2-TPR measurements were carried out to study the reduction behaviors of the TiO_2 supports calcined under different atmosphere of sol-gel TiO_2 and the results are shown in Figure 5.3. All the prepared TiO_2 supports showed only one reduction peak at above 500 °C attributing to the reduction of surface capping oxygen of TiO_2 [1]. The TPR profiles of all TiO_2 supports exhibited similar peak position.

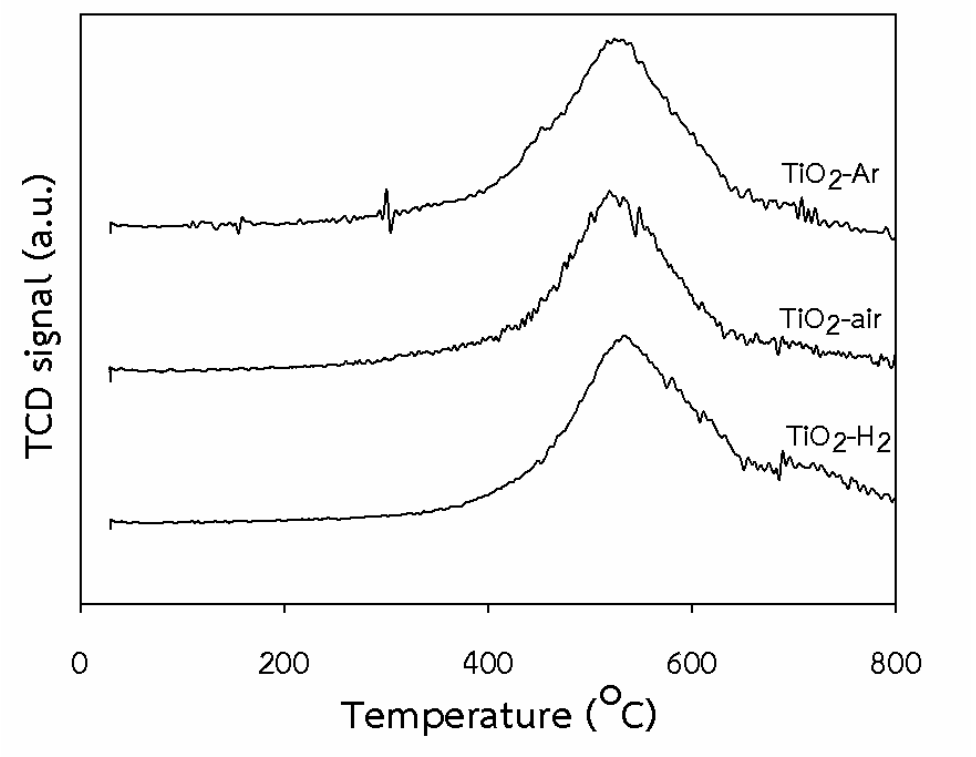

.

Figure 5.3 H_2-TPR profiles of the TiO_2 supports calcined under H_2 air and Ar atmosphere

5.1.4 X-ray photoelectron spectroscopy (XPS)

XPS is the technique to determine the elemental composition of the catalyst sample at surface and electronic states. The deconvolution of O1s XPS peak are shown in Figure 5.4, there are three peaks of XPS spectra observed in TiO_2 support calcined under difference atmospheres. The peaks located at 530.3, 532.2 and 533.9 were assigned to the lattice oxygen, surface hydroxyl groups and adsorbed oxygen mainly from adsorbed water molecules, respectively [55]. The binding energies of Ti 2p in TiO_2 for Ti^{4+} were located at 458.9 and 464.8 eV, which were assigned to Ti^{4+} $2p_{3/2}$ and Ti^{4+} $2p_{1/2}$, respectively [22]. The XPS spectra peaks for Ti 2p of the TiO_2 supports are presented in Figure 5.5. The TiO_2-Ar showed binding energies of Ti at 458.9 eV for Ti $2p_{3/2}$, attributing to Ti^{4+}, while TiO_2-H_2 and TiO_2-air exhibited the XPS shifting to the lower BE. The TiO_2 catalyst calcined under Ar and air showed higher Ti binding energy than the calcined under H_2, vacuum and N_2 according to Wu, N.L. et al. [21]. They indicated that a non-oxidizing atmosphere such as N_2 vacuum and H_2, resulted in Ti

ions of lower valences, likely Ti^{3+}. In this work, it is believed that the sol-gel TiO_2 calcined under H_2 atmosphere proceed more Ti^{3+} on the surface of TiO_2 support. The investigation of defect on TiO_2 from ESR spectra are presented in the next section.

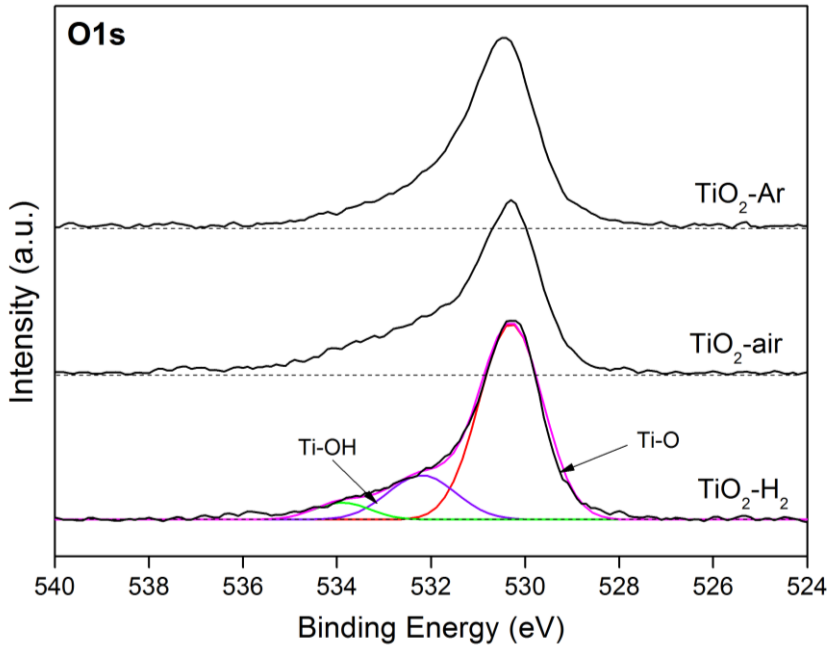

Figure 5.4 XPS spectra of O1s of TiO_2 supports.

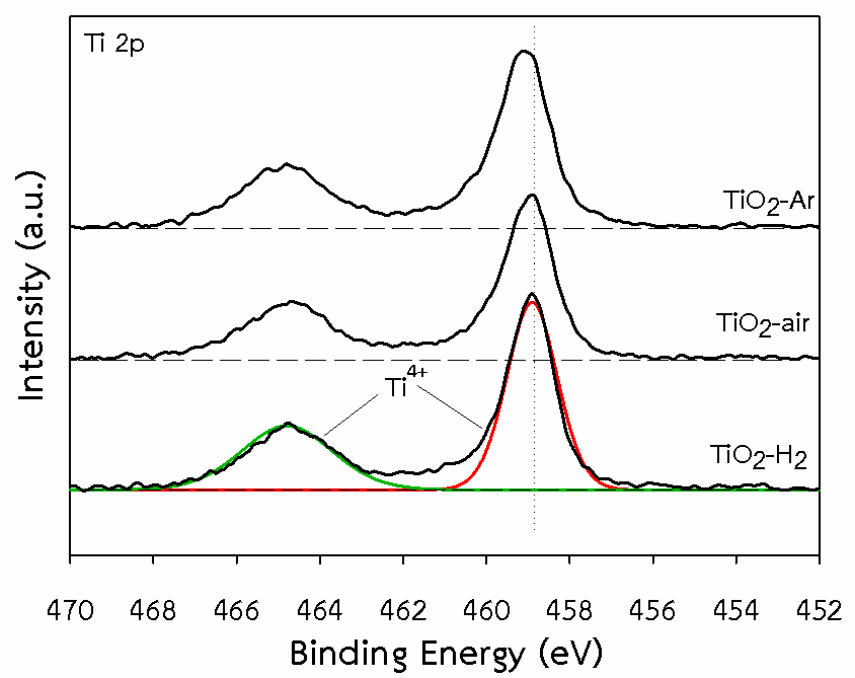

Figure 5.5 XPS spectra of Ti 2p of TiO_2 supports.

5.1.5 Electron Spin Resonance (ESR)

Electron spin resonance is a highly sensitive technique for studying chemical species having one or more unpaired electrons. In this work, ESR technique was used determined the defective site of TiO_2. Nakaoka et al. [56] and Hirakawa et al. [57] reported the g values of the ESR signals occurring on the TiO_2 powders. There are six signals of ESR spectra: i) $Ti^{4+}O^{-}Ti^{4+}OH^{-}$, ii) surface Ti^{3+}, iii) adsorbed oxygen (O^{2-}), iv) $Ti^{4+}O^{2-}$ $Ti^{4+}O^{2-}$, v) inner Ti^{3+}, and vi) adsorbed water. The ESR spectra of the sol-gel TiO_2 supports calcined under different atmosphere are shown in Figure 5.6 and two signal were also obtained on TiO_2 with board peak and asymmetry may be overlap. Corresponding to Strunk, J. [58], all the ESR spectra of the partially reoxidized sample showed a second paramagnetic signal centered around g=2.010 apart from the paramagnetic Ti^{3+} signal. It is possible that some of components might overlap with Ti^{3+} signal. It was found that the sol-gel TiO_2 calcined under H_2 and air exhibited signal at the g value of 1.997, which can be attributed to surface Ti^{3+} [59, 60]. The Ti^{3+} species are produced by trapping of electrons at defective sites of TiO_2 and the amount of accumulated electrons may therefore reflect the number of defective sites [61]. Another signal at g= 2.012, corresponded to oxygen vacancy. The signals between 1.998 and 2.012 are ascribed to the electrons trapped by oxygen vacancy on the TiO_2 surface [62]. Pan, X. [63] shows that all the defects identified in TiO_2, oxygen vacancy is one of the most importance and is supposed to be the prevalent defect in many metal oxides. The formation of oxygen vacancy in TiO_2 leads to the creation of unpaired electrons or Ti^{3+} centers. Suriye, K. et al [20] reported that dispersion of cobalt increased with the amount of surface defect (Ti^{3+}) present in titania support as used for preparation Co/TiO_2 catalysts. Xiong, L. [64] show that the dominant defects in TiO_2 surfaces are Ti^{3+} defects and oxygen vacancies and defects in TiO_2 plays a significant role in enhancing the dispersion and stability of supported metal via the strong interaction between defect site and metal cluster. The TiO2–Ar founded only signal assigned to oxygen vacancies.

The intensity of the ESR spectra also indicated the amount of defects on the sol-gel TiO_2. It was found that the intensity of ESR signal of TiO_2-H_2 was stronger than the TiO_2-air and TiO_2-Ar, indicating the amount of defects on the surface of TiO_2 increased when calcined under H_2 atmosphere. It was in good agreement with the XPS results. Thus, it demonstrates that the formation of defect on TiO_2 can be favoured by sol-gel TiO_2 when calcined under H_2 atmosphere. The amounts of Ti^{3+} defects increase with increasing crystallite size of TiO_2 as prepared by solvothermal method [60]. In this work, all the prepared TiO_2 supports possessed similar average crystallite size and BET surface area. According to the presence of defects on the surface of TiO_2 as shown by the XPS and ESR results, it is demonstrated that calcination atmosphere for preparation of sol-gel TiO_2 at mild temperature led to the creation of defect on the TiO_2 without phase transformation.

Liu, H. et al. [65], reported that the oxygen vacancy and Ti^{3+} species generated during the H_2 treatment appears as defects in the TiO_2 structure and it seems that oxygen vacancies and Ti^{3+} may be present in the modified TiO_2. The peaks with a g factor of 1.955 and 2.002 were assigned to Ti^{3+} and oxygen vacancies, respectively when the H_2 treatment was lower than 400 °C. When the H_2 temperature was further increased, the oxygen vacancy reached a saturated status and the electrons in the oxygen vacancies were transferred out to form Ti^{3+}. If the H_2 treatment occurred at low temperature, oxygen vacancies was deduced alone. The ESR results showed that during the hydrogen treatment, oxygen vacancies was first produced and Ti^{3+} was then generated.

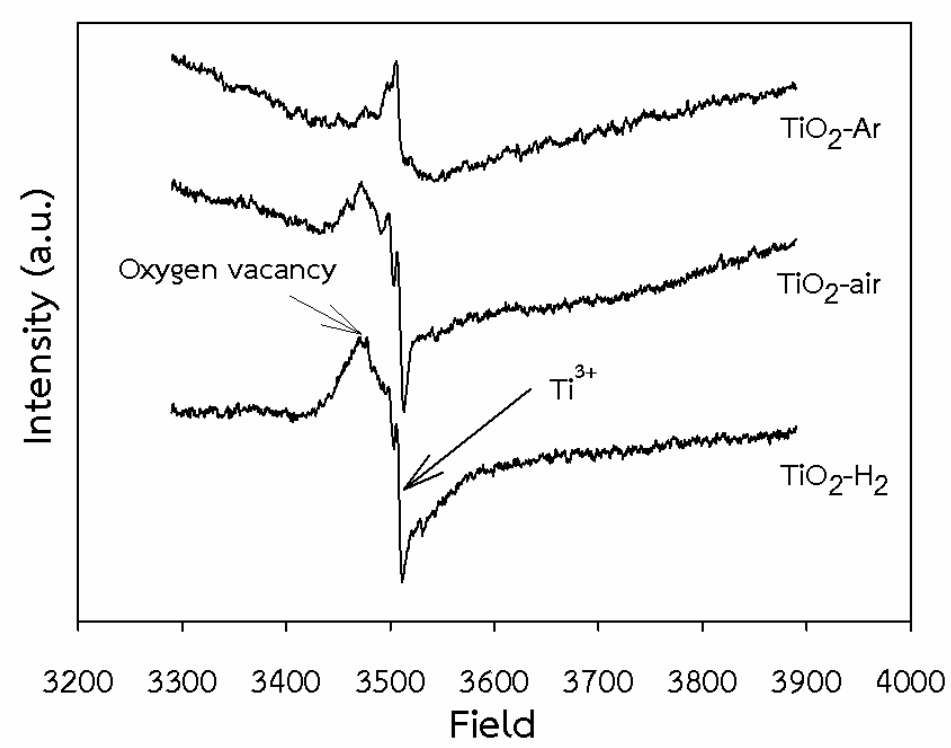

Figure 5.6 The ESR results of TiO_2 calcined under H_2, air and Ar atmosphere at 350 °C

5.2 Properties of 0.5%Pt/TiO_2 catalysts prepared by incipient wetness impregnation method.

In this section, the sol-gel TiO_2 calcined under H_2, air and Ar were employed as the supports for preparation of 0.5%Pt/TiO_2 catalysts by incipient wetness impregnation method and studied in the selective hydrogenation of 3-NS. The properties of Pt/TiO_2 catalysts were investigated by XRD, BET surface areas, H_2-TPR, CO-IR, TEM and CO-chemisorption.

5.2.1 XRD

The XRD patterns of 0.5%Pt/TiO_2 catalysts prepared by incipient wetness impregnation are shown in Figure 5.7. The measurements were carried out at the diffraction angles (2θ) between 20° and 80°. From the XRD results, all the Pt/TiO_2 synthesized samples exhibited anatase phase TiO_2 at 2θ degrees 25° (major), 37°, 48°, 55°, 56°, 62°, 71° and 75° and the small peak at 30.81° corresponded to brookite phase TiO_2. After Pt loading, there were no changes in crystalline phase of TiO_2 for all the catalysts. No sharp peaks for Pt can be observed in all the XRD patterns after platinum loading due to the low metal loading and/or Pt nanoparticles were highly dispersed on TiO_2 supports. The average crystallite sizes of TiO_2 after Pt loading were calculated by the Scherrer's equation from the full width at half maximum of the XRD peak at 2θ = 25°. There were no change of the average crystallite size of TiO_2 upon Pt loading. The crystallite size was maintained at about 7-8 nm as shown in Table 5.2

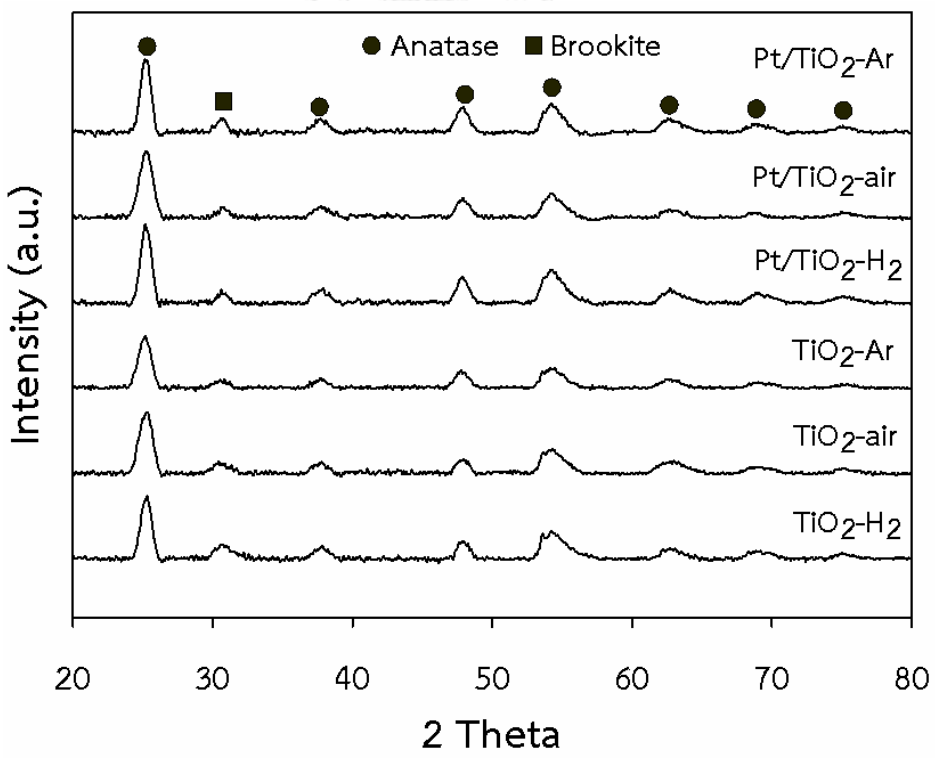

Figure 5.7 The XRD patterns of Pt/TiO_2 catalysts.

5.2.2 N_2-Physisorption

The BET surface area, pore volume, and pore diameter of the Pt/TiO_2 catalysts prepared by incipient wetness impregnation method and calcined at 400 °C are shown in Table 5.2. The BET surface areas of all the Pt/TiO_2 catalysts were ranging 129-143 m^2/g and average pore diameter about of 4.9 nm were obtained. There were no changes of the average pore diameter of TiO_2 upon Pt loading. However, the BET surface areas and pore volume of TiO_2 after Pt loading slightly decreased due to pore blockages.

Table 5.2 Physical properties of the Pt/TiO_2 catalysts.

Catalysts	Crystallite size[a] of anatase TiO_2 (nm)	BET surface area (m^2/g)	Pore volume[b] (cm^3/g)	Pore diameter[b] (nm)
TiO_2-H_2	7.9	139	0.32	4.92
TiO_2-Air	7.5	159	0.30	4.74
TiO_2-Ar	7.8	134	0.28	4.95
Pt/TiO_2-H_2	8.1	129	0.31	5.21
Pt/TiO_2-Air	7.9	143	0.30	4.95
Pt/TiO_2-Ar	8.1	137	0.30	5.03

[a] Base on the XRD results.

[b] Determined from the Barret-Joyner-Halenda (BJH) desorption method.

5.2.3 Hydrogen Temperature program reduction (H_2-TPR)

The H_2-TPR measurements were carried out to study the reduction behaviors of the Pt/TiO_2 catalysts under different atmosphere of sol-gel TiO_2 and the results are shown in Fig 5.8. All the prepared TiO_2 supported Pt showed three reduction peaks. The first peak at around 95 °C was associated to the reduction of PtO_x crystallites to metallic Pt [66, 67]. The reduction of Pt oxide on the Pt/TiO_2-H_2 and Pt/TiO_2-air occurred at slightly lower temperature compared to the Pt/TiO_2-Ar, corresponding to a higher dispersion of Pt on the support surface. In the literature, decomposition of Pd hydride on the TiO_2- N_2 occurred at lower temperature than TiO_2-O_2, resulting higher

dispersion of Pd dispersion [43]. The reduction peak of Pt oxide on the Pt/TiO_2-Ar showed larger peak area than over the Pt/TiO_2-air and Pt/TiO_2-H_2, indicating the agglomeration of Pt oxide or lower Pt dispersion. The second peak appeared as a larger peak from 250 °C to 500 °C, which can be attributed to the reduction of Pt species interacting with the TiO_2 support to form Pt-TiO_x interface sites and the hydrogen consumption above 500 °C was due to the reduction of surface capping oxygen of TiO_2 [1, 67]. The TPR profiles of all catalysts exhibited similar peak position. Some reported that the Pt/TiO_2 catalyst, the supported metallic Pt can catalyse molecular H_2 dissociation and induce spillover of H atoms from the metal to the oxide support, hence lower the reduction temperature of support [68]. However, in this work, hydrogen spillover behavior was not observed.

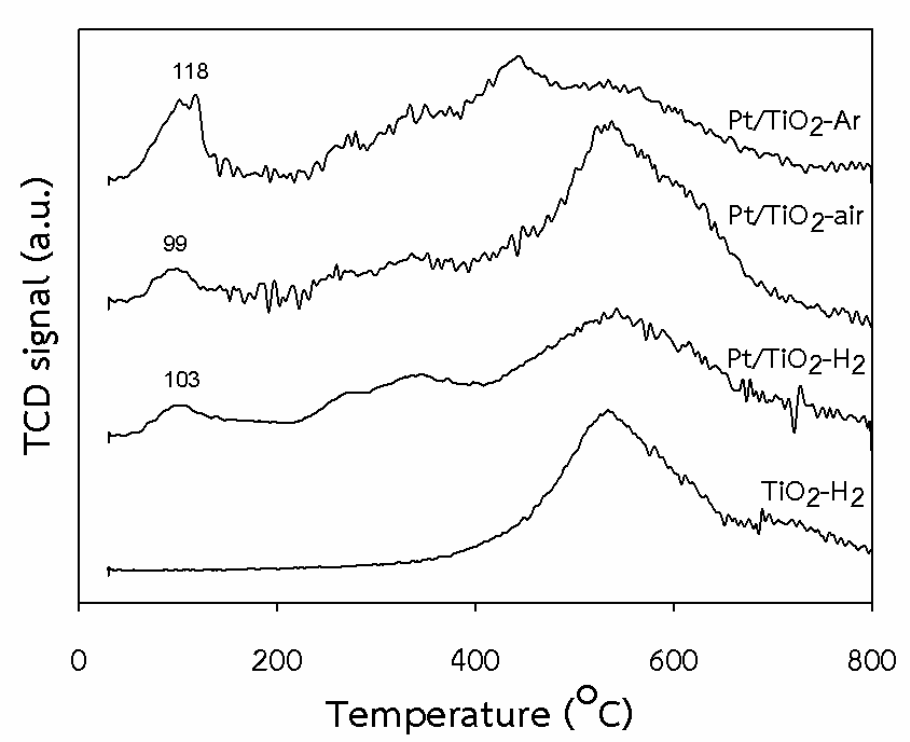

Figure 5.8 The H_2 –TPR profiles of Pt/TiO_2 catalysts.

5.2.4 Transmission electron microscopy (TEM)

The TEM images of 0.5wt%Pt/TiO_2 catalysts are shown in Figure 5.9. All the catalyst particles showed spherical shape. The average particle size determined from the TEM images was about 8 nm, which was consistent to that calculated from the XRD results. It is indicated that the TiO_2 obtained from both methods was single crystalline. From TEM images, Pt/PtO metal were not distinguishable from TiO_2 supports probably due to low metal loading.

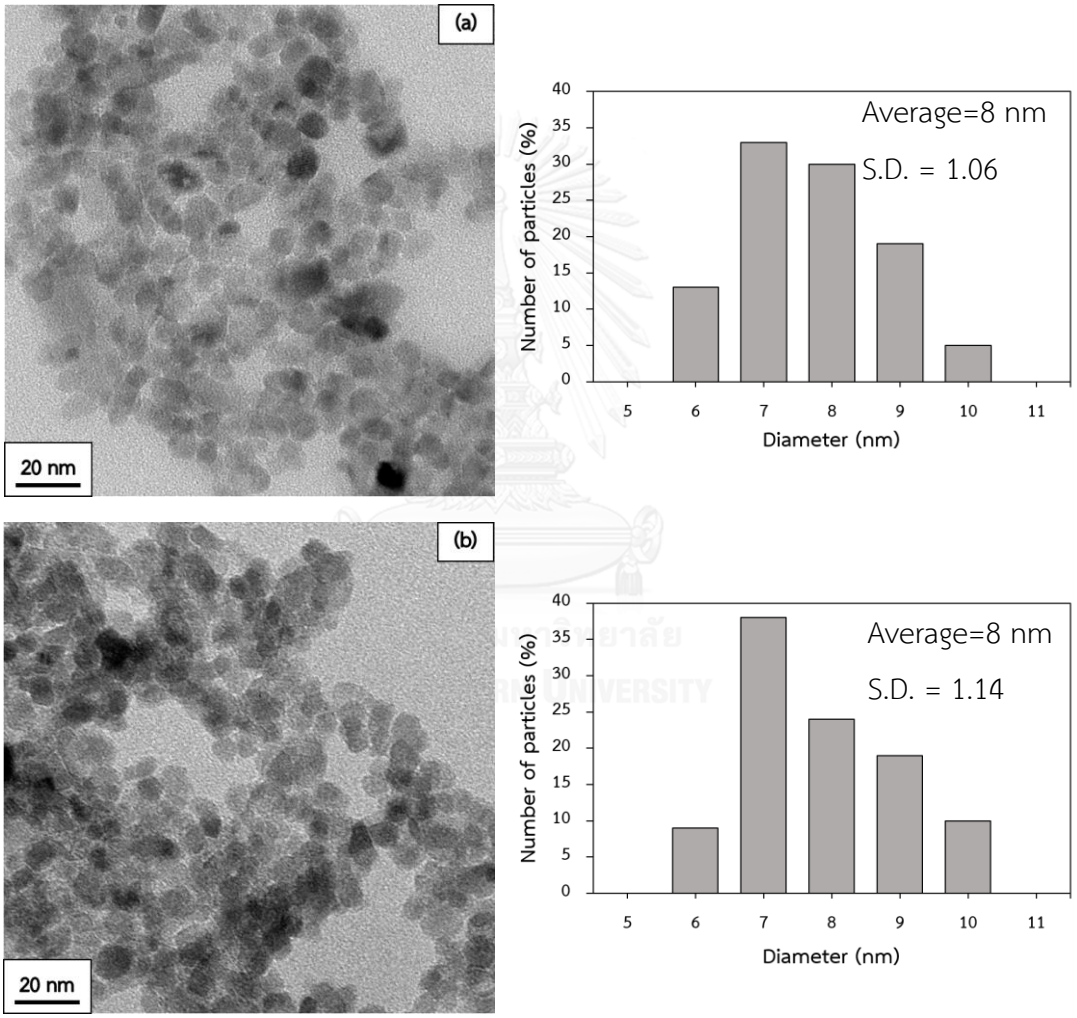

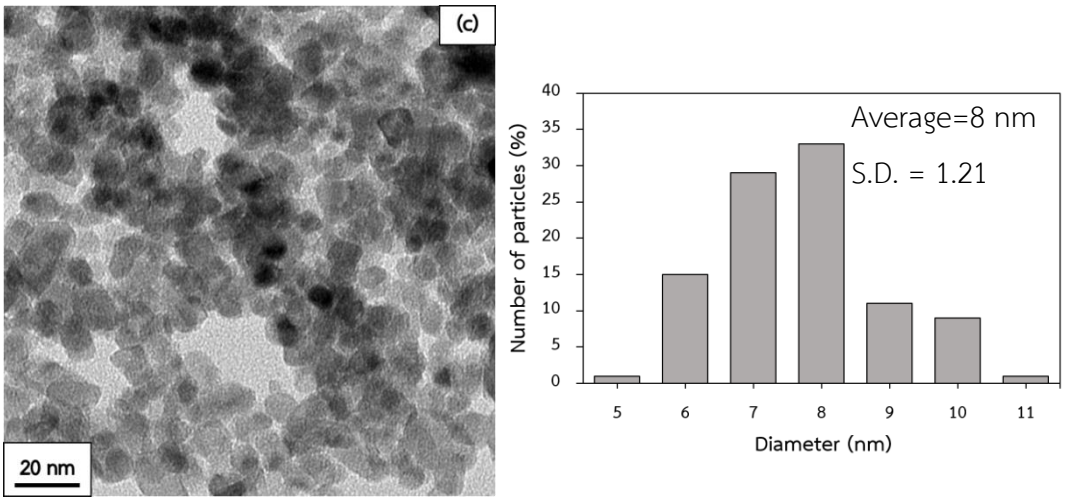

Figure 5.9 TEM images and size distribution of a) Pt/TiO_2-H_2 b) Pt/TiO_2-air c) Pt/TiO_2-Ar

5.2.5 Infrared spectroscopy of adsorbed CO (CO-IR)

Figure 5.10 illustrates FT-IR spectra of adsorbed CO on the Pt/TiO_2 catalysts prepared with different calcination atmospheres of the sol-gel TiO_2 supports. The IR spectrum of adsorbed CO shows bands in the range of frequency of 2200-1800 cm^{-1}.The adsorption band at around 2000-2100 cm^{-1} was assigned to a linear type of CO adsorption [69] while IR bands in the 1825 cm^{-1} corresponded to bridged-type adsorbed CO. It was reported that bridge-type adsorbed CO formed on large Pt particles, while linear-type adsorbed CO form on small Pt particles [1]. The high-frequency band at 2070-2100 cm^{-1} was assigned to the adsorption of CO adsorbed on highly coordinate Pt surfaces like Pt (111) terraces and Pt (100) while that lower frequencies at 2000-2066 cm^{-1} was on low coordinated Pt sites like kink, edge and corner [32]. Yoshida, H. et al. [32] reported that low coordinated Pt sites are more active for the hydrogenation of nitro group of NS in to VA. In this work, the adsorption band at 2065 cm^{-1}, which corresponded to the CO adsorbed of Pt on edge site and this band was asymmetry toward the lower wave number side, suggesting the presence of another band around 2035 cm^{-1},which assigned to CO adsorbed on corner and/or kink sites [15]. The Pt/TiO_2-H_2 caused the increase in the relative quantity of low-coordinated Pt sites on edge and corner while the peaks became very small for the

Pt/TiO_2-air and Pt/TiO_2-Ar, corresponding to the CO-chemisorption results that the Pt/TiO_2-air and Pt/TiO_2-Ar exhibited much lower Pt active sites than the Pt/TiO_2-H_2. It is effective for the formation of a large of low coordinate Pt sites on the surface of dispersed Pt particles. The hydrogenation of NS on Pt/TiO_2 catalyst is a structure-sensitive reaction and low coordinated Pt sited are more active for the hydrogenation of nitro group than vinyl group [32]. The linear adsorbed CO stretch bands on theTiO_2-supported metallic Pt catalyst were reported at frequencies vary between 2050 and 2090 cm^{-1}, which depend on catalyst dispersion and charge transfer in the neighborhood of Pt adsorption sites [70]. In this work, Pt supported on TiO_2 which TiO_2 supports calcined under different atmosphere had different degrees of Pt dispersion. The adsorption band of Pt/TiO_2-H_2, Pt/TiO_2-air and Pt/TiO_2-Ar appeared at 2070, 2065 and 2062 cm^{-1}, respectively. Yoshida, H. et al [32] reported that the larger fraction of low coordinated Pt sites existed on the surface of smaller TiO_2 crystallites which promoted the electron donation from Ti to Pt particles. The larger fraction of less coordinated Pt site exist on the surface of TiO_2-H_2, which promotes the electron donation from the Ti to Pt particles. It is confirmed by the FT-IR results of CO adsorption that the adsorption band of the CO adsorbed on Pt was red-shifted to more extent in the TiO_2-H_2.

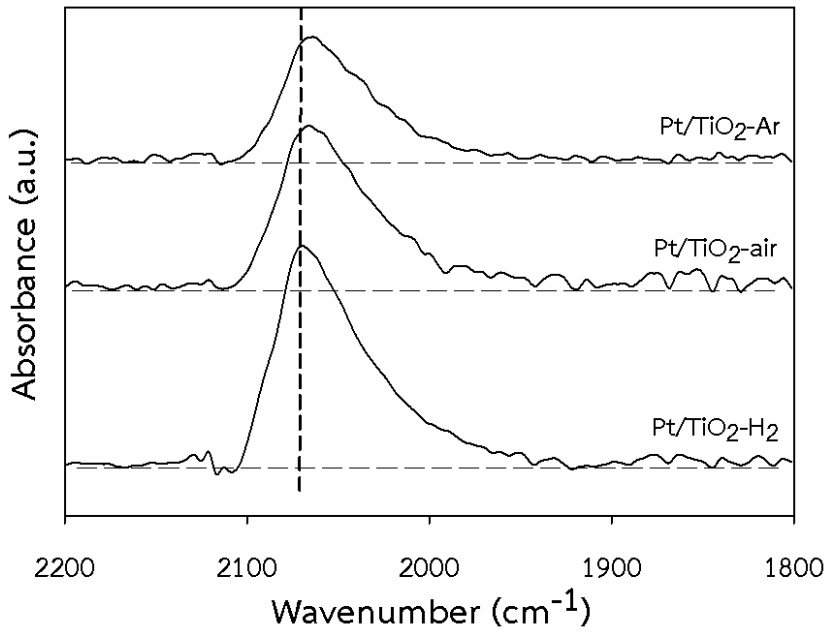

Figure 5.10 CO-IR spectra of 0.5%Pt/TiO_2 catalysts.

5.2.6 CO-pulses chemisorption

The relative amount of Pt active sites on the catalyst samples were usually calculated from the chemisorption results based on the assumption that one CO molecule adsorbed on one Pt site. The amounts of CO chemisorption on Pt/TiO_2 catalysts reduced at 200 °C and 500 °C are shown in Table 5.3. The Pt dispersion reduced at 200 °C and 500 °C on TiO_2-H_2 were 57% and 36%, respectively, while those of Pt/TiO_2-air were 29% and 25%, respectively. The Pt/TiO_2-Ar exhibited the lowest Pt dispersion between 27 and 20%, respectively. It was found that Pt dispersion on TiO_2-H_2 was much higher than those supported on TiO_2-Air and TiO_2-Ar. Comparing between the two reduction temperature used, the Pt/TiO_2 catalysts reduced at 200 °C showed higher Pt dispersion than catalysts reduced at 500 °C. The higher Pd dispersion and the stronger metal–support interaction were correlated with the presence of surface Ti^{3+}, leading to improved catalyst performance [43]. Suriye, K. et al [20] reported that dispersion of cobalt increased with the amount of surface defect (Ti^{3+}) present in titania support as used for preparation Co/TiO_2 catalysts. The presence of surface Ti^{3+} on the TiO_2 support prepared by sol-gel method gives the higher Pd dispersion [18]. Thus, the Pt supported on the TiO_2 containing higher amount of defect, exhibited higher Pt dispersion. In our results, the effect of the calcination atmosphere used during preparation of the sol-gel TiO_2 supports had influence on the amount defective sites on the TiO_2 surface, and as a consequence affected the dispersion of Pt on TiO_2 surface.

Table 5.3 CO chemisorption and reaction results of the 0.5%Pt/TiO_2 catalyst

Catalyst	Red.T (°C)	CO chemisorption (molecule CO x 10^{18}/g cat.)	Pt dispersion (%)	Time (min)	Conversion (%)	Selectivity (%)		
						VA	EA	ENB
Pt/TiO_2-H_2	200	8.8	57	20	76	92.1	4.9	3.0
				80	100	90.8	8.8	0.4
	500	5.6	36	20	38	70.8	5.2	24.0
				80	52	74.6	9.7	15.7
Pt/TiO_2-air	200	4.5	29	20	29	77.9	5.0	17.1
				80	100	92.8	6.9	0.3
	500	3.9	25	20	21	81.0	4.0	15.0
				80	60	73.8	9.7	16.5
Pt/TiO_2-Ar	200	4.2	27	20	27	75.5	4.6	19.8
				80	100	90.4	9.4	0.2
	500	3.1	20	20	12	72.0	4.9	23.1
				80	52	71.4	7.7	20.9

Reaction (3.6 mmol NS in 10 ml ethanol) at 40 °C with a 20 mg catalyst under 20 bar

5.3 Reaction study in the liquid phase selective hydrogenation of 3-nitrostyrene

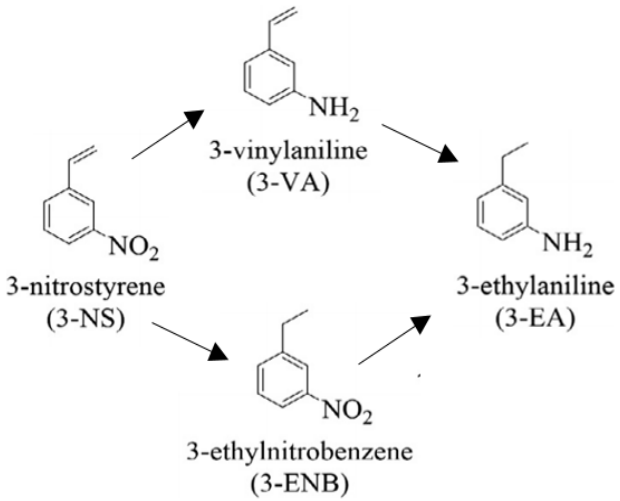

Figure 5.11 Simplified reaction scheme of the hydrogenation of 3-NS.

As shown in Figure 5.11, NS hydrogenation is quite a complex reaction, which has two main reaction pathways occurring from hydrogenation of a C=C double bond and a nitro group [2]. The reaction involves a nitro group reduction towards 3-VA, which can be further transformed to the undesired 3- ethylaniline (3-EA) and 3-ethylnitrobenzene (3-ENB) which can be further converted to 3-EA [49]. The catalytic performance of 0.5%Pt catalysts supported on sol-gel derived TiO_2 calcined under different atmospheres were investigated in the selective hydrogenation of NS under the following reaction conditions: 40 °C, 2 MPa of H_2. The catalytic behaviors of the Pt/TiO_2 catalysts prepared with different calcination atmospheres of TiO_2 supports including NS conversion and product selectivity are summarized in Table 5.3. The main hydrogenation products were ENB and VA. The desired product is VA without formation of intermediates hydrogenation products. It was found that a proper selection of the catalysts by system of small Pt crystallites on TiO_2 support could improve the catalytic performance with avoiding the formation of hydroxylamine intermediates. For any reduction temperature, the Pt/TiO_2-H_2 catalysts exhibited much higher catalytic activity than the Pt/TiO_2-air and Pt/TiO_2-Ar catalysts, which could be attributed to the higher Pt dispersion. The catalytic activity was dropped when Pt supported

on sol-gel TiO_2 support calcined under Ar atmosphere due to the low dispersion of Pt as supported by the co-chemisorption. Combining the results of the reaction of the reaction study and those of the FT-IR measurement. It was found that the higher selectivity of Pt/TiO_2-H_2 for VA formation resulted from the larger relative quantity of low coordinated Pt sites on edge, corner and kink sites. Ichiro, S. et al. [15] reported that the hydrogenation of the nitro group would preferentially proceed on low coordinated Pt sites while the vinyl group would occur on the terrace sites. The catalytic activity in the selective hydrogenation of 3-NS related with availability of Pt surface atoms in Pt dispersion but VA selectivity depend on the number of Pt-TiOx interface sites [1]. At low reduction temperature, all Pt/TiO_2 catalysts had slightly higher VA selectivity. The Pt/TiO_2-H_2 showed the highest VA selectivity among the catalysts studied at around 90 % at 76 % conversion comparing at high reduction temperature. The high reduction temperature at 500 °C decreased both the conversion of 3-NS and VA selectivity on Pt/TiO_2-H_2 due to Pt metal sintering led to migration over the catalyst surface. Increasing of the activation temperature (T_A=573-773K) results in nanoparticles (NPs) of bigger sizes, thus, decrease of VA selectivity with T_A=473 to 573 K can be attributed to a NP size effect [49]. It was reported that bridge-type adsorbed CO formed on large Pt particles, while linear-type CO adsorbed on low coordinate form on small Pt particles and Yoshida, H.et al [32] reported that low coordinated Pt sites are more active for the hydrogenation of nitro group of NS in to VA. In this work, it is suggested that all the Pt/TiO_2 catalysts reduced at 500 °C promoted the reduction of the C=C double bond so that the ENB selectivity increased comparing to the lower reduction temperature.

The relationship between the NS conversion and the VA selectivity of Pt/TiO_2 catalysts reduced at 200 °C as a function of reaction time over Pt/TiO_2-H_2 and Pt/TiO_2-air catalysts are shown in Figure 5.12. Increasing of reaction time, the conversion of 3-NS increased while the selectivity of 3-VA remained essentially unchanged at approximately 90%, except when the conversion was below 20% for Pt/TiO_2-H_2 and when the conversion was below 40% for Pt/TiO_2-air. It was found that the VA selectivity did not depend on the NS conversion but affected by Pt surface sites.

The Pt/TiO_2-H_2 showed high selectivity at all conversion levels. The Pt/TiO_2-H_2 showed higher conversion of 3-NS than the Pt/TiO_2-air. Complete conversion of NS was obtained within 80 min for both catalysts.

It is known that the TiO_2 and Pt metal exhibits strong metal–support interaction (SMSI) phenomenon due to reduction at high temperatures by the decoration of the metal surface by partially reducible metal oxides or by an electron transfer between the support and the metals. Fujita, S,I. et al [15] reported that strong-metal support interaction (SMSI) between Pt and TiO_2 improved selectivity of VA by partially reduced TiO_2 (TiO_x) decorates Pt metal surface when catalysts were reduced at high temperature but at the expense of activity. In this study, both activity and selectivity of all catalyst increased when low reduction temperature at 200 °C were used. Kang et al. [71] reported that Pd/TiO_2 reduced at 500 °C improved ethylene selectivity when compared to Pd/TiO_2 catalyst reduced at 300 °C, due to the SMSI effect. Riyapan, S. et al [43] showed that the presence of Ti^{3+} promoted SMSI effect and ethylene desorption, thus, high reduction temperature was not necessary for improved catalytic performance. The large crystallite size of solvothermal-derived TiO_2 correlated with the higher amount of Ti^{3+} surface defect, resulting in higher dispersion of cobalt due to strong interaction between Co and TiO_2 [72]. In the present work, the large amount of defect on surface of TiO_2 supports led to increased dispersion of Pt on the TiO_2 supports, which resulted in an improvement of catalysts activity and promoted the reduction of the nitro group so that the VA selectivity increased. High reduction temperature was not necessary for the selective hydrogenation NS to VA over these catalysts.

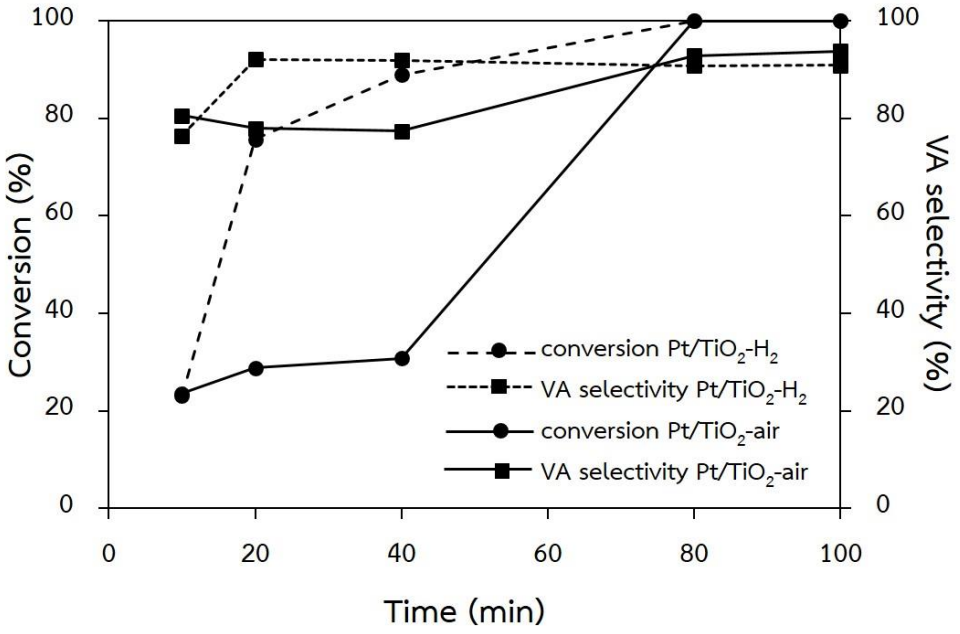

Figure 5.12 NS conversion and VA selectivity of Pt/TiO_2

5.4 The characteristics and properties of a sol-gel TiO_2 calcined under N_2 and O_2 atmosphere.

From the last part, the Pt/TiO_2-air exhibited the lower activity and VA selectivity compared to the Pt/TiO_2-H_2. However, air is composed of N_2 and O_2 so the O_2 and N_2 atmospheres were studied and compared in this section. The nanocrystalline TiO_2 supports were prepared by a sol-gel method and calcined at 350 °C under different atmospheres (N_2 and O_2) for 2 h. The properties of TiO_2 supports were investigated by X-ray diffraction (XRD), BET surface areas, hydrogen temperature program reduction (H_2-TPR), Electron spin resonance (ESR), and X-ray photoelectron spectroscopy (XPS).

5.4.1 X-ray diffraction (XRD)

The XRD patterns of TiO_2 supports prepared by sol-gel method and calcined under N_2 and O_2 atmospheres are shown in Figure 5.13. The XRD peaks were similar to the results in previous part. The average crystallite size of the anatase phase TiO_2 calcined under N_2 and O_2 atmospheres was similar at about 7-8 nm. According to Riyapan, S. et al. [43] showed that the average crystallite size of the TiO_2 calcined

under different atmosphere (N_2 and O_2) was similar at 6 nm. From the XRD results, it can suggests that the calcination atmosphere of sol-gel TiO_2 supports did not have any influence on the average crystallite size and exhibited similar in XRD pattern.

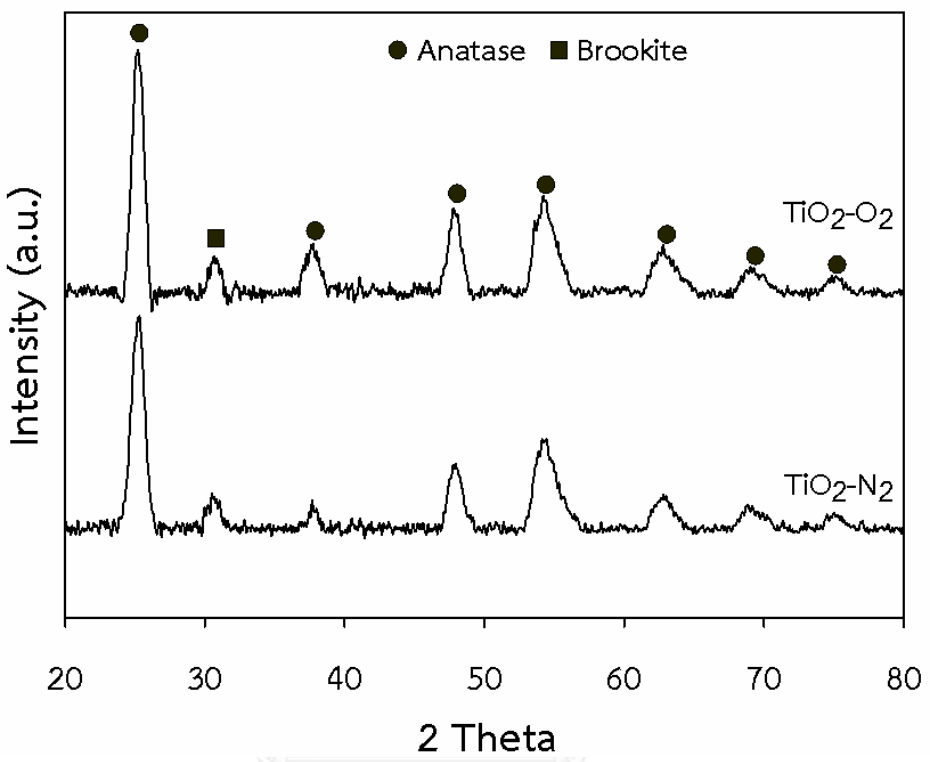

Figure 5.13 The XRD patterns of TiO_2 calcined under N_2 and O_2 atmosphere.

5.4.2 N_2-physisorption

The BET surface area, pore volume, and pore diameter of the sol-gel TiO_2 calcined under N_2 and O_2 atmosphere were shown in Table 5.4. The BET surface areas of the TiO_2 supports calcined under N_2 and O_2 were 138 and 154 m^2/g, pore volume about of 0.3 cm^3/g and average pore diameter about of 4.9 nm. The physisorption isotherms of TiO_2-N_2 and TiO_2-O_2 supports are shown in Figure.5.14. All the TiO_2 supports exhibited type-IV physisorption isotherm with hysteresis loop, corresponding the characteristic of mesoporous materials with pore diameters between 2 and 50 nm. The shape characteristic of hysteresis loop for all TiO_2 supports as calcined under different atmosphere were type H1, which describes a narrow distribution of relatively

uniform pores. Thus, suggest that the calcination atmosphere did not have any influence on the structural properties of the sol-gel TiO_2.

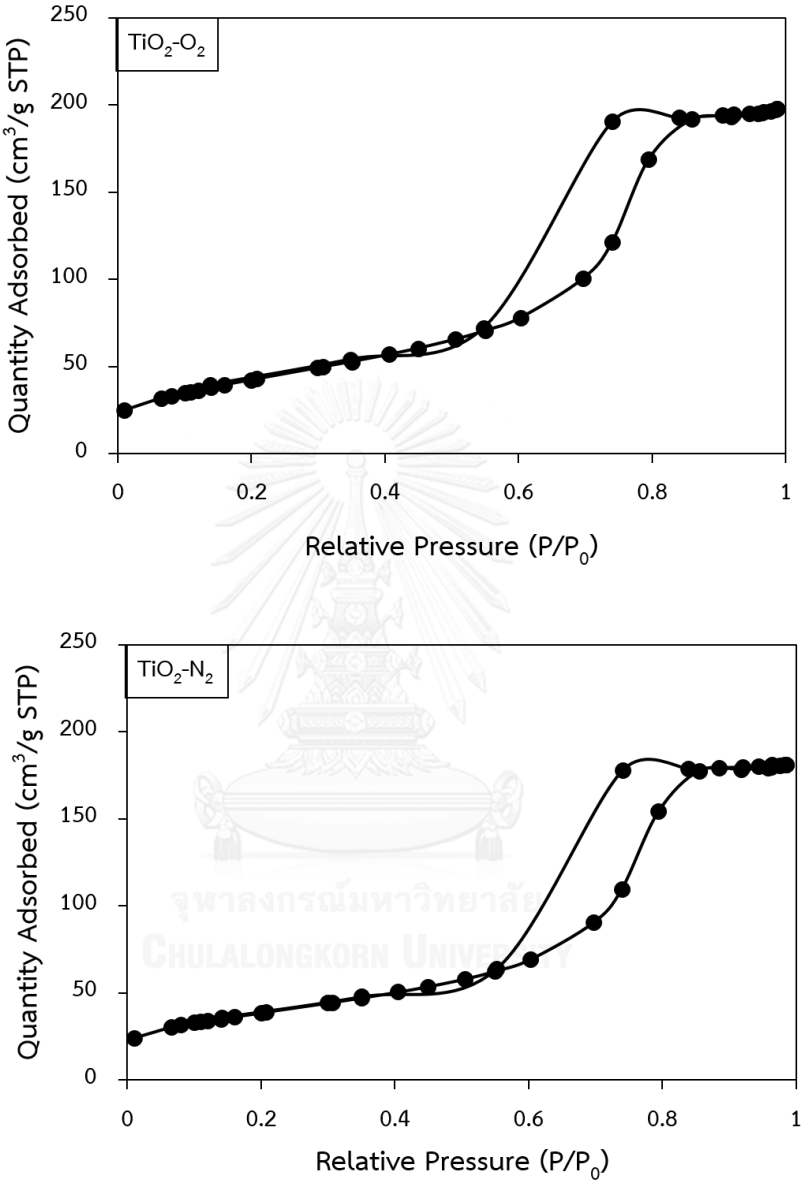

Figure 5.14 N_2 adsorption isotherm of TiO_2 supports calcined under N_2 and O_2 atmosphere

Table 5.4 Physical properties of the TiO_2

Catalysts	Crystallite size[a] of anatase TiO_2 (nm)	BET surface area (m^2/g)	Pore volume[b] (cm^3/g)	Pore diameter[b] (nm)
TiO_2-N_2	7.9	138	0.28	4.96
TiO_2-O_2	7.7	154	0.31	4.92

[a] Base on the XRD results.

[b] Determined from the Barret-Joyner-Halenda (BJH) desorption method.

5.4.3 Hydrogen Temperature program reduction (H_2-TPR)

The H_2-TPR measurements were carried out to study the reduction behaviors of the TiO_2 supports under N_2 and O_2 atmosphere of sol-gel TiO_2 and the results are shown in Figure 5.15. All the prepared TiO_2 supports showed only one reduction peak at above 500 °C attributing to the reduction of surface capping oxygen of TiO_2 [1, 67]. The TPR profiles of all TiO_2 supports exhibited similar peak position.

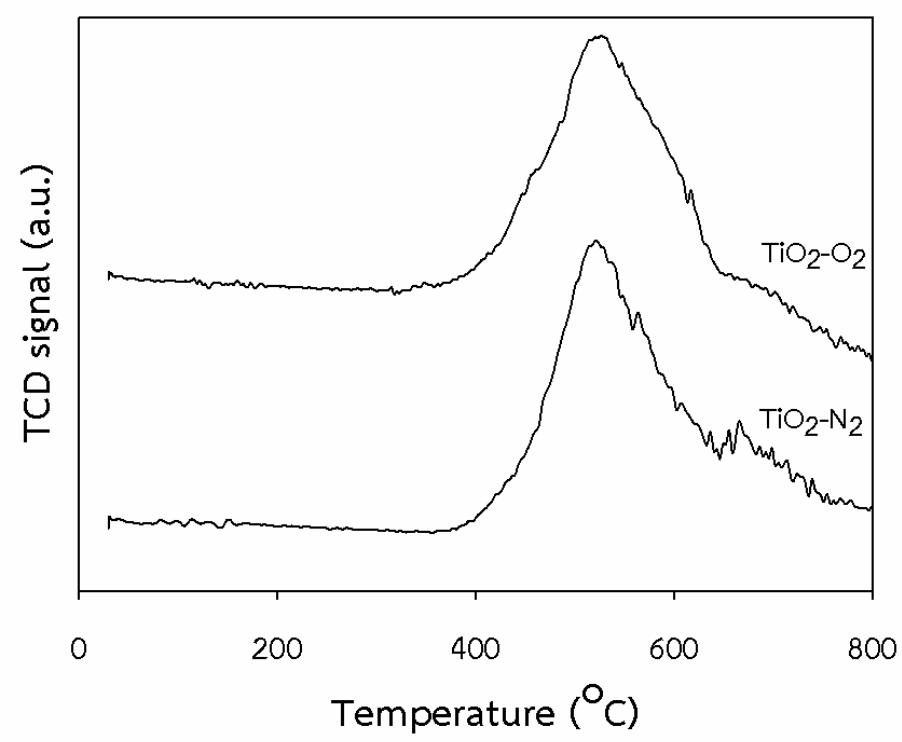

Figure 5.15 H_2-TPR profiles of the TiO_2 supports calcined under N_2 and O_2 atmosphere

5.4.4 X-ray photoelectron spectroscopy (XPS)

The deconvolution of O1s XPS peak are shown in Figure 5.16, there are three peaks of XPS spectra observed in TiO_2 support calcined under N_2 and O_2 atmospheres. The O1s XPS peak were similar to the results in previous part. Figure 5.17, the TiO_2-N_2 and TiO2-O_2 supports showed binding energies of Ti at 458.9 eV for Ti $2p_{3/2}$, attributing to Ti^{4+} [22]. In this work, it is not different in peak composition and did not Ti^{3+} peak in both catalysts, due to small amount of Ti^{3+}.

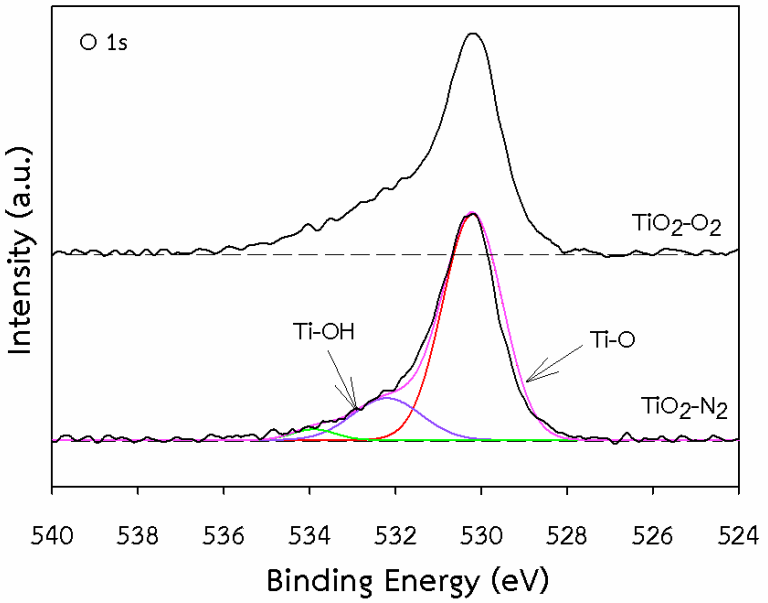

Figure 5.16 XPS spectra of O1s of TiO_2 supports.

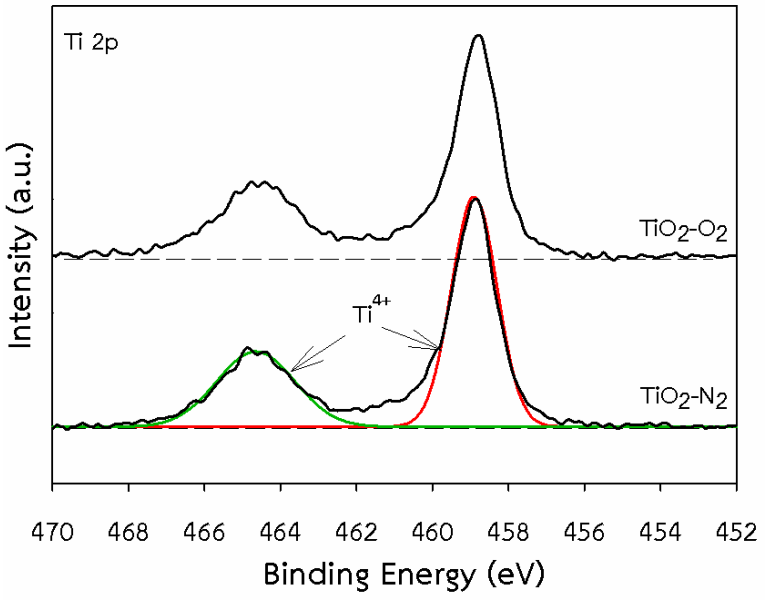

Figure 5.17 XPS spectra of Ti 2p of TiO_2 supportts.

5.4.5 Electron Spin Resonance (ESR)

The ESR spectra of the sol-gel TiO_2 supports calcined under N_2 and O_2 atmosphere are shown in Figure 5.18. It was found that the sol-gel TiO_2 calcined under N_2 exhibited one signal at the g value of 1.997, which can be attributed to surface Ti^{3+} [59, 60]. The Ti^{3+} species are produced by trapping of electrons at defective sites of TiO_2 and the amount of accumulated electrons may therefore reflect the number of defective sites. The TiO_2-O_2 support had a board peak and asymmetry may be overlap between Ti^{3+} and oxygen vacancies, thus, assigned to two signal were also obtained. Corresponding to [58], all ESR spectra of the partially reoxidized sample showed a second paramagnetic signal centered around g=2.010 apart from the paramagnetic Ti^{3+} signal, it is possible that some of components might overlap with Ti^{3+} signal. Zhang, K. et al [62] reported that signals between 1.998 and 2.012 are ascribed to the electrons trapped by oxygen vacancy on the TiO_2 surface. The increased Ti^{3+} amount in oxygen atmosphere did not from the reduction of Ti^{4+} to Ti^{3+} due to low calcination temperature used and absence of hydrogen. They propose that the removal of the surface hydroxyl group when exposed to increase oxygen concentration for the formation of the surface defect [73].

The intensity of the ESR spectra indicates that the amount of defects on the sol-gel TiO_2. The intensity of ESR signal as assigned to Ti^{3+} of TiO_2-N_2 was stronger than the TiO_2-O_2, indicating the amount of Ti^{3+} defects on the surface of TiO_2 increased when calcined under N_2 atmosphere. Thus, it demonstrates that the formation of Ti^{3+} defect on TiO_2 can be favoured by sol-gel TiO_2 which calcined under N_2 atmosphere. In this work, all the prepared TiO_2 supports possessed similar average crystallite size and BET surface area. Thus, the presence of Ti^{3+} defects on the surface of TiO_2 demonstrates that calcination atmosphere for preparation of sol-gel TiO_2 at mild can create defects on the TiO_2 without phase transformation.

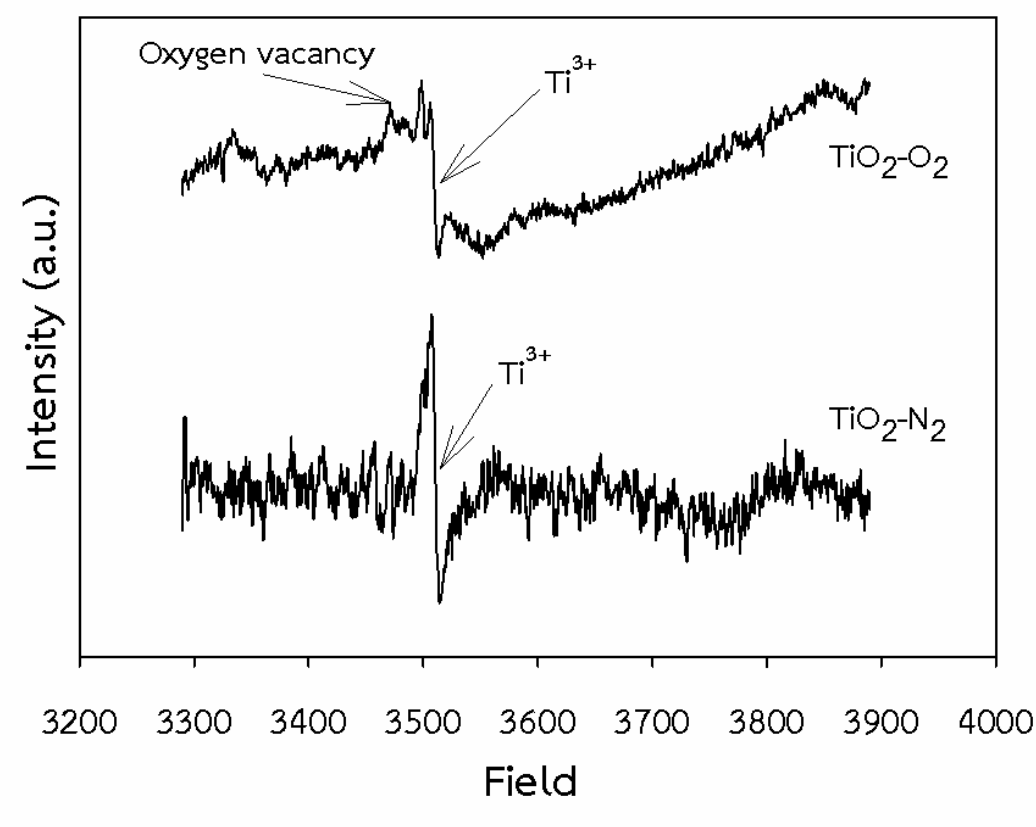

Figure 5.18 The ESR results of TiO_2 calcined under N_2 and O_2 atmosphere at 350 °C

5.5 Properties of 0.5%Pt/TiO_2 catalysts prepared by incipient wetness impregnation method

In this section, the sol-gel TiO_2 calcined under N_2 and O_2 were employed as the supports for preparation of 0.5%Pt/TiO_2 catalysts by incipient wetness impregnation method and studied in the selective hydrogenation of 3-NS. The properties of Pt/TiO_2 catalysts were investigated by X-ray diffraction (XRD), BET surface areas, Hydrogen temperature programmed reduction (H_2-TPR), infrared spectroscopy of adsorbed CO (CO-IR), CO-chemisorption and transmission electron microscopy (TEM).

5.5.1 X-ray diffraction (XRD)

The XRD patterns of 0.5%Pt/TiO_2 supports prepared by incipient wetness impregnation are shown in Figure 5.19. From the XRD results, the XRD peaks were similar to the results in previous part. After Pt loading, there were no changes in crystalline phase of TiO_2 for all the catalysts. No sharp peaks for Pt can be observed in all the XRD patterns after platinum loading due to the low metal loading and/or Pt nanoparticles were highly dispersed on TiO_2 supports. There were no change of the average crystallite size of TiO_2 upon Pt loading. The crystallites size was maintained at about 7-8 nm are shown in Table 5.6.

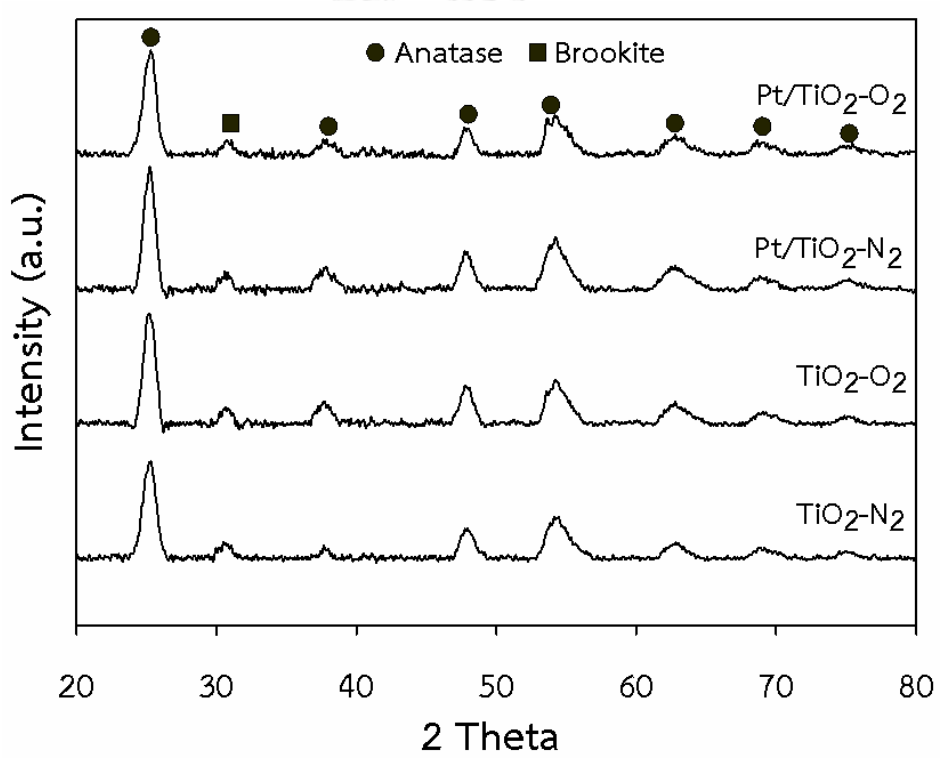

Figure 5.19 The XRD patterns of Pt/TiO_2 catalysts

5.5.2 N_2-Physisorption

The BET surface area, pore volume, and pore diameter of the Pt/TiO_2 catalysts prepared by impregnation method and calcined 400 °C are shown in Table 5.5. The BET surface areas of all the Pt/TiO_2 catalysts were ranging 136-141 m^2/g and average pore diameter about of 4.9 nm were obtained. There were no changes of the average pore diameter of TiO_2 upon Pt loading. However, the BET surface areas and pore volume of TiO_2 after Pt loading slightly decreased due to pore blockages.

Table 5.5 Physical properties of the Pt/TiO_2 catalysts.

Catalysts	Crystallite size[a] of anatase TiO_2 (nm)	BET surface area (m^2/g)	Pore volume[b] (cm^3/g)	Pore diameter[b] (nm)
TiO_2-N_2	7.9	138	0.28	4.96
TiO_2-O_2	7.7	154	0.31	4.92
Pt/TiO_2-N_2	8.0	141	0.30	4.92
Pt/TiO_2-O_2	8.1	136	0.30	4.93

[a] Base on the XRD results.

[b] Determined from the Barret-Joyner-Halenda (BJH) desorption method.

5.5.3 Hydrogen Temperature program reduction (H_2-TPR)

The H_2-TPR measurements were carried out to study the reduction behaviors of the Pt/TiO_2 catalysts under different atmosphere of sol-gel TiO_2 and the results are shown in Figure 5.20. All the prepared TiO_2 supported Pt showed three reduction peaks. The first peak at around 95 °C was associated to the reduction of PtO_x crystallites to metallic Pt [66, 67]. The second peak appeared as a larger peak from 250 °C to 500 °C, which can be attributed to the reduction of Pt species interacting with the TiO_2 support to form Pt-TiO_x interface sites and the hydrogen consumption above 500 °C was due to the reduction of surface capping oxygen of TiO_2 [1, 67]. The TPR profiles of all catalysts exhibited similar peak position.

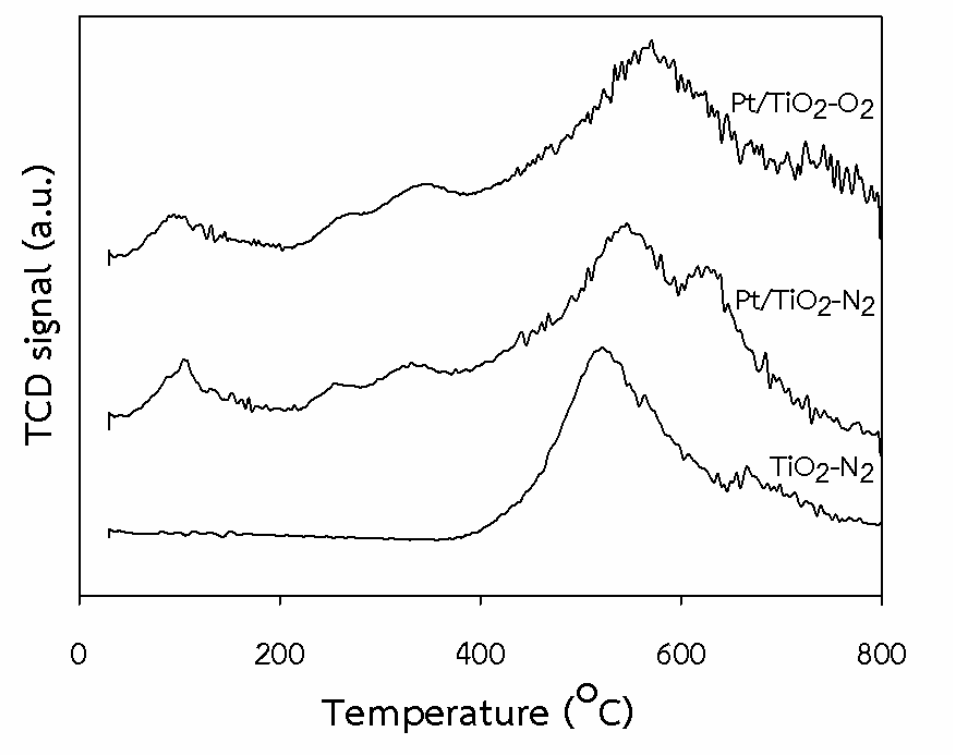

Figure 5.20 The TPR profiles of Pt/TiO_2 catalysts.

5.5.4 Transmission electron microscopy (TEM)

The TEM images of 0.5wt%Pt/TiO_2 catalysts are shown in Figure 5.21. All the catalysts particles showed spherical shape. The average particle size determined from the TEM images was about 7-8 nm, which was consistent to that calculated from the XRD results. From TEM images, Pt/PtO metal were not distinguishable from TiO_2 supports probably due to low metal loading.

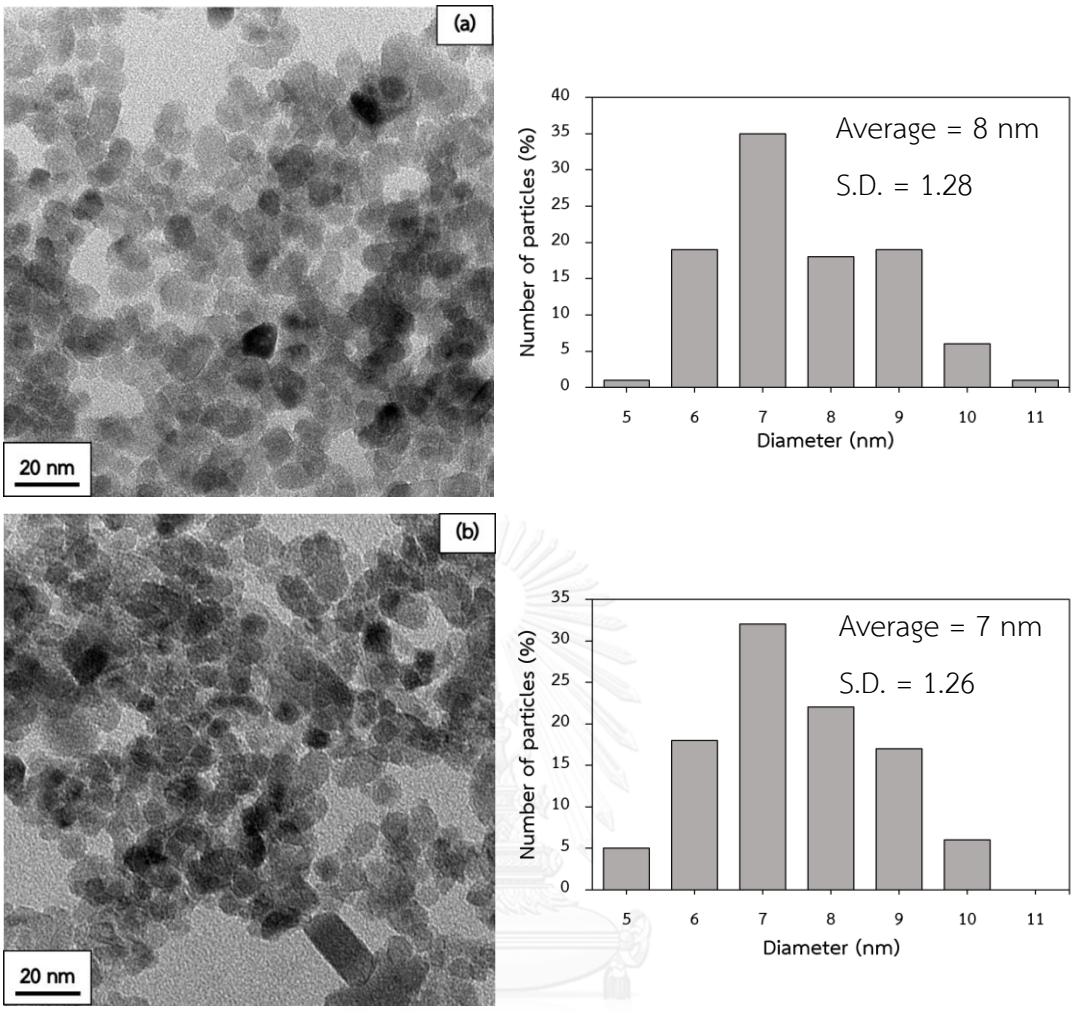

Figure 5.21 TEM images and size distribution of a) Pt/TiO_2-N_2 b) Pt/TiO_2-O_2

5.5.5 Infrared spectroscopy of adsorbed CO (CO-IR)

Figure 5.22 illustrates FT-IR spectra of adsorbed CO on the Pt/TiO_2 catalysts with the sol-gel TiO_2 supports calcined under N_2 and O_2 atmosphere. In this work, the adsorption band at 2065 cm^{-1}, which corresponded to the CO adsorbed of Pt on edge site and this band was asymmetry toward the lower wave number side, suggesting the presence of another band around 2035 cm^{-1},which assigned to CO adsorbed on corner and/or kink sites. The adsorption band were similar to the results in previous part. The Pt/TiO_2-N_2 catalyst caused the same in the relative quantity of low-coordinated Pt sites on edge and corner comparing to the Pt/TiO_2-O_2 catalyst.

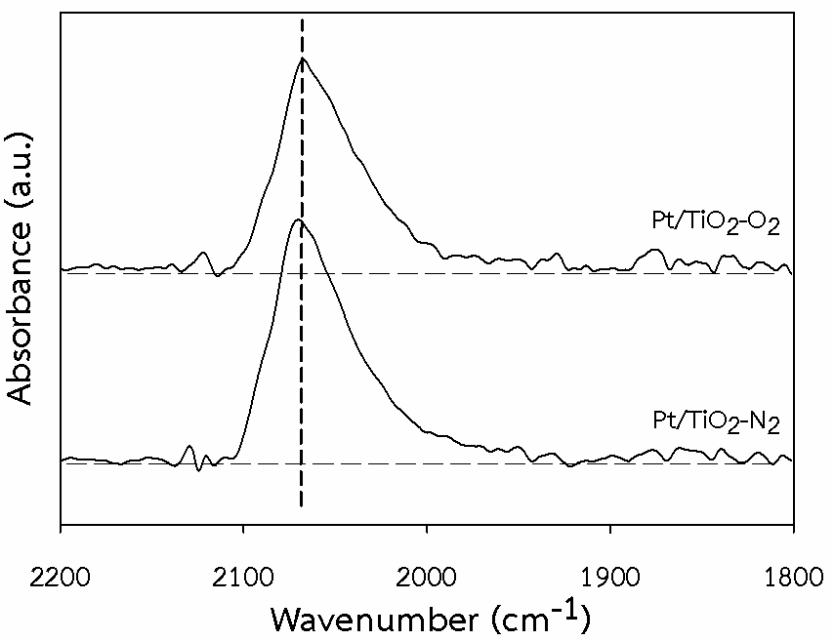

Figure 5.22 CO-IR spectra of 0.5%Pt/TiO_2 catalysts.

5.5.6 CO-pulses chemisorption

The amounts of CO chemisorption on Pt/TiO_2 catalysts reduced at 200 °C and 500 °C are shown in Table 5.6. The Pt dispersion reduced at 200 °C and 500 °C on TiO_2-N_2 were 56% and 44%, respectively, while those of Pt/TiO_2-O_2 were 49% and 39%, respectively. It was found that Pt dispersion on TiO_2-N_2 was higher than those supported on TiO_2-O_2. Comparing between the two reduction temperature used, the Pt/TiO_2 catalysts reduced at 200 °C showed higher Pt dispersion than catalysts reduced at 500 °C. The higher Pd dispersion and the stronger metal–support interaction were correlated with the presence of surface Ti^{3+}, leading to improved catalyst performance [43]. Thus, the Pt supported on the TiO_2 containing higher amount of defect, exhibited higher Pt dispersion. In our results, the effect of the calcination atmosphere used during preparation of the sol-gel TiO_2 supports had influence on the amount defective sites on the TiO_2 surface, and as a consequence affected the dispersion of Pt on TiO_2 surface.

Table 5.6 CO chemisorption and reaction results of the 0.5%Pt/TiO_2 catalysts.

Catalyst	Red.T (°C)	CO chemisorption (molecule CO x 10^{18}/g cat.)	Pt dispersion (%)	Time (min)	Conversion (%)	Selectivity (%)		
						VA	EA	ENB
Pt/TiO_2-N_2	200	8.7	56	20	73	95.5	3.0	1.5
				80	100	92.8	7.1	0.1
	500	6.8	44	20	52	69.0	6.7	24.3
				80	73	89.6	5.6	4.8
Pt/TiO_2-O_2	200	7.5	49	20	67	94.5	3.1	2.4
	500	6.0	39	20	40	87.4	3.6	9.0
				80	77	87.5	7.3	5.2

Reaction (3.6 mmol NS in 10 ml ethanol) at 40 ºC with a 20 mg catalyst under 20 bar

5.6 Reaction study in the liquid phase selective hydrogenation of 3-nitrostyrene

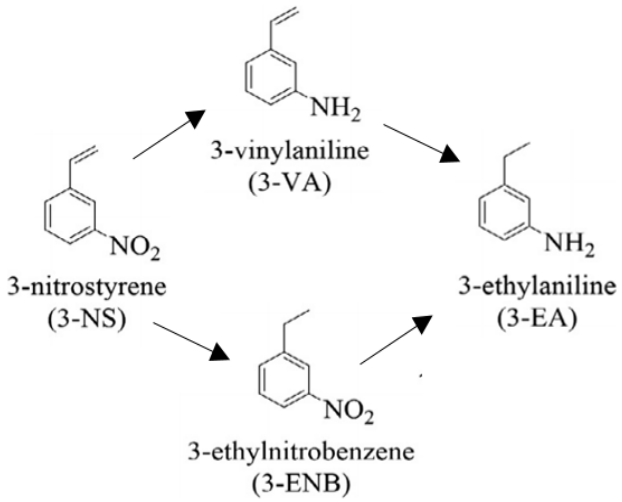

Figure 5.23 Simplified reaction scheme of the hydrogenation of 3-NS.

The catalytic behaviors of the Pt/TiO_2 catalysts at prepared with N_2 and O_2 calcination atmospheres of TiO_2 supports including NS conversion and product selectivity are summarized in Table 5.6. For reduction temperature at 200 °C, the Pt/TiO_2-N_2 catalysts exhibited slightly higher catalytic activity than the Pt/TiO_2-O_2 catalysts, which could be attributed to the higher Pt dispersion. Combining the results of the reaction of the reaction study and those of the FT-IR measurement. It

was found that the selectivity of Pt/TiO_2-N_2 and Pt/TiO_2-O_2 reduced at 200 °C were not different for VA formation corresponding to the same in the relative quantity of low-coordinated Pt sites on edge and corner. Comparing the reduction temperature, the both catalysts did not difference in VA selectivity.

It was known that the TiO_2 and Pt metal exhibited exhibits strong metal–support interaction (SMSI) phenomenon due to reduction at high temperatures by the decoration of the metal surface by partially reducible metal oxides or by an electron transfer between the support and the metals. In this study, both activity and selectivity of all catalyst increased when low reduction temperature at 200 °C were used. In the present work, the large amount of defect on surface of TiO_2 supports led to increased dispersion of Pt on the TiO_2 supports, which resulted in an improvement catalysts activity and promoted the reduction of the nitro group so that the VA selectivity increased. High reduction temperature was not necessary for the selective hydrogenation NS to VA over these catalysts.

PART II

The properties of Pt/TiO_2 catalysts prepared by strong electrostatic adsorption method on the selected sol-gel TiO_2 compared to the incipient wetness impregnation method in the liquid-phase hydrogenation of 3-nitrostyrene.

In this part, the effect of calcination atmosphere of TiO_2 were further investigated under H_2 and air atmosphere and used as the supports for preparation of Pt/TiO_2 catalysts by strong electrostatic adsorption method. The properties of Pt/TiO_2 catalysts were investigated by XRD, H_2-TPR, CO-Chemisorption and TEM.

5.7 Characteristic and catalytic properties of Pt/TiO_2 prepared by strong electrostatic adsorption.

5.7.1 Inductively Coupled Plasma optical emission spectroscopy (ICP)

5.7.1.1 PZC of TiO_2 supports

In this preparation method, the PZC of the TiO_2 supports were first determined. Figure 5.24 and 5.25 displays the pH final which is plotted versus pH initial without metal in the solution at a surface loading of 1000 m^2/L. The point of zero chart (PZCs) of TiO_2-H_2 and TiO_2-air equaled to 5.8 for TiO_2-H_2 and 3.1 for TiO_2-air.

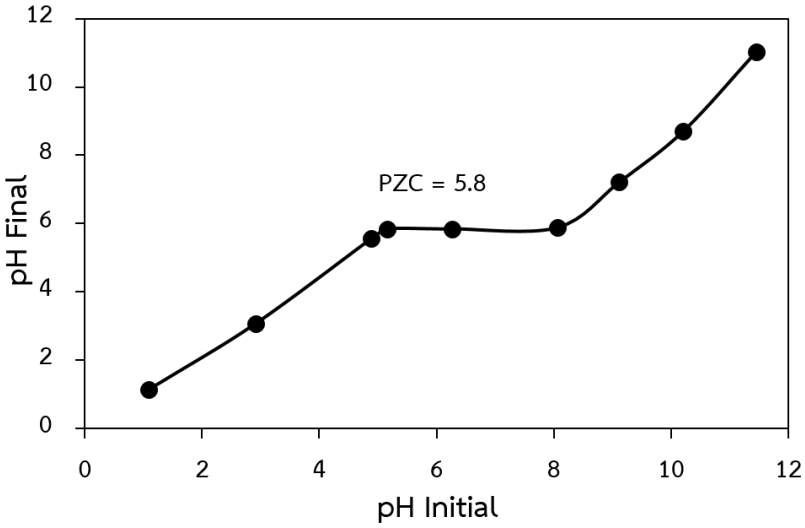

Figure 5.24 The point of zero chart of TiO_2-H_2

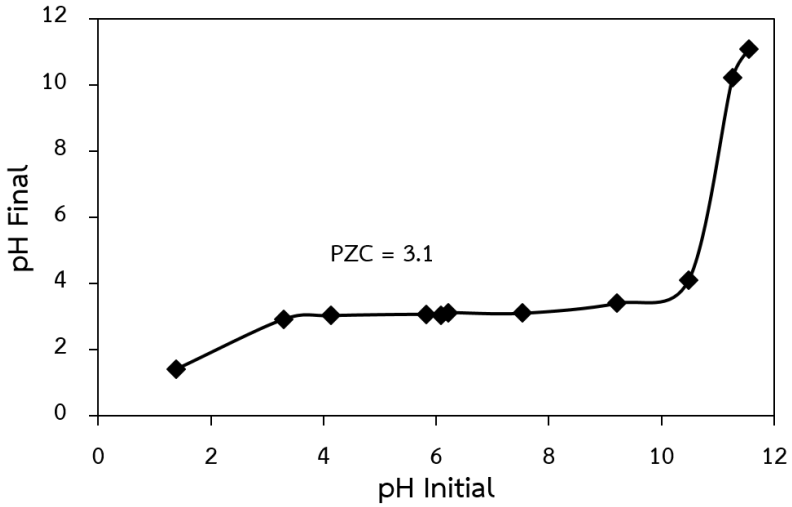

Figure 5.25 The point of zero chart of TiO_2-air

5.7.1.2 Determination of Pt uptakes

The Pt uptake curve was reported as the Pt surface density, defined as the amount of Pt per m^2 of the support versus the final pH of the slurry after 1 h on the rotary shaker. The TiO_2-H_2 and TiO_2-air began to adsorb Pt metal ammine complexes at a pH greater than pH_{PZC} and reached a maximum uptake at a initial pH around 11.6 for both supports. In order to determine the optimal pH condition leading to metal loading around 0.5 wt%, Pt uptake was observed at initial pH around 10.53 for TiO_2-H_2 and around 10.85 for TiO_2-air. The adsorption curve shows the Pt uptake, which corresponds to a Pt loading is defined as the percentage of the Pt mass per the total mass of the catalyst.

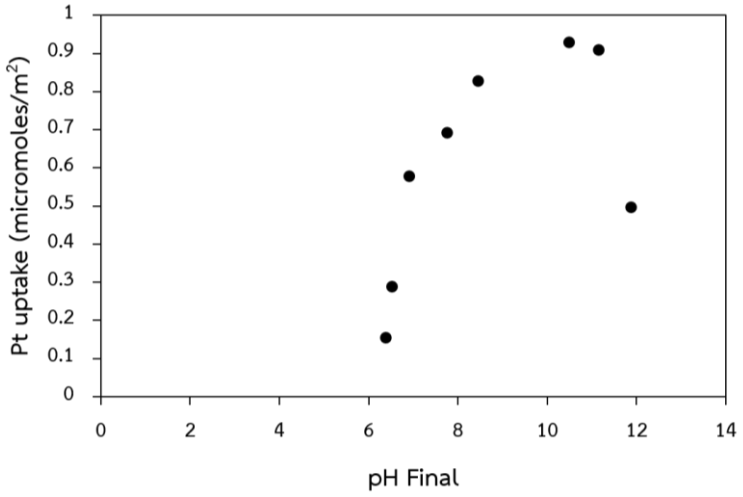

Figure 5.26 The uptake of Pt on TiO_2-H_2 support as a function of pH

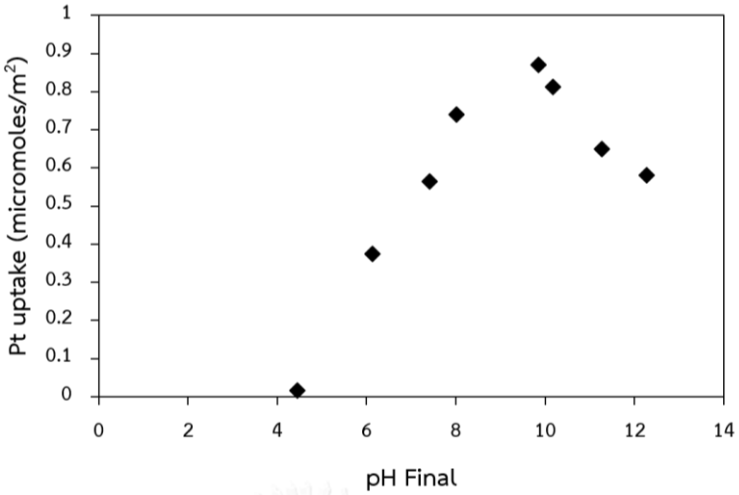

Figure 5.27 The uptake of Pt on TiO_2-air support as a function of pH

5.7.2 X-ray diffraction (XRD)

The XRD patterns of TiO_2 supports and 0.5%Pt/TiO_2 supports prepared by strong electrostatic adsorption method are shown in Figure 5.28. The measurements were carried out at the diffraction angles (2θ) between 20° and 80°. From the XRD results, all the Pt/TiO_2 synthesized samples exhibited anatase phase TiO_2 at 2θ degrees 25° (major), 37°, 48°, 55°, 56°, 62°, 71° and 75° and the small peak at 30.81° corresponded to brookite phase TiO_2. After Pt loading, there were no changes in crystalline phase of TiO_2 for all the catalysts. No sharp peaks for Pt can be observed in all the XRD patterns after platinum loading due to the low metal loading and/or Pt nanoparticles were highly dispersed on TiO_2 supports.

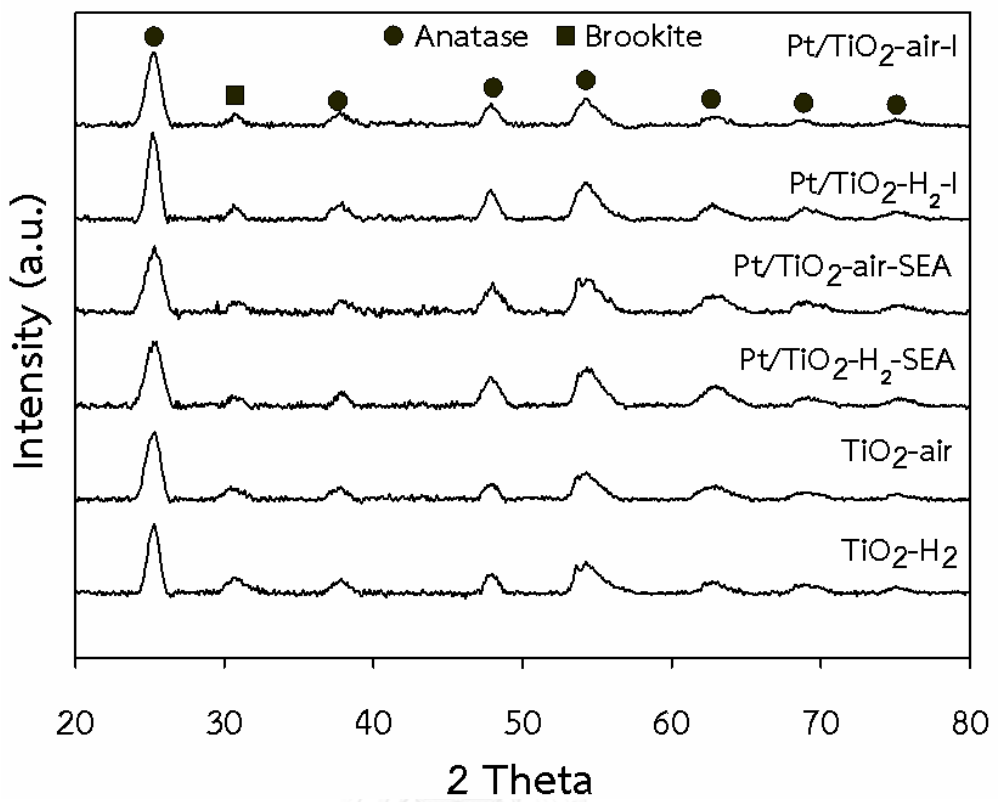

Figure 5.28 The XRD patterns of the TiO_2 supports and Pt/TiO_2 catalysts prepared by strong electrostatic adsorption method.

5.7.3 Transmission Electron Microscopy (TEM)

The TEM images of 0.5wt%Pt/TiO_2 catalysts prepared by strong electrostatic adsorption are shown in Figure 5.29. All the catalysts particles showed spherical shape. From TEM images, Pt/PtO metal were not distinguishable from TiO_2 supports probably due to low metal loading. It was found that SEA method generated small and homogeneous particles resulted in well dispersed particles [25, 53].

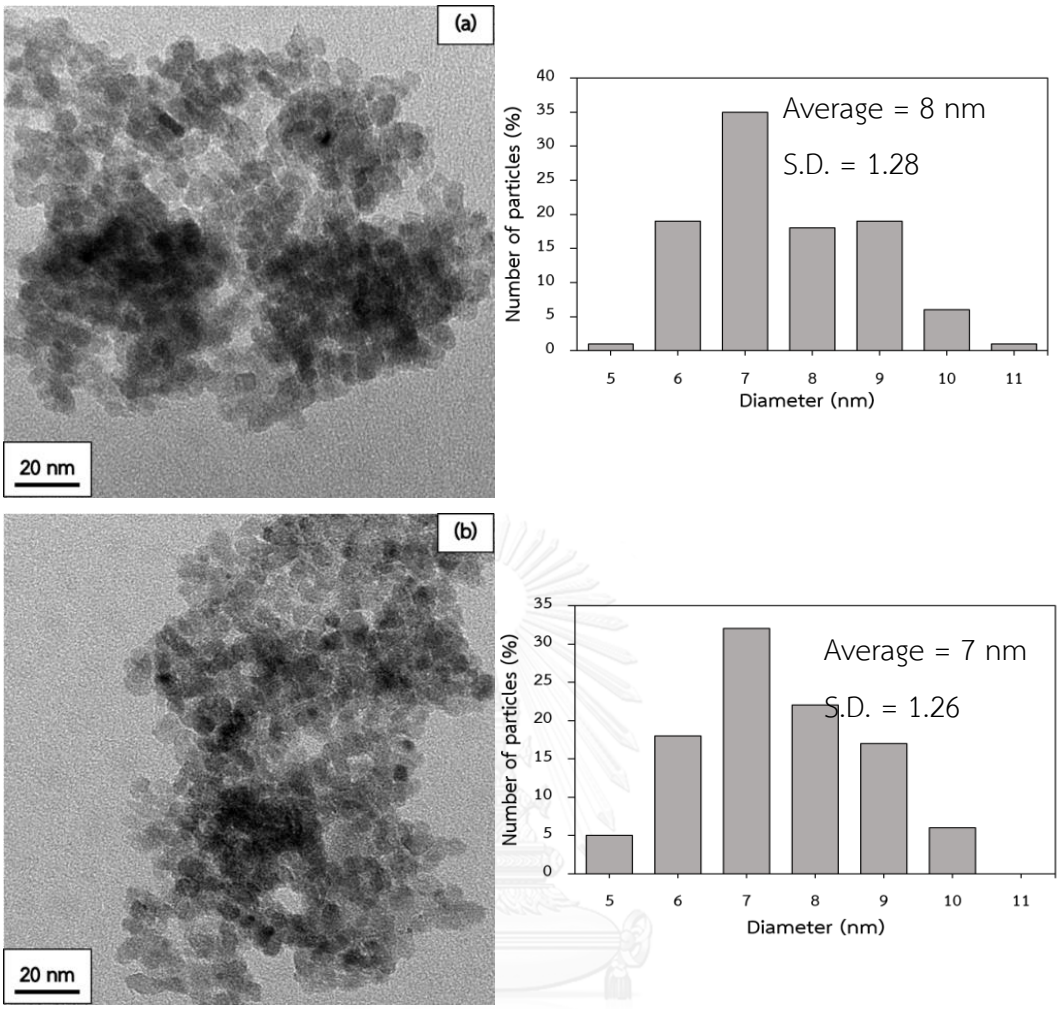

Figure 5.29 TEM images and size distribution of a) Pt/TiO_2 -N_2 b) Pt/TiO_2-O_2

5.7.4 Hydrogen Temperature program reduction (H_2-TPR)

The H_2-TPR measurements were carried out to study the reduction behaviors of the Pt/TiO_2 catalysts prepared by SEA method and the results are shown in Figure 5.30. All the TiO_2 supported Pt showed larger reduction peaks from 250 °C to 600 °C which can be attributed to the reduction of Pt species interacting with the TiO_2 support to form Pt-TiO_x interface sites and the hydrogen consumption above 600 °C was due to the reduction of surface capping oxygen of TiO_2. The TPR profiles of all the catalysts exhibited similar peak position. The reduction peak of the SEA-prepared catalysts shifted to higher temperatures and were broader relative to the impregnation-prepared catalysts due to stronger interaction between adsorbed species and TiO_2 than

impregnation method resulting in more difficult to reduce Pt species. Similar results were observed on [53] which reported that TPR patterns of SEA method shifted to higher temperatures and boarder than the impregnation method due to strong interaction between adsorbed species and silica resulting from the SEA preparation makes the metal precursor much more difficult to reduce. For all the SEA-prepared catalysts, the peak at around 95 ºC which was associated to the reduction of PtO_x crystallites to metallic Pt was not observed as in impregnation-prepared catalysts, due to SEA method generated small particles, confirmed by TEM image.

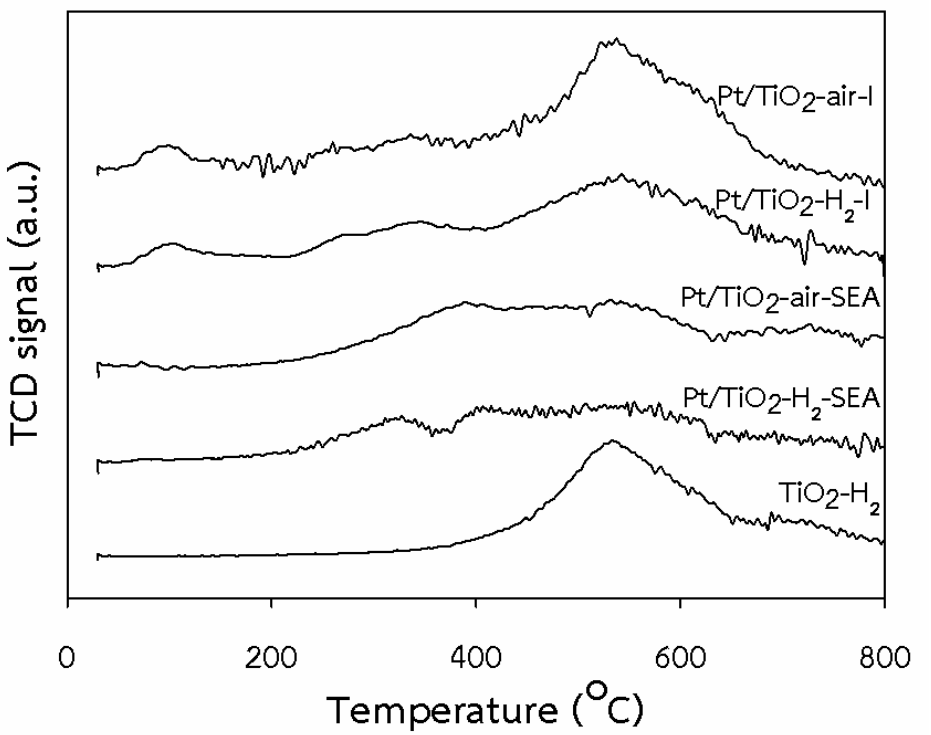

Figure 5.30 The TPR profiles of Pt/TiO_2 catalysts

5.7.5 CO-pulses chemisorption

The relative amount of Pt active sites on the catalyst samples were calculated from the chemisorption results based on the assumption that one CO molecule adsorbed on one Pt site. The amounts of CO chemisorption on Pt/TiO_2 catalysts reduced at 200 ºC are shown in Table 5.7. Preparation of catalysts by SEA method,

Pt/TiO_2-H_2 and Pt/TiO_2-air catalysts showed Pt dispersion at 54% and 50%, respectively. It was found that Pt dispersion on TiO_2-H_2 was slightly higher than supported on TiO_2-air, suggesting that calcination atmosphere of TiO_2 supports did not affect dispersion of metal when prepared by SEA method. Comparing between the different preparation method, the Pt/TiO_2-H_2 catalysts prepared by both methods did not show different of Pt dispersion, while the Pt/TiO_2-air catalysts can improve Pt dispersion from 29 % to 50 % when prepared by SEA method. Thus, it is suggested that preparation of Pt/TiO_2 catalysts by SEA method resulted in an increased dispersion of Pt on all the TiO_2 surface. According to [25], SEA method were used to the preparation of supported metal catalysts with highly dispersion.

Table 5.7 CO chemisorption and reaction results of the 0.5%Pt/TiO_2 catalysts

Catalyst	CO chemisorption (molecule CO x 10^{18}/g cat.)	Pt dispersion (%)	Time (min)	Conversion (%)	Selectivity (%)		
					VA	EA	ENB
Pt/TiO_2-H_2-SEA	8.4	54	20	69	87.9	5.1	7.0
			40	90	88.6	8.5	2.9
Pt/TiO_2-air-SEA	7.7	50	20	64	88.2	5.7	6.1
			40	80	85.6	8.3	6.0
Pt/TiO_2-H_2-I	8.8	57	20	76	92.1	4.9	3.0
			40	89	91.9	5.9	2.2
Pt/TiO_2-air-I	4.5	29	20	29	77.9	5.0	17.1
			40	31	77.4	5.0	17.6

Reaction (3.6 mmol NS in 10 ml ethanol) at 40 °C with a 20 mg catalyst under 20 bar

5.8 Reaction study in selective hydrogenation of 3-NS

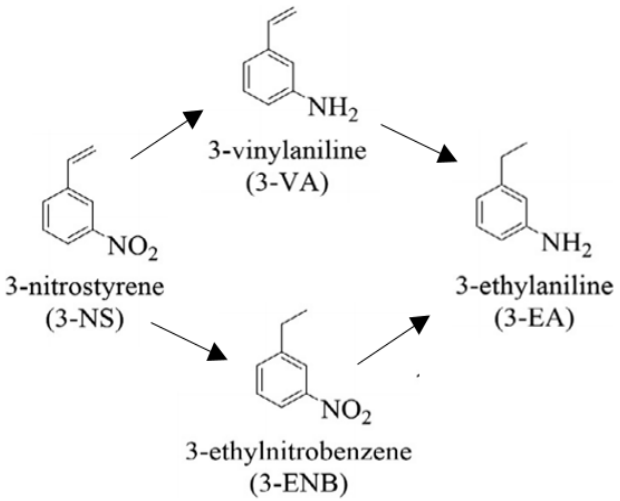

Figure 5.31 Simplified reaction scheme of the hydrogenation of 3-NS.

The catalytic performance of 0.5%Pt catalysts supported on sol-gel derived TiO_2 calcined under different atmospheres were investigated in the selective hydrogenation of NS under the following reaction conditions: 40 °C, 2 MPa of H_2. The catalytic behaviors of the Pt/TiO_2 catalysts at difference calcination atmosphere of TiO_2 supports including NS conversion and product selectivity are summarized in Table 5.7. The main hydrogenation products were ENB and VA, which the desired product is VA without formation of intermediates hydrogenation products. Compared to the reaction at 20 min of reaction time of the Pt/TiO_2-H_2 and Pt/TiO_2-air catalysts prepared by SEA method, both catalysts gave the same conversion of 3-NS and same selectivity to 3-VA when reduced at 200 °C. It is was suggested that the calcination atmosphere of sol-gel TiO_2 support did not affect to change of catalytic performance of Pt/TiO_2 catalysts prepared by SEA method. When increasing the reaction time to 40 min, the conversion of 3-NS increased from 69% to 90% over the Pt/TiO_2-H_2, while the Pt/TiO_2-air increased from 64% to 80%. However, the selectivity of 3-VA was not different in both catalysts and maintained the same with increased reaction time. The Pt/TiO_2-H_2 prepared by SEA method was not improved in terms of both conversion of 3-NS and 3-VA selectivity compared to those prepared by incipient wetness impregnation method. The conversion of 3-NS approximate 70% with 90 % of

3-VA selectivity were obtained from both preparation methods. The preparation of the Pt/TiO_2-air catalysts by SEA method can improve the conversion of 3-NS from 29% to 64% at 20 min of reaction time while slightly increased 3-VA selectivity comparing to those prepared by incipient wetness impregnation method.

CHARPTER VI
CONCLUSIONS

6.1 Conclusions

1) The TiO_2 supports prepared by sol-gel method and calcined under different gas atmospheres (H_2, air, N_2, O_2 and Ar) at 350 °C for 2 h. exhibited similar average crystallite size, crystalline phase, and BET surface area. The calcination atmosphere did not have any influence on the structural properties of the TiO_2 supports. However, as shown by the ESR results, the amount of defects on the surface of TiO_2 increased when calcined under H_2 and N_2 atmosphere compared to those calcined in air, O_2, and Ar. Improvement in the selective hydrogenation of 3-NS of Pt/TiO_2 catalysts after treatment under different atmosphere of TiO_2 supports achieved might be resulted from all the species (i.e. oxygen vacancies and Ti^{3+}), a proper ratio of oxygen vacancies and Ti^{3+} in the modified TiO_2 structure.

2) The catalytic performances of Pt/TiO_2 catalysts prepared by impregnation method in the selective hydrogenation of 3-NS were improved when the TiO_2 support were calcined in H_2 and N_2 atmosphere. The Pt/TiO_2-H_2 and Pt/TiO_2-N_2 catalysts exhibited high conversion of 3-NS (>70%) with high selectivity to 3-VA (>90%) in short reaction time (20 min) when reduced at 200 °C. The improved catalytic activities of Pt/TiO_2 were correlated to the high Pt dispersion. The selectivity of desired product (VA) was related to the presence of linearly CO bond with Pt sites and the metal-support interaction, which were influenced by defects on TiO_2 support. High reduction temperature is not necessary for selectively improvement in the selective hydrogenation of 3-NS.

3) For the Pt/TiO_2-H_2 and Pt/TiO_2-air catalysts prepared by SEA method and reduced at 200 °C, the calcination atmosphere of sol-gel TiO_2 support did not affect the catalytic performances. Both catalysts gave the same conversion of 3-NS and same selectivity to 3-VA under similar reaction conditions. However, the conversion of 3-NS of the Pt/TiO_2-air catalysts was improved from 29% to 64% when prepared by SEA method.

6.2 Recommendation

1. The effects of defects on TiO_2 in the other reactions should be investigated in the next researches.

2. The further study the other factors which has the influence on defects on TiO_2.

REFERENCES

[1] Pisduangdaw, S., Mekasuwandumrong, O., Yoshida, H., Fujita, S.-I., Arai, M., and Panpranot, J. Flame-made Pt/TiO2 catalysts for the liquid-phase selective hydrogenation of 3-nitrostyrene. Applied Catalysis A: General 490 (2015): 193-200.

[2] Pisduangdaw, S., Mekasuwandumrong, O., Fujita, S.-I., Arai, M., Yoshida, H., and Panpranot, J. One step synthesis of Pt–Co/TiO2 catalysts by flame spray pyrolysis for the hydrogenation of 3-nitrostyrene. Catalysis Communications 61 (2015): 11-15.

[3] Corma, A., Serna, P., Concepcion, P., and Calvino, J.J. Transforming nonselective into chemoselective metal catalysts for the hydrogenation of substituted nitroaromatics. J Am Chem Soc 130(27) (2008): 8748-53.

[4] Corma, A., González-Arellano, C., Iglesias, M., and Sánchez, F. Gold complexes as catalysts: Chemoselective hydrogenation of nitroarenes. Applied Catalysis A: General 356(1) (2009): 99-102.

[5] Shimizu, K.-i., Miyamoto, Y., and Satsuma, A. Size- and support-dependent silver cluster catalysis for chemoselective hydrogenation of nitroaromatics. Journal of Catalysis 270(1) (2010): 86-94.

[6] Reis, P.M. and Royo, B. Chemoselective hydrogenation of nitroarenes and deoxygenation of pyridine N-oxides with H2 catalyzed by MoO2Cl2. Tetrahedron Letters 50(8) (2009): 949-952.

[7] Beier, M.J., Andanson, J.-M., and Baiker, A. Tuning the Chemoselective Hydrogenation of Nitrostyrenes Catalyzed by Ionic Liquid-Supported Platinum Nanoparticles. ACS Catalysis 2(12) (2012): 2587-2595.

[8] Macwan, D.P., Dave, P.N., and Chaturvedi, S. A review on nano-TiO2 sol–gel type syntheses and its applications. Journal of Materials Science 46(11) (2011): 3669-3686.

[9] Wang, C., Deng, Z.-X., Zhang, G., Fan, S., and Li, Y. Synthesis of nanocrystalline TiO2 in alcohols. Powder Technology 125(1) (2002): 39-44.

[10] Yu, J., Zhao, X., and Zhao, Q. Effect of surface structure on photocatalytic activity of TiO2 thin films prepared by sol-gel method. Thin Solid Films 379(1–2) (2000): 7-14.

[11] Bamwenda, G.R., Tsubota, S., Nakamura, T., and Haruta, M. Photoassisted hydrogen production from a water-ethanol solution: a comparison of activities of Au□TiO2 and Pt□TiO2. Journal of Photochemistry and Photobiology A: Chemistry 89(2) (1995): 177-189.

[12] Lin, H., Huang, C., Li, W., Ni, C., Shah, S., and Tseng, Y. Size dependency of nanocrystalline TiO2 on its optical property and photocatalytic reactivity exemplified by 2-chlorophenol. Applied Catalysis B: Environmental 68(1-2) (2006): 1-11.

[13] Teoh, W.Y., Mädler, L., Beydoun, D., Pratsinis, S.E., and Amal, R. Direct (one-step) synthesis of nanoparticles for photocatalytic mineralisation of sucrose. Chemical Engineering Science 60(21) (2005): 5852-5861.

[14] Kominami, H., et al. Novel synthesis of microcrystalline titanium(IV) oxide having high thermal stability and ultra-high photocatalytic activity: thermal decomposition of titanium(IV) alkoxide in organic solvents. Catalysis Letters 46(3-4) (1997): 235-240.

[15] Fujita, S.-i., Yoshida, H., Asai, K., Meng, X., and Arai, M. Selective hydrogenation of nitrostyrene to aminostyrene over Pt/TiO2 catalysts: Effects of pressurized carbon dioxide and catalyst preparation conditions. The Journal of Supercritical Fluids 60 (2011): 106-112.

[16] Zhao, J., Gu, Y., and Huang, J. Flame synthesis of hierarchical nanotubular rutile titania derived from natural cellulose substance. Chem Commun (Camb) 47(38) (2011): 10551-3.

[17] Kajitvichyanukul, P., Ananpattarachai, J., and Pongpom, S. Sol–gel preparation and properties study of TiO2thin film for photocatalytic reduction of chromium(VI) in photocatalysis process. Science and Technology of Advanced Materials 6(3-4) (2005): 352-358.

[18] Riyapan, S., et al. Improved catalytic performance of Pd/TiO2 in the selective hydrogenation of acetylene by using H2-treated sol–gel TiO2. Journal of Molecular Catalysis A: Chemical 383-384 (2014): 182-187.

[19] *Wu, D.C., Qiyuan; Yin, Zhoulan; Li, Jie. The influence of different calcination atmosphere on the photocatalytic reactivity of water splitting to O(2) over rutile TiO(2). in *EPD Congress 2008 held at the 2008 Annual TMS Meeting and Exhibition*. 2008: New Orleans, LA. 89-94.

[20] Suriye, K., Praserthdam, P., and Jongsomjit, B. Impact of Ti3+ Present in Titania on Characteristics and Catalytic Properties of the Co/TiO2 Catalyst. Industrial & Engineering Chemistry Research 44(17) (2005): 6599-6604.

[21] Wu, N.-L., Lee, M.-S., Pon, Z.-J., and Hsu, J.-Z. Effect of calcination atmosphere on TiO2 photocatalysis in hydrogen production from methanol/water solution. Journal of Photochemistry and Photobiology A: Chemistry 163(1-2) (2004): 277-280.

[22] Klaysri, R., et al. Impact of calcination atmospheres on the physiochemical and photocatalytic properties of nanocrystalline TiO2 and Si-doped TiO2. Ceramics International 41(9) (2015): 11409-11417.

[23] Hao, X., Barnes, S., and Regalbuto, J.R. A fundamental study of Pt impregnation of carbon: Adsorption equilibrium and particle synthesis. Journal of Catalysis 279(1) (2011): 48-65.

[24] Lambert, S., et al. Synthesis of very highly dispersed platinum catalysts supported on carbon xerogels by the strong electrostatic adsorption method. Journal of Catalysis 261(1) (2009): 23-33.

[25] Jiao, L. and Regalbuto, J.R. The synthesis of highly dispersed noble and base metals on silica via strong electrostatic adsorption: II. Mesoporous silica SBA-15. Journal of Catalysis 260(2) (2008): 342-350.

[26] Ramsurn, H. and Gupta, R.B. Hydrogenation by Nanoparticle Catalysts. (2013): 347-374.

[27] Nerozzi, F. Heterogeneous Catalytic Hydrogenation. Platinum Metals Review 56(4) (2012): 236-241.

[28] Rylander, P.N. PLATINUM METALS IN CATALYTIC HYDROGENATION. Annals of the New York Academy of Sciences 145(1) (1967): 46-51.

[29] Satterfield, C.N. Heterogeneous Catalysis in Industrial Practice, 2nd Edition. New-York : McGraw Hill (1991).

[30] Hossain, N.S.a.M.M. synthesis and Size-control of TiO2 photocatalyst nanoparticles Preparation Using Sol-Gel Method. World Applied Sciences Journal (2011): 1981-1986.

[31] Li, B., Wang, X., Yan, M., and Li, L. Preparation and characterization of nano-TiO2 powder. Materials Chemistry and Physics 78(1) (2003): 184-188.

[32] Yoshida, H., Igarashi, N., Fujita, S.-i., Panpranot, J., and Arai, M. Influence of Crystallite Size of TiO2 Supports on the Activity of Dispersed Pt Catalysts in Liquid-Phase Selective Hydrogenation of 3-Nitrostyrene, Nitrobenzene, and Styrene. Catalysis Letters 145(2) (2014): 606-611.

[33] Tauster, S.J., Fung, S.C., and Garten, R.L. Strong metal-support interactions. Group 8 noble metals supported on titanium dioxide. J Am Chem Soc 100(1) (1978): 170-175.

[34] Colmenares, J.C., et al. Influence of the strong metal support interaction effect (SMSI) of Pt/TiO2 and Pd/TiO2 systems in the photocatalytic biohydrogen production from glucose solution. Catalysis Communications 16(1) (2011): 1-6.

[35] Zhang, J., Zhang, M., Jin, Z., Wang, J., and Zhang, Z. Study of high-temperature hydrogen reduced Pt0/TiO2 by X-ray photoelectron spectroscopy combined with argon ion sputtering—Diffusion-encapsulation effect in relation to strong metal–support interaction. Applied Surface Science 258(8) (2012): 3991-3999.

[36] Devi, R.S., Venckatesh, D.R., and Sivaraj, D.R. Synthesis of Titanium Dioxide Nanoparticles by Sol-Gel Technique. International Journal of Innovative Research in Science, Engineering and Technology 03(08) (2014): 15206-15211.

[37] Kim, C.-S., Moon, B.K., Park, J.-H., Tae Chung, S., and Son, S.-M. Synthesis of nanocrystalline TiO2 in toluene by a solvothermal route. Journal of Crystal Growth 254(3-4) (2003): 405-410.

[38] Chen, X. and Mao, S.S. Titanium Dioxide Nanomaterials: Synthesis, Properties, Modifications, and Applications. Chemical Reviews 107(7) (2007): 2891-2959.

[39] Prasad, K., Pinjari, D.V., Pandit, A.B., and Mhaske, S.T. Phase transformation of nanostructured titanium dioxide from anatase-to-rutile via combined ultrasound assisted sol-gel technique. Ultrason Sonochem 17(2) (2010): 409-15.

[40] Wang, C.-C. and Ying, J.Y. Sol–Gel Synthesis and Hydrothermal Processing of Anatase and Rutile Titania Nanocrystals. Chemistry of Materials 11(11) (1999): 3113-3120.

[41] Karami, A. Synthesis of TiO2 nano powder by the sol-gel method and its use as a photocatalyst. Journal of the Iranian Chemical Society 7(2) (2010): S154-S160.

[42] S. Mu& *, M.G., M. Ivanda, S. PopoviC, A. TurkoviC, R. Trojko, A. SekuliC, and FuriC, K. Chemical and microstructural properties of Ti02 synthesized by sol-gel procedure Materials Science and Engineering (1997): 33-40.

[43] Riyapan, S., Boonyongmaneerat, Y., Mekasuwandumrong, O., Praserthdam, P., and Panpranot, J. Effect of surface Ti3+ on the sol–gel derived TiO2 in the selective acetylene hydrogenation on Pd/TiO2 catalysts. Catalysis Today 245 (2015): 134-138.

[44] Wei, H., et al. Supported Au-Ni nano-alloy catalysts for the chemoselective hydrogenation of nitroarenes. Chinese Journal of Catalysis 36(2) (2015): 160-167.

[45] Xu, G., Wei, H., Ren, Y., Yin, J., Wang, A., and Zhang, T. Chemoselective hydrogenation of 3-nitrostyrene over a Pt/FeOxpseudo-single-atom-catalyst in CO2-expanded liquids. Green Chem. 18(5) (2016): 1332-1338.

[46] Yarulin, A., Berguerand, C., Yuranov, I., Cárdenas-Lizana, F., Prokopyeva, I., and Kiwi-Minsker, L. Pt–Zn nanoparticles supported on porous polymeric matrix for selective 3-nitrostyrene hydrogenation. Journal of Catalysis 321 (2015): 7-12.

[47] Serna, P., Boronat, M., and Corma, A. Tuning the Behavior of Au and Pt Catalysts for the Chemoselective Hydrogenation of Nitroaromatic Compounds. Topics in Catalysis 54(5-7) (2011): 439-446.

[48] Furukawa, S., Yoshida, Y., and Komatsu, T. Chemoselective Hydrogenation of Nitrostyrene to Aminostyrene over Pd- and Rh-Based Intermetallic Compounds. ACS Catalysis 4(5) (2014): 1441-1450.

[49] Yarulin, A., Berguerand, C., Alonso, A.O., Yuranov, I., and Kiwi-Minsker, L. Increasing Pt selectivity to vinylaniline by alloying with Zn via reactive metal–support interaction. Catalysis Today 256 (2015): 241-249.

[50] Yoshida, H., et al. Hydrogenation of Nitrostyrene with a Pt/TiO2Catalyst in CO2-Dissolved Expanded Polar and Nonpolar Organic Liquids: Their Macroscopic and Microscopic Features. The Journal of Physical Chemistry C 115(5) (2011): 2257-2267.

[51] Makosch, M., et al. Organic Thiol Modified Pt/TiO2Catalysts to Control Chemoselective Hydrogenation of Substituted Nitroarenes. ACS Catalysis 2(10) (2012): 2079-2081.

[52] Job, N., Lambert, S., Zubiaur, A., Cao, C., and Pirard, J.-P. Design of Pt/Carbon Xerogel Catalysts for PEM Fuel Cells. Catalysts 5(1) (2015): 40-57.

[53] Jiao, L. and Regalbuto, J.R. The synthesis of highly dispersed noble and base metals on silica via strong electrostatic adsorption: I. Amorphous silica. Journal of Catalysis 260(2) (2008): 329-341.

[54] Job, N., et al. Synthesis and characterization of highly loaded Pt/carbon xerogel catalysts prepared by the Strong Electrostatic Adsorption method. 175 (2010): 169-176.

[55] Li, L. and Liu, C.-y. Facile Synthesis of Anatase-Brookite Mixed-Phase N-Doped TiO2Nanoparticles with High Visible-Light Photocatalytic Activity. European Journal of Inorganic Chemistry 2009(25) (2009): 3727-3733.

[56] Nakaoka, Y. and Nosaka, Y. ESR investigation into the effects of heat treatment and crystal structure on radicals produced over irradiated TiO2 powder. Journal of Photochemistry and Photobiology A: Chemistry 110(3) (1997): 299-305.

[57] Hirakawa, T., Kominami, H., Ohtani, B., and Nosaka, Y. Mechanism of photocatalytic production of active oxygens on highly crystalline TiO2 particles by means of chemiluminescent probing and ESR spectroscopy. The Journal of Physical Chemistry B 105(29) (2001): 6993-6999.

[58] Strunk, J., Vining, W.C., and Bell, A.T. A Study of Oxygen Vacancy Formation and Annihilation in Submonolayer Coverages of TiO2 Dispersed on MCM-48†. The Journal of Physical Chemistry C 114(40) (2010): 16937-16945.

[59] Weerachawanasak, P., Praserthdam, P., Arai, M., and Panpranot, J. A comparative study of strong metal–support interaction and catalytic behavior of Pd catalysts supported on micron- and nano-sized TiO2 in liquid-phase selective hydrogenation of phenylacetylene. Journal of Molecular Catalysis A: Chemical 279(1) (2008): 133-139.

[60] Kongsuebchart, W., Praserthdam, P., Panpranot, J., Sirisuk, A., Supphasrirongjaroen, P., and Satayaprasert, C. Effect of crystallite size on the surface defect of nano-TiO2 prepared via solvothermal synthesis. Journal of Crystal Growth 297(1) (2006): 234-238.

[61] Ikeda, S., et al. Quantitative analysis of defective sites in titanium (IV) oxide photocatalyst powders. Physical Chemistry Chemical Physics 5(4) (2003): 778-783.

[62] Zhang, J., et al. Increasing the oxygen vacancy density on the TiO2 surface by La-doping for dye-sensitized solar cells. The Journal of Physical Chemistry C 114(43) (2010): 18396-18400.

[63] Pan, X., Yang, M.Q., Fu, X., Zhang, N., and Xu, Y.J. Defective TiO2 with oxygen vacancies: synthesis, properties and photocatalytic applications. Nanoscale 5(9) (2013): 3601-14.

[64] Xiong, L.-B., Li, J.-L., Yang, B., and Yu, Y. Ti3+in the Surface of Titanium Dioxide: Generation, Properties and Photocatalytic Application. Journal of Nanomaterials 2012 (2012): 1-13.

[65] Liu, H., Ma, H., Li, X., Li, W., Wu, M., and Bao, X. The enhancement of TiO 2 photocatalytic activity by hydrogen thermal treatment. Chemosphere 50(1) (2003): 39-46.

[66] Zhang, C., He, H., and Tanaka, K.-i. Catalytic performance and mechanism of a Pt/TiO2 catalyst for the oxidation of formaldehyde at room temperature. Applied Catalysis B: Environmental 65(1-2) (2006): 37-43.

[67] Ekou, T., et al. Citral hydrogenation over Rh and Pt catalysts supported on TiO2: Influence of the preparation and activation protocols of the catalysts. Journal of Molecular Catalysis A: Chemical 337(1-2) (2011): 82-88.

[68] Soria, J.C.C.a.J. Reversible Ti3+ Formation by H2 Adsorption on M/Tt02 Catalysts. J. Phys. Chem. 86 (1982): 1392-1395.

[69] Pisduangdaw, S., Mekasuwandumrong, O., Fujita, S.-I., Arai, M., Yoshida, H., and Panpranot, J. One step synthesis of Pt–Co/TiO 2 catalysts by flame spray pyrolysis for the hydrogenation of 3-nitrostyrene. Catalysis Communications 61 (2015): 11-15.

[70] Li, X., Zheng, W., Pan, H., Yu, Y., Chen, L., and Wu, P. Pt nanoparticles supported on highly dispersed TiO2 coated on SBA-15 as an efficient and recyclable catalyst for liquid-phase hydrogenation. Journal of Catalysis 300 (2013): 9-19.

[71] Kang, J.H., Shin, E.W., Kim, W.J., Park, J.D., and Moon, S.H. Selective Hydrogenation of Acetylene on TiO2-Added Pd Catalysts. Journal of Catalysis 208(2) (2002): 310-320.

[72] Kongsuebchart, W., Panpranot, J., Satayaprasert, C., and Praserthdam, P. Effect of TiO2 crystallite size on the dispersion of Co on nanocrystalline TiO2. Reaction Kinetics and Catalysis Letters 91(1) (2007): 119-126.

[73] Suriye, K., Praserthdam, P., and Jongsomjit, B. Control of Ti3+surface defect on TiO2 nanocrystal using various calcination atmospheres as the first step for surface defect creation and its application in photocatalysis. Applied Surface Science 253(8) (2007): 3849-3855.

APPENDIX

APPENDIX A

CALCULATION FOR CATALYST PREPARATION

For 0.5%Pt/TiO_2 catalysts prepared by incipient wetness impregnation method was shown.

TiO_2 supports calcined under H_2, air, N_2, O_2 and Ar and used as the supports for preparation of Pt/TiO_2 catalysts. The calculation of 0.5 wt%Pt/TiO_2 catalysts prepared by incipient wetness impregnation method were shown below. In this work, 4 g of the TiO_2 supports were used for all preparation and calculation based on 100 g of catalyst used.

Precursor:

-Chloroplatinic acid hexahydrate 37.5% (H_2PtCl_6•$6H_2O$) MW. = 517.90 g/mol

-TiO_2 supports were prepared by sol-gel method and calcined under H_2, air, N_2, O_2 and Ar.

Calculation:

TiO_2 100-0.5 = 99.5 g

Plattinum 0.5 g

For TiO_2 4 g

Plattinum reguired = (4x0.5)/99.5 = 0.0201 g

Chloroplatinic acid hexahydrate dissolved in DI water, which Pt precursor was stock in solution form

$$\text{Pt required in stock solution} = \frac{\text{weight of Pt required}}{\text{MW of Pt}} \times \text{MW of } H_2PtCl_6 \bullet 6H_2O$$

$$= \frac{0.0201 \text{ g} \times 517.9 \text{ g precursor}}{195.078 \text{ g Pt}}$$

$$= 0.0534 \text{ g precursor}$$

From N_2 physisorption results, pore volume of the titanium dioxide supports are about 0.3 cm^3/g (ml/g) in all catalysts. For incipient wetness impregnation method, total volume of DI water which is used to dissolve Chloroplatinic acid hexahydrate muse be equal to the pore volume of titania support. According to the total volume of precursor solution which for impregnation is 0.3 ml for 0.95 g of titania support.

APPENDIX B

CALCULATION OF THE CRYSTALLITE SIZE

Calculation of the crystallite size by Debye-Scherrer equation

The crystallite size was calculation from the half-height width of the diffraction peak of XRD pattern using the Debye-Scherrer equation.

From Scherrer equation

$$D = \frac{K\lambda}{\beta \cos\theta}$$

Where D= Crystallite size, Å

K = crystallite-shape factor=0.9

λ = X-ray wavelength, 1.5418 Å for CuK_α

θ = Observed peak angle, degree

β = X-ray diffraction broadening, radian

The X-ray diffraction broadening (β) is the corrected width of a powder diffraction free from all broadening due to the instrument. The α-alumina was used as a standard sample to observe the instrumental broadening data. The most common correction for the X-ray diffraction broadening (β) can be obtained by using Warren's formula

From Warren's formula:

$$\beta = \sqrt{B_M^2 - B_S^2}$$

Where B_M = The measured peak width in radians at half peak height

B_S = The corresponding width of the standard material

Example: Calculation of the crystallite size of anatase TiO_2

The major peak of anstase TiO_2 was observed at $25.42^\circ 2\theta$

The half-height width of the diffraction peak at $25.42^\circ = 1.04^\circ$

$$= \frac{2\Pi \times 1.04}{360}$$

= 0.0182 radian (B_M)

Corresponding the half-height width of α -alumina of the diffraction peak at 25.42° = 0.0041 radian (B_S)

$$\beta = \sqrt{B_M^2 - B_S^2}$$
$$= \sqrt{0.0182^2 - 0.0041^2}$$
$$= 0.0177 \text{ radian}$$

Thus, $\beta = 0.0177$

$2\theta = 25.42 \Rightarrow \theta = 12.71^\circ$

$\lambda = 1.5418$ Å for CuK_α

$$\text{Crystallite size, } D = \frac{K\lambda}{\beta \cos\theta}$$
$$= \frac{0.9 \times 1.5418}{0.0177 \times \cos(12.71)}$$
$$= 80.36 \text{ Å}$$
$$= 8.036 \text{ nm}$$

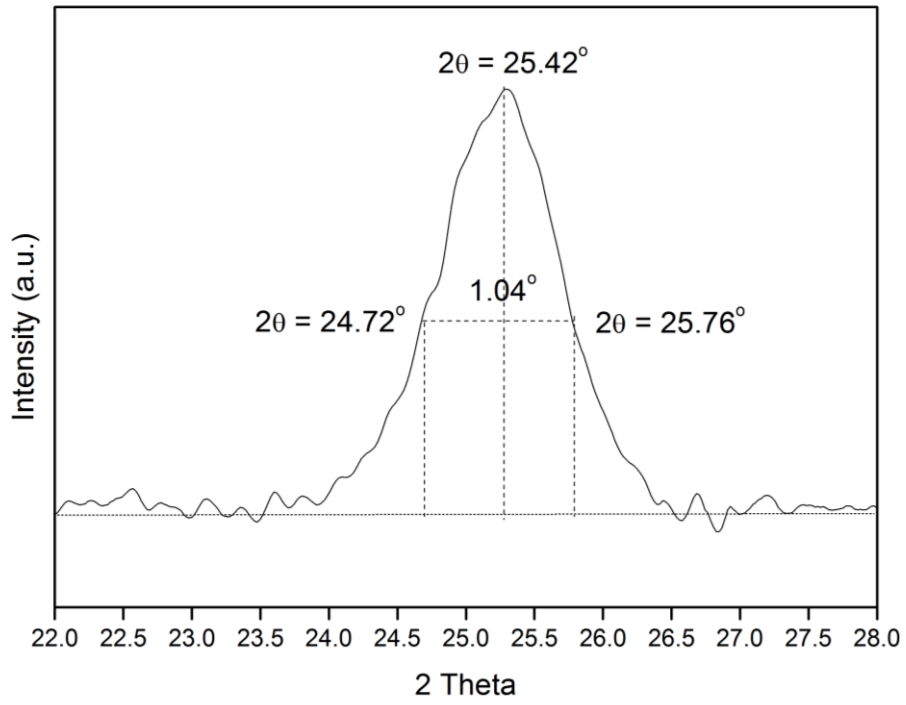

Figure B.1 The measured XRD peak of anatase TiO_2 for calculation of crystallite size of anatase TiO_2

APPENDIX C

CALCULATION FOR METAL ACTIVE SITES AND DISPERSION

Calculation of Pt active sites and Pt dispersion of the catalyst by CO-chemisorption is as follows:

Volume of CO adsorption on catalyst, $V_{ads} = \frac{V_{inj}}{m} \times \sum_{i=1}^{n} (1 - \frac{A_i}{A_f})$

Where V_{inj} = volume injected, 0.02 cm^3

m = mass of catalyst used, g

A_i = area of peak i

A_f = area of last peak

Pt active sites

$$\text{Pt active sites} = S_f \times \frac{V_{ads}}{V_g} \times N_A$$

S_f = stoichiometer factor, CO adsorbed on Pt, CO:Pt=1

V_{ads} = volume adsorbed

V_g = molar volume of gas at STP, 22414 cm^3/mol

N_A = Avogadro's number, 6.023×10^{23} molecules/mol

Metal dispersion

$$\text{Metal dispersion (\%)} = 100 \times \frac{\text{molecule of Pt from CO adsorption}}{\text{molecule of Pt loaded}}$$

$$\%D = S_f \times \frac{V_{ads}}{V_g} \times \frac{MW}{\%M} \times 100\% \times 100\%$$

S_f = stoichiometer factor, CO adsorbed on Pt, CO:Pt=1

V_{ads} = volume adsorbed

V_g = molar volume of gas at STP, 22414 cm^3/mol

MW = molecular weight of the metal

%M = weight percent of the active metal

APPENDIX D

Calculation for catalytic performance

Calculation of NS conversion and selectivity of the catalysts are shown in this below. Decane was used as internal standard for calibration in reactant and products in hydrogenation of 3-NS. Molar ratio and area ratio were plotted and then the relation of decane and the NS were written in the equation for calculation the conversion.

The calibration of 3-NS are exhibited.

	area (0.9 mmol NS)	area (1.8 mmol NS)	area (3.6 mmol NS)
NS	60432750.9	64683467.3	40640706
Decane	2327119.8	4269411.2	5463047
area ratio	0.038507593	0.066004674	0.134423034
mol decane	3.018E-07	3.018E-07	3.018E-07
mol NS	1.2066E-08	2.4132E-08	4.8264E-08
molar ratio	0.039980119	0.079960239	0.159920477

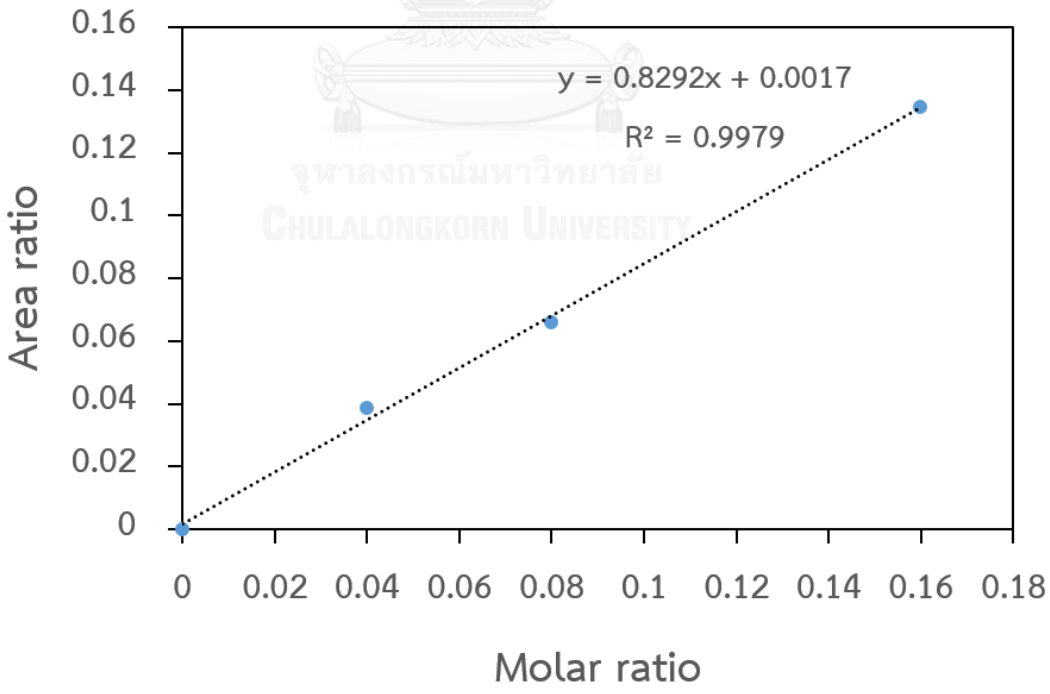

Figure D.1 Calibration curve of NS

From this data we get the relation of decane and 3-nitrostyrene as:

$$\text{Mole ratio of } \left(\frac{\text{NS}}{\text{Decane}}\right) = 0.8292 \times \text{Area ratio of } \left(\frac{\text{NS}}{\text{Decane}}\right)$$

$$\text{Mole NS} = \left(\frac{\text{Mole Decane}}{\text{Area Decane}}\right) \times 0.8292 \times \text{Area NS}$$

Calculation of NS conversion

$$\%\text{NS conversion} = \frac{\text{Mole}_{in} - \text{Mole}_{out}}{\text{Mole}_{in}} \times 100$$

$$\%\text{NS conversion} = \frac{\text{Mole NS}_{in} - \text{Mole NS}_{out}}{\text{Mole NS}_{in}} \times 100$$

$$\%\text{seletivity of VA} = \frac{\text{Mole VA}}{\text{Mole VA} + \text{Mole ENB} + \text{Mole EA}} \times 100$$

VITA

Miss Sasithorn Kuhaudomlap was born on April 6th, 1991 in Kanchanaburi, Thailand. She received the Bachelor's Degree in Chemical Engineering from Department of Chemical Engineering, Faculty of Engineering and Industrial Technology, Silpakorn University, Nakhonpathom, Thailand in March 2014. Thereafter, she entered to study in Master's Degree of Chemical Engineering at Department of Chemical Engineering, Chulalongkorn University, Bangkok Thailand since 2014 and joined center of excellence on catalysis and catalytic reaction engineering research group.